ADAPTIVE AND NON-ADAPTIVE EVOLUTION OF THE CONTROL OF GENE EXPRESSION

by

Kun Xiong

A Dissertation Submitted to the Faculty of the

DEPARTMENT OF MOLECULAR AND CELLULAR BIOLOGY

In Partial Fulfilment of the Requirements
For the Degree of

DOCTOR OF PHILOSOPHY

In the Graduate College

THE UNIVERSITY OF ARIZIONA

2019

THE UNIVERSITY OF ARIZONA
GRADUATE COLLEGE

As members of the Dissertation Committee, we certify that we have read the dissertation prepared by ***Kun Xiong***, titled ***Adaptive and Non-adaptive Evolution of the Control of Gene Expression*** and recommend that it be accepted as fulfilling the dissertation requirement for the Degree of Doctor of Philosophy.

Joanna Masel Date: (4/12/2019)

Andrew Capaldi Date: (4/12/2019)

Guang Yao Date: (4/12/2019)

Ryan Gutenkunst Date: (4/12/2019)

Final approval and acceptance of this dissertation is contingent upon the candidate's submission of the final copies of the dissertation to the Graduate College.

I hereby certify that I have read this dissertation prepared under my direction and recommend that it be accepted as fulfilling the dissertation requirement.

Joanna Masel Date: (4/12/2019)
Professor
Ecology & Evolutionary Biology

Acknowledgement

I sincerely thank Dr. Joanna Masel for her dedicated mentoring in the past 5 years. She showed me how good science was done, and pushed me forward with her high standard for research. Along the way, she helped me through problems with her expertise and generously supported my career development. I also thank members of my thesis committee, for their guidance and support to my research. I need to thank the Department of Molecular and Cellular Biology for giving me a rich and enjoyable life during my study. I am eternally grateful to my parents. They allowed me to freely explore my childhood interests and offered careful education that enabled me to purse my dream.

Table of Contents

Abstract

Non-adaptive evolution refers to evolutionary processes that are primarily driven not by natural selection, but by factors such as a bias towards generating certain mutations over others. Although non-adaptive evolution is supported by abundant data, it is obscure outside the field of evolutionary biology, potentially for historical reasons. Considering non-adaptive evolution helps us to understand the origins and roles of traits at molecular and cellular levels, where research is often dominated by adaptationist assumptions. To demonstrate that a balanced view on evolution is necessary, my thesis research asks how adaptive and non-adaptive evolution shape the control of gene expression. I start by simulating the evolution of mechanisms for quality control of gene expression. I show that the error rate associated with gene expression is determined by both the mutational bias that tends to increase the error rate and by the effective population size of the species, which determines the strength of natural selection on the error rate. This offers an explanation for the observed non-monotonic relationship between transcriptional error rate and effective population size. I next study the evolution of transcriptional regulatory networks (TRNs). The adaptationist view hypothesizes that the enrichment of a subnetwork called coherent type 1 feed-forward loops (C1-FFLs) in TRNs is an adaptation for filtering out short spurious signals, but this and similar hypotheses about other enriched subnetworks are widely questioned by evolutionary biologists, because the adaptive hypothesis fails to consider network topologies that evolve non-adaptively. To help resolve this debate, I developed a highly mechanistic computational model that captures non-adaptive factors that can shape the topology of TRNs. I show that functional C1-FFLs evolve readily under selection for filtering out a spurious signal, but not under control selection conditions. While this result supports the adaptive origin of C1-FFLs, I show that non-adaptive subnetworks can also be enriched in TRNs evolved for filtering out a spurious signal, suggesting that inferring functions of TRNs from topology alone can be problematic. A further complication comes from the fact that a subnetwork that is topologically different from C1-FFLs also evolves to filter out spurious signals. In conclusion, I argue that non-adaptive evolution can explain the origins and roles of traits that are difficult to understand under adaptationism, and that considering non-adaptive evolution is necessary to carry out scientific research in all fields of biology. Molecular and cellular biologists should actively consider non-adaptive evolution in their research.

Introduction

Aim of the study

As molecular and cellular biologists, we are often interested in characterizing the functions of bio-molecules and cellular structures. Function, in this context, means not any effect that can result from the bio-molecule according the laws of the universe, but a specific effect that is likely important for the cell and thus explains the existence of the molecule (Graur et al. 2013). This means that when we ask "what's the function of protein X?", we are essentially asking "what effect of X causes X to exist and/or persist during evolution?". More importantly, we also implicitly assume that the reason protein X evolves must be to meet the need for a certain biological effect. This assumption is known as adaptationism in evolutionary biology. However, we molecular and cellular biologists are often unaware that adaptationism is criticized by many evolutionary biologists. As will be explained in the next section, factors other than natural selection can drive evolution, causing non-adaptive evolution. For these reasons, my research focuses on the control of gene expression, one of the most important research subject in molecular and cellular biology, and asks what control mechanisms of gene expression may have arisen through evolution by natural selection and what may have arisen through non-adaptive evolution. I hope my research can show molecular and cellular biologists the necessity of having a balanced view when interpreting the origins of molecular and cellular traits.

Introduction to non-adaptive evolution

A flavor of non-adaptive evolution

In 1970s, researchers studying domestication started an experiment on silver foxes in Siberia. They bred wild fox based on a single criterion: parental foxes must not be aggressive and must not avoid humans when they are hand fed and petted (Trut, Oskina, and Kharlamova 2009). The selective breeding produced tamed foxes that are obedient and eager for human touch in several generations. Interestingly, the tamed foxes also developed curly tails, floppy ears, lightened fur color, and other traits that are commonly found in domesticated animals, even though none of these traits was a criterion for the selective breeding. One reason behind the development of these tameness-unrelated traits is that selection for tameness has changed the neurohormonal status, such as a reduction in glucocorticord, which induces stress-response, and an increase in serotonin, which inhibits aggressive behavior (Trut, Oskina, and Kharlamova 2009). Neurohormones can affect gene expression and cell differentiation during development, leading to morphological changes (Trut, Oskina, and Kharlamova 2009).

Morphological traits like curly tails, floppy ears, and lightened fur color, are common in domesticated mammals, such dogs, cows, and pigs, but are rare in the wild counterparts of these animals. Therefore, before the Siberian fox experiment, it was generally believed that the morphological changes in domesticated mammals were not caused by species-specific processes, but were the results of our preference for cute appearance during domestication. The experiment on foxes clearly showed that such traits can arise even with no selection for them during domestication. Because cuteness traits should not increase the fitness of a fox, i.e. increasing the fox's offspring, these traits are not adaptations.

Similarly, certain genes in the olfactory receptor (OR) gene family are unlikely to be adaptations for detecting odors. The human OR gene family has about 400 functional genes and 400 pseudogenes, but because olfactory receptors work in combination, fewer functional genes may be sufficient to differentiate odors (Nei, Niimura, and Nozawa 2008). The huge variation of functional OR gene numbers among human individuals also suggests that gaining or losing OR genes does not considerably affect fitness (Nei,

Niimura, and Nozawa 2008). Evolution of the OR gene family likely involves rounds of gene duplication and pseudogenization of functional genes; many such mutations are likely neutral (Nei, Niimura, and Nozawa 2008).

If the emergence of a trait is not driven by natural selection for that trait, the trait and its evolution are often called "non-adaptive" by evolutionary biologists. However, being "non-adaptive" is not about whether the trait provides benefit nowadays – this is critically important. A trait that evolved non-adaptively may become beneficial. For example, suppose the Siberian fox farm becomes a pet company, and starts to breed cute foxes from the docile ones. Floppy ears will be a beneficial trait in this situation, but was neutral when docile foxes were selected for.

A brief history of theories of (non-)adaptive evolution

The concept of non-adaptive evolution can be highly counter-intuitive; after all, evolution is usually associated with adaptation and natural selection. Understanding the history of evolutionary theories is helpful to demonstrate how adaptive evolution is mistakenly equated with evolution, which is a frequent misconception in fields outside of evolutionary biology. As we will see, although non-adaptive evolution first arose as an alternative to Darwin's theory of evolution by natural selection, it is now an inseparable part of modern evolutionary theories.

In 1858, Darwin published *On the Origin of Species*, proposing that species form through evolution and natural selection as a driver of evolution. In his theory of evolution by natural selection, Darwin proposed that individuals vary in phenotype, and a "struggle for existence" among individuals makes sure that only those carrying beneficial phenotypic variants can survive and reproduce, passing those variants to the next generation.

Although Darwin's theory of evolution by natural selection is regarded as one of the most important scientific theories in history, it was far from solid when Darwin first proposed it. Because the relationship between abnormal chromosomes and mutation was not discovered until Morgan and Dobzhansky's work in the 1930s, Darwin had to assume that phenotypic variation arose through mechanisms like acquired inheritance, i.e. the use (disuse) of a trait creates inheritable enhancement (degradation) of the trait. This is now rejected by the field. Darwin was not aware of Mendel's work on inheritance, and this led him to propose pangenesis as the mechanism of inheritance (Darwin 1894). Pangenesis states that all parts of the body produce tiny particles, which can grow into the parts from which they are produced, and that these particles are pooled in reproductive cells to generate the bodies of offspring. A major problem of pangenesis, as pointed out by Fisher (1932), is that it implies that sexual reproduction will quickly average out phenotypic variation among individuals: fertilization blends the parental particle, therefore a trait in offspring should be the average of the parental traits. However, evolution by natural selection requires phenotypically different individuals. According to Fisher (1932), Darwin was aware of this problem and assumed that the mechanisms to generate phenotypic variation proposed in the *Origin* could replenish the variation lost due to sexual reproduction. That natural selection must act on phenotypic variation that is generated by mechanisms like acquired inheritance cast a shadow on Darwin's theory of evolution by natural selection.

Flaws in Darwin's theory of evolution by natural selection and discoveries in paleontology quickly led to what's known as the "eclipse of Darwinism" around 1900s, during which several alternatives to the theory of evolution by natural selection received significant attention. Darwin assumed that natural selection accumulated "slight, successive, and favorable variations" (Darwin 1858, 346), but the fossil record often lacked forms that resemble intermediates during the formation of new species. Instead, fossils of multiple new species were often discovered in batches, suggesting rapid speciation in a relatively short amount of time. This apparent discontinuity in evolution was explained by saltationism.

Saltationism argued that speciation was driven by mutations that could “instantaneously” create new species, which were different from mutations that cause phenotypic variation among individuals within a species (Bowler 1983). Followers of saltationism debated among themselves whether speciation-driving mutations were under natural selection (Bowler 1983).

Additional major alternatives are acquired inheritance and orthogenesis, which share some similarities. Acquired inheritance, also known as neo-Larmarckism, proposes that individuals can actively refine a trait and pass the refined trait to the next generation, causing the trait to evolve. Orthogenesis proposes that there is a direction in the evolution of a species, and the direction is determined by factors intrinsic to the species. The nature of such intrinsic factors were never made clear, although many considered the developmental process as a candidate (Bowler 1983). Acquired inheritance proposed that the active use of a trait by an organism refines the trait, implying that the "desires" of organisms and/or "a primordial property" of living tissues to modify themselves to meet the excess use (Fisher 1930) are what determine the evolution of the trait. Certain scholars thus considered acquired inheritance as the mechanism underlying orthogenetic evolution (Bowler 1983). Both theories essentially call on some internal factors to create a bias in the direction of mutation, and consider the biased mutation as the direct driver of evolution. Both theories, particularly orthogenesis, were supported by so-called long-term trends in the fossil record. As a commonly cited example, the fossil record of a mollusk *Gryphaea* showed that the shell of the animal displayed a trend of overcoiling, and the overcoiling was believed to be so extreme such that the animal could barely open its shell (Bowler 1983). The apparently harmful trend toward overcoiling could be not explained by natural selection, therefore it was considered a case of evolution driven by the internal factors of the organism.

The re-vitalization of the theory of natural selection occurred during the Modern Synthesis in the early 20th century. The Synthesis was an effort to bring together Darwin’s rudimentary theory of evolution by natural selection and mainly genetics, and synthesize a mature theory of evolution (Smocovitis 1992). It started with the establishment of population genetics. Building on Mendel’s theory of particulate inheritance, population geneticists consider an individual as a set of loci, and each locus carries an allele that has certain fitness value. Individuals carrying high-fitness alleles should on average have more offspring than those carrying low-fitness alleles. Under this simplification, a population can be summarized by the frequencies of different alleles at each locus, and evolution can be described as changes in allele frequencies, which can be predicted given appropriate parameters. For example, Fisher (1932) studied how random deviations from an expected number of offspring, commonly known as genetic drift, could affect the frequency of an allele. He argued that most beneficial alleles only increase fitness to a small degree, therefore a common beneficial allele has only a slightly better chance of surviving genetic-drift-induced lost than a neutral allele does. Which allele eventually reaches high frequency in a population, i.e. has the most descendants, is partially determined by chance. Following this line, Wright proposed that in small populations, changes in allele frequency are mostly random, i.e. non-adaptive (Wright 1931). As we will see, genetic drift offered an explanation for the apparent discontinuities in the fossil record. Additional contributions of population genetics to evolutionary theories during the synthesis are reviewed by historian William Provine (Provine 1978).

The work of Theodosius Dobzhansky on fruit fly chromosomes demonstrated the mechanisms underlying mutations, lending genetic support to the mathematical equations of evolution (Smocovitis 1992). His work attracted biologists from many fields “to bind the heterogeneous practices of evolution into an evolutionary network grounded in genetics and selection theory” (Smocovitis 1992). For example, paleontologist Simpson proposed that the apparent discontinuities in the fossil record can be explained by changes in the rate of evolution (Simpson 1944). Building primarily on Wright’s theory of shifting balance, Simpson argued that environmental changes, such as fragmentation of habitat, can divide a species into small populations, which, through strong genetic drift, can rapidly evolve in random directions. Because a mutation could be pre-adaptive, i.e. it does not provide a benefit in the current

environment but is beneficial under a particular new environment, a population in which a pre-adaptive mutation had fixed could thrive in an appropriate new environment. The mutant trait could be further refined by selection in the new environment. Thus, the combined effect of genetic drift and selection could explain rapid speciation, removing the need for saltationism which called for mutations produced by unknown mechanisms.

Towards the end of the synthesis, there was a trend that considered natural selection as the primary or, for some, the only, driver of evolution. Such thoughts are known as adaptationism, selectionism, and sometimes neo-Darwinism. For example, in *Evolution*: *the Modern Synthesis*, the book that proposed and popularized the term "modern synthesis", Huxley listed many examples of adaptive traits to demonstrate the "omnipresence of adaption". Although he acknowledged the existence of a few non-adaptive traits, he considered them rare exceptions or adaptations that were unrecognized due to lack of knowledge of their function (Huxley 1942). Enrst Mayr, a major contributor to the synthesis, concluded the 1947 Princeton Conference on Genetics, Paleontology, and Evolution with "an agreement among all the participants on the gradual mode of evolution, with natural selection as the basic mechanism of evolution and only direction-giving force in evolution" (Mayr and Provine 1981), and consistently defended the exclusive role of natural selection (Mayr 1993). Because the timing of the modern synthesis coincided with the establishment of many branches of biological sciences (Smocovitis 1992), e.g. molecular genetics, it is arguably an inevitable consequence that adaptationism was absorbed by many branches of biological sciences at their foundation.

There were certainly concerns about adaptationism. While general working models of natural selection had been quantitatively described by population geneticists, and had been successfully applied to explain major evolutionary events like speciation, many were unconvinced that these were sufficient to support a dominant role of natural selection in evolution. Gould called the rise of adaptationism the "hardening of the modern synthesis" (Gould 1983). William Provine considered the whole modern synthesis a constriction of the plethora of evolutionary theories developed since the 19th century, and agreed with Gould on adaptationism, calling it a "further constriction of evolutionary constriction" (Provine 1988). Perhaps the most well-known criticism of adaptationism is "*The spandrels of San Marco and the Panglossian paradigm: a critique of the adaptationist programme*" by Gould and Lewontin (1979). A spandrel is the gap between a rectangle and an arc that is tangential to both arms of the rectangle. Spandrels are common in San Marco Basilica, because the rectangular door frames in San Marco often embed a dome inside. These spandrels are always decorated with beautiful paintings. Because adaptationists assume traits always evolve adaptively, Gould and Lewontin mocked that adapationists would consider the spandrels of San Marco an adaptation for containing paintings, although spandrels are geometrically inevitable under the design of the building (Gould and Lewontin 1979). To Gould and Lewontin, adaptationists could always propose that a specific trait evolves as an adaptation for a new function when arguments in favor of an old function were no longer supported. They complained that once an adaptationist explanation became the working hypothesis to explain the origin of a trait, it would be essentially impossible to reject it. Therefore, any working hypothesis should also consider the possibility that a trait evolved non-adaptively through factors such as genetic drift and developmental constraint (Gould and Lewontin 1979).

To demonstrate how deeply non-adaptive evolution has been integrated in modern evolutionary theories, I will introduce several modern evolutionary theories in the next three sections. We will see that population genetics provides a platform to seamlessly integrate adaptive evolution and non-adaptive evolution induced by genetic drift, therefore evolutionary theories based on population genetics form the major school in evolutionary studies. In a different school of evolutionary biology, research focuses on revealing the role of organismal development in evolution.

The (nearly) neutral theory of evolution

The role of genetic drift in evolution had been brought to attention by Wright and Simpson, but some scholars suggested that it was dismissed later during modern synthesis (Mayr 1993; Gould 1983). The importance of genetic drift was recognized after Motoo Kimura proposed the neutral theory of evolution.

The invention of protein sequencing techniques in the 1950s allowed researchers to see the differences in the amino acid sequences of the same protein among species. Given these differences and the evolutionary time since the species diverged from their last common ancestor, one can calculate an amino acid substitution rate of a protein. In 1968, Kimura noticed that the amino acid substitution rates of several mammalian proteins were too high when compared with a previous calculation that had assumed substitutions to be adaptive (Haldane 1957); instead, amino acid substitutions were more likely to be neutral (Kimura 1968).

Kimura considered an amino acid substitution as occurring when the allele frequency of a rare allele increased to 1 ("fixes") in a population. For a diploid population of N individuals, Kimura calculated the probability that an allele of a given initial frequency reaches fixation. For an initial frequency of $1 / 2N$, the probability is given by Eq.1.

$$\begin{cases} \frac{1-e^{-2s}}{1-e^{-2sN_e}}, |s| > 0 \\ \frac{1}{2N_e}, \ s \approx 0 \end{cases} \quad (1)$$

In Eq.1, s is the selection coefficient of allele X relative to other alleles at the same locus, and is defined as $s = (f1 - f0) / f1$, where the fitness offered by allele X to the individual is $f0$, and the fitness offered by any other allele is $f1$. Therefore, $s < 0$ means allele X is deleterious relative to other alleles, $s > 0$ means beneficial, and $s \approx 0$ means neutral (neutral is defined more precisely as $|2sN_e| << 1$ in the original work of Kimura). N_e is the "effective" population size that accounts for the fact that real-world populations can deviate from an idealized population due to, for example, fluctuations in population size.

Eq. 1 shows that a neutral allele fixes with probability $1 / 2N$. Assuming the per-individual amino acid mutation rate is μ, each generation there will be $2N\mu$ alleles entering the population and potentially becoming fixed. If these alleles are neutral, there will be $2N\mu \times 1/2N = \mu$ alleles reaching fixation in the population per generation. In other words, the substitution rate of neutral amino acids in a population is equal to the per-individual mutation rate of neutral amino acids.

Soon, the amino acid substitution rates of hemoglobin and cytochrome C were measured by new techniques, and the variance in substitution rates among species was larger than predicted by the neutral theory (Ohta and Kimura 1971). To explain this discrepancy, Ohta and Kimura (1971) proposed that if most substitutions were slightly deleterious, the substitution rate should negatively correlate with the N_e and/or the generation time of the species (this is explained in the next paragraph). Additionally, certain regions in cytochrome C and tRNA displayed higher substitution rates than predicted by neutral theory, suggesting a stepwise substitution where one slightly deleterious substitution creates a need for compensation, facilitating additional substitutions (Ohta 1973). The revised theory proposed that most mutations should be slightly deleterious rather than neutral, and is therefore known as the nearly neutral theory of evolution (Ohta and Gillespie 1996). Nearly neutral mutations initially referred to slightly deleterious mutations that satisfy $-sN_e \approx 1$ (Ohta and Kimura 1971), but the theory was later revised to also include slightly beneficial mutations (Ohta and Gillespie 1996) and thus refers to mutations that satisfy $|sN_e| \approx 1$ or equivalently $|s| \approx 1 / N_e$.

Within the regime of near-neutrality ($|s| \approx 1 / N_e$), the fate of a mutation is sensitive to the effective population size N_e. This can be seen from the probability of fixation of a rare deleterious mutation with $s = -0.01$, which is 4×10^{-11} in a diploid population of $N_e = 1000$, but is 0.0032 in a relatively small diploid population of $N_e = 100$; the second probability is not much smaller than that of a neutral mutation, which is 0.005. Before the nearly neutral theory of evolution proposed this population-size-dependent probability of fixation, studies on substitution rates suffered from the so-called generation-time effect. When evolutionary rate is defined as the number of substitutions *per generation*, the evolutionary rate of neutral substitutions is a constant that does not change with population size. However, organisms with large population sizes, e.g. bacteria, usually have shorter generation times than those with small population sizes, e.g. humans. Consequently, when measured as number of substitutions *per year*, the evolutionary rate of neutral substitutions should decrease as population size decreases -- this is known as the generation-time effect. It was found that, while the evolutionary rate of non-coding DNA displays the generation-time effect, that of proteins does not (Laird, McConaughy, and McCarthy 1969). The nearly neutral theory argued that mutations in proteins could fall into the regime of near-neutrality. Because large populations narrow the nearly neutral regime, proteins in large populations should experience less substitution, canceling out the effect from short generation times.

More recently, the nearly neutral theory of evolution has been used to explain phenotypic differences between species. Lynch proposed that the effective population size of a species essentially set a characteristic "drift barrier", a selection coefficient $s = -1 / N_e$ (Lynch and Walsh 2007). Mutations with $s > -1 / N_e$ are strictly purged by natural selection and only the rest are tolerated. The differences among species in tolerance of deleterious mutations could explain phenotypic differences among species. Specifically, Lynch proposed that the large effective population sizes of bacteria allow them to suppress non-coding sequences in genomes, such as introns, keeping the genome slim, while the bloated genomes of multi-cellular eukaryotes are evidence of reduced selection due to relatively small effective population sizes (Lynch and Walsh 2007; Lynch and Conery 2003). Differences in effective population size are also used to explain the increasing complexity of the assembly of protein-protein interactions, i.e. interactome, from bacteria to multicellular organisms (Fernández and Lynch 2011).

Revisiting mutationism

When studying evolution, early population genetics focused on changes in the frequency of alleles that are already present in the population, and generally ignored the creation of a new alleles by mutation (Yampolsky and Stoltzfus 2001). Under this doctrine, even if an allele is recurrently mutated into one with lower fitness, natural selection will prevent the fixation of the inferior allele, i.e. complete replacement of the original allele by the inferior allele, in a population (Yampolsky and Stoltzfus 2001). With saltationism being rejected during the modern synthesis, mutation was generally considered a less important factor in evolution, comparing with natural selection (Yampolsky and Stoltzfus 2001; Stoltzfus 2006).

The neutral and nearly neutral theory of evolution suggest a different conclusion. Given two neutral alleles A and a that are produced by mutation at rate u and v, respectively, because the probability of fixation is equal for A and a, the probability that A is fixed in a population is just $u / (u + v)$. According to the neutral and nearly neutral theory of evolution, most mutations have only slight fitness effects, therefore the outcomes of evolution, at least at molecular level, should depend largely on the rates of mutations. Mutation bias between nucleotides is one possible reason for the difference in genomic GC content across species (Sueoka 1988).

More recently, Yampolsky and Stoltzfus (2001) argue that, when mutation acts to create *de novo* alleles rather than converting between existing alleles, the mutation rate of beneficial mutations also matters. Older versions of the modern synthesis treat evolution as a buffet where various beneficial alleles are already present in the population and natural selection can always pick the one providing the most benefit

(Stoltzfus 2015). In contrast, *de novo* beneficial alleles are dishes on the conveyor belt in a sushi bar; those occuring at higher frequency tend to be picked up more often by natural selection (Stoltzfus 2015). Empirically, Rokyta et al. (2005) calculated the frequency of beneficial nucleotide substitutions in a viral genome, and found that the most frequent substitutions are not the most fit; instead, fitness combined with mutation rates of different nucleotides could explain the observed substitution frequencies.

Theories about constraints to evolution

While population-genetic evolutionary theories focus on quantifying changes in allele frequencies, evolutionary biologists of a different school are interested in identifying "constraints to evolution". The distinction between these two schools can be illustrated by their attitudes to mutation. Population geneticists usually care about the fitness distribution of mutations, and about mutation rates, in order to predict what alleles can evolve *de novo* and how allele frequencies change. In contrast, a central question for the other school is what factors determine the phenotypic effects and rates of mutations, thus indirectly shaping evolution. This is not claiming that population geneticists are only interested in plugging the fitness of a mutation or mutation rate into equations. In fact, inferring the fitness distribution of alleles entering into or segregating in a population is an important topic in population genetics. Fisher himself also tried to explain the distribution of fitness effects of mutations (Fisher 1932).

Organismal development is the process that produces morphology, and had long been considered a driving force of evolution since neo-Larmackism and orthogenesis (Bowler 1983). However, it was widely believed that developmental biologists were not actively involved in the discussions during the modern synthesis (Smocovitis 1992; Mayr and Provine 1981; Gilbert, Opitz, and Raff 1996; Pigliucci 2007), which might have delayed the growth of evolutionary theories that are based on development. The potential roles of development in evolution were systematically discussed in 1985. This discussion (Smith et al. 1985) proposed that developmental processes could limit the generation of novel traits, narrowing the possible outcomes of evolution. Any developmental process must obviously obey fundamental physical and chemical laws; otherwise a zebra evolving a machine gun rather than black-and-white stripes as a defense against lions (Sober 1984) would lose its absurdity. A particular developmental process could bias the fitness distribution of mutations. A mutation that makes a kangaroo better at leaping is more likely to be beneficial than a mutation that makes the animal better at running (Smith et al. 1985). Robustness of a developmental process against mutation, as a result of canalizing selection, reduces the chance of generating a novel trait.

Evolutionary theories that emphasize the role of development are now known as evo-devo (Carroll 2008; Müller 2007). Advances in technology have allowed scholars to discover that regulatory programs that underlie developmental processes are highly similar among different species, for example the Hox genes regulating the formation of body segments are conserved from invertebrates to vertebrates (Carroll 2008). Researchers are beginning to understand how morphological diversity among species is generated from the conserved regulatory programs (Carroll 2008). Students of evo-devo believe that, to make sense of evolution, "the evo-devo framework assigns much of the explanatory weight to the generative properties of development, with natural selection providing the boundary condition" (Müller 2007), and have been calling for a new synthesis focusing on evo-devo (Pigliucci 2007; Carroll 2008; Müller 2007).

Summary

I hope the previous sections have demonstrated that evolution is a complex process and both natural selection and non-adaptive factors can influence the outcome of evolution. The division between adaptationism and theories of non-adaptive evolution does not mean that evolution is generally dichotomous. Understanding evolution requires a balanced view of adaptive and non-adaptive processes. While the iterative nature of evolution makes it philosophically difficult to determine the ultimate causal factor of evolution (Sober 1984; Sansom 2003), researchers usually seek a plausible but specific explanation for the origin of a trait. In particular, many are interested in whether selection for a particular

biological effect the trait can perform leads to the evolution of the trait. In other words, the function, in terms of the "selected effect" rather than the "causal role" (Graur et al. 2013), is of interest. In response to "the spandrels of San Marco", Mayr (1983) argued that by repeatedly rejecting unreasonable hypothetical functions of a trait, the true function of the trait could be revealed, and that such practice was a tradition of science. However, the missing point, as Gould and Lewontin (1979) suggested, is that unless one of the working hypotheses also accounts for non-adaptive explanations for the origin of a trait, one can hardly escape from the adaptationism framework.

Dissertation format

The next chapter summarizes my two studies on the adaptive and non-adaptive evolution of the control of gene expression. Study one is about the evolution of quality-control mechanisms acting on gene expression. In this study, genes are expressed independently from each other. The second study addresses non-adaptive evolution of regulation of gene expression with interacting genes. Specifically, I will show how the topology of transcriptional regulatory networks (TRNs) is shaped by non-adaptive factors. The background and specific aims of each study will be introduced in the next chapter, since this chapter is devoted to introducing the concept and theories of non-adaptive evolution.

The results and conclusion of the first study have been published (Xiong et al. 2017). The study is a collaborative work with Jay McEntee, David Porfirio, and Joanna Masel. Specifically, Masel designed the computational model and wrote the manuscript (with input and editing from me), McEntee implemented an early version of the computational model, and Porfirio wrote a pipelining program to run simulations in batches. My roles were re-writing the program in Matlab to increase speed, performing all the computational simulations included in the paper, and analyzing simulation results.

For the second study, a manuscript reporting the results and conclusion is under review at *Nature Communications* for the second time in response to requested revisions (Xiong et al. 2019). The second study is a collaboration with Alex Lancaster, Mark Siegal, and Joanna Masel. Specifically, Masel and Siegal designed a highly mechanistic computational model to simulate gene expression. Masel and Lancaster wrote an early version of the developmental (but not evolutionary) portion of the code, but suspended the project before the computer program was completed. I designed and implemented methods to simulate mutations, reviewed all and updated many aspects of the developmental algorithm in light of more recent mechanistic data, designed a computationally more efficient simulation of transcription factor (TF) binding, and parallelized the program. Even with the substantial computational resources available through High Performance Computing at the University of Arizona, these last two revisions were essential in order to complete all the simulations. I then chose the topic of type 1 coherent feed-forward loops (defined in Chapter 2), designed experiments to study their origin, performed the computational simulations, analyzed the results, and wrote a first draft of the manuscript. Masel then rewrote the final manuscript with input and editing from me.

Present Study

The methods, results, and conclusions of this study are presented in the papers appended to this dissertation. The following is a summary of the most important findings of these papers.

Evolution of mechanisms for the quality control of gene expression

The drift barrier theory proposes that certain differences in traits among species can be explained by the different effective population sizes of the species. A recent study shows that mutation rates of different species tend to increase as the population sizes of the species decrease (Lynch 2010). To explain this trend, Lynch (2010) proposed that because mutations tend to break the delicate DNA machinery, error rate in DNA duplication should increase when the counter-effect of natural selection is absent. When natural selection pushes back against this mutational bias, it can eliminate more mutations that damage the DNA machinery in large populations, where selection is strong, than in small ones, where selection is weak (Lynch 2010).

Similar to DNA replication, the expression of genes is also an error-prone process. Erroneous gene expression, for example mis-transcription, can turn a normal product into a harmful erroneous product. Reducing either the error rate of gene expression, or the damage per erroneous product, can avoid or mitigate the loss in fitness caused by erroneous gene expression. Evolving towards perfecting one solution can reduce the need to perfect the other. Given that mutations tend to reduce the accuracy of molecular machineries in gene expression, and to reduce the robustness of genes that to incorrect expression, the less needed solution should be eroded by mutation. Between the two solutions, which one is expected in species with large effective population sizes, and in species with small effective population sizes?

A simple way to reduce an error rate is to improve the accuracy of the molecular machinery of gene expression. Because such an improvement reduces the error rate in the expression of potentially all genes, we call it a global solution. The amount of erroneous product can also be reduced through actively degrading or converting abnormal product to normal product, e.g. using chaperones to help defective proteins fold, which can handle expression errors from multiple genes and hence is also a global solution. In contrast, mutation to a single gene can create a mutant that not only maintains the wild-type function, but is also robust to being expressed improperly. An example is a mutation that creates a backup stop codon right after the normal stop codon of a gene. When ribosomes read through the first stop codon, the backup stop codon can terminate translation and limit damage to the protein. Because such a mutation is gene-specific, we call it a local solution.

From the perspective of each solution's cost, reducing error rates in gene expression can be subject to the "speed vs. accuracy" tradeoff, and so comes at the price of energy, material, and/or other opportunity. On the other hand, the local solution is free or nearly free.

To quantitatively study the evolution of the two strategies, Rajon and Masel (2011) developed a mathematical model based on stop codon read-through during translation. Their model assumes that the expression of a gene produces normal protein in the absence of an error, and abnormal protein that carries an extra sequence in the presence of a translational read-through error. The extra sequence in the

abnormal protein, which they call the cryptic sequence, is gene-specific, and determines whether the abnormal protein is neutral in fitness or harmful. Rajon and Masel assume that the reduction in fitness due to translational read-through is proportional to the amount of harmful abnormal proteins produced from all genes. They simulate evolution, allowing mutations to convert a harmful cryptic sequence to neutral, and to reduce the read-through rate at the price of reducing fitness.

A key assumption of Rajon and Masel's model is that all genes have the same expression level. Because the rate of translational read-through is also the same for all genes in the model, each gene produces the same amount of abnormal proteins. This essentially makes every gene that carries a harmful cryptic sequence equally dangerous, which is biologically unrealistic. I expanded their model to allow expression level to vary among genes. When carrying harmful cryptic sequences, highly-expressed genes do more damage than lowly-expressed genes, following translational read-through. For simplicity, I did not consider other factors that can also determine the magnitude of damage of reading through a gene that carries a harmful cryptic sequence, for example, the essentiality of a gene. Nevertheless, making the magnitude of damage proportional to gene expression level captures a variance of the magnitude of damage among genes. The value of the variance can be changed to reflect a magnitude of damage that also depends on other gene-specific factors.

I found that large populations always evolve the local solution. Even after starting with a low read-through rate and a harmful cryptic sequence in every gene, large populations evolve a high read-through rate and neutral cryptic sequences in nearly all genes. Small populations always invest in the global solution, evolving a low read-through rate and tolerating harmful cryptic sequences in most genes. This is expected under the drift barrier theory: because mutation tends to produce harmful cryptic sequences, only large populations have strong enough selection to purge harmful cryptic sequences in most genes, saving the need for a costly global solution. While these results agree with Rajon and Masel (2011), the behavior of intermediate populations differs between the two studies. In Rajon and Masel, intermediate populations can evolve either solution, evolving toward whichever solution they start near. However, in the expanded model, fewer intermediate populations maintain this bistability in evolution, as the variance in expression levels among genes increases. When the variance of expression levels among genes is equal to that in yeast, all intermediate populations evolve intermediate read-through rates and intermediate numbers of genes that carry harmful cryptic sequences.

The expanded model also shows that the local solution tends to evolve in highly-expressed genes, even in a small population where the global solution is preferred. This suggests that the quality-control mechanisms acting on gene expression can vary depending on the expression level of a gene. Analyzing the frequency of mis-incorporated nucleotides in the transcriptome is a way to test this prediction, and I am a coauthor on a submitted manuscript that agrees with this prediction (Meer et al. 2019).

I also expanded the model to include the bias that mutations are more likely to increase rather than decrease the read-through rate. With this bias, I found a non-monotonic relation between the error rate and population size: while the error rate increases from small to large populations, it also increases as small populations keep shrinking. Extremely small populations do not have strong enough selection to overcome the mutational bias that favor an increase in read-through rate – although the genome of these populations are full of harmful cryptic sequences. A recent study shows that both the large-population *E. coli* and the small-population endosymbiont bacteria, *Buchnera*, have similarly high transcriptional error rate (Traverse and Ochman 2016), while medium-population *S. cerevisiae* and *C. elegans* have

intermediate transcriptional error rate (Gout et al. 2017). Our result provides an explanation to this non-monotonic relationship between transcriptional error rate and population size.

Evolution of transcriptional regulatory networks

Two genes can interact with each other through transcriptional regulation in which gene A encodes a TF that regulates the expression of gene B. Transcriptional regulatory interactions among genes are often depicted as transcriptional regulatory networks (TRNs), and there have been many efforts to infer the functions of natural TRNs (Alon 2007). A popular hypothesis is that the topology of natural TRNs reflects adaptations for functions in terms of performing particular dynamics of gene expression. For example, when compared with randomized networks, natural TRNs are enriched in certain sub-networks, commonly known as network motifs (Alon 2007). Theoretical analysis and experiments show that network motifs can generate special dynamics of gene expression, supporting the adaptive origin of network motifs.

Many evolutionary biologists are unconvinced by the adaptive origin of network motifs (Lynch 2007; Sole and Valverde 2006; Wagner 2003; Artzy-Randrup et al. 2004). The turnover of individual genes changes the topology of TRNs differently than the turnover of individual regulatory interactions between genes, therefore natural bias between the rates of gene duplication/deletion and that of mutation to TF binding sites has the potential to promote network motifs. The hypothesis that network motifs evolve adaptively needs to be tested against a null that accounts for the non-adaptive evolution of TRNs.

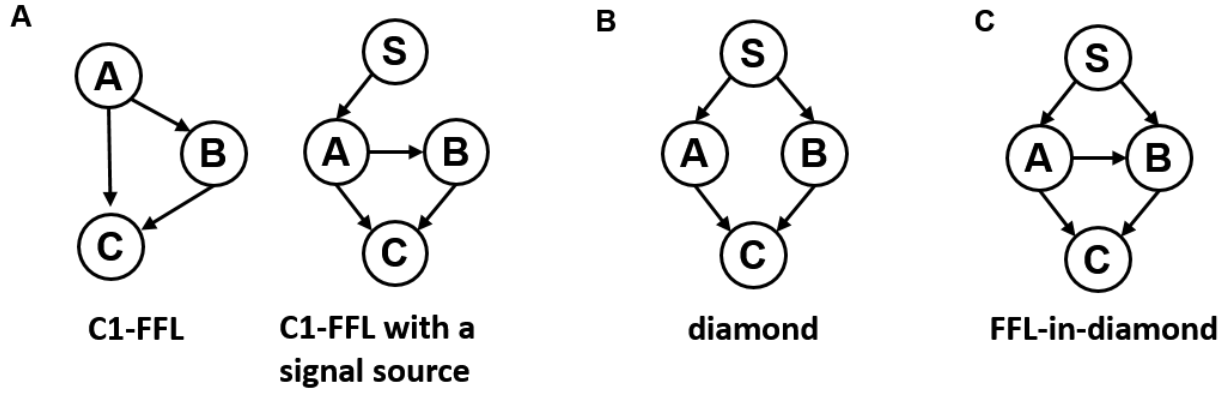

Figure 1. Network motifs involved in the study. (A) Left is a C1-FFL by itself; right is a C1-FFL with the master TF A regulated by a signal. **(B)** In a diamond, the signal induces the expression of two TFs, A and B, which then activate the expression of C. We found that in AND-gated diamonds that evolved for filtering out a short spurious signal caused by environmental fluctuations, A and B differ in the speed of gene expression. **(C)** FFL-in-diamonds can evolve non-adaptively from C1-FFLs and from diamonds.

My study focus on a network motif called type 1 coherent feed-forward loops (C1-FFLs). A C1-FFL is formed when gene A encodes a TF that can bind to a TF gene B and activate the expression of the latter, but TF B cannot bind to gene A, and both TF A and TF B can bind to a third gene C and activate C's expression (**Fig. 1A**). It has been shown that AND-gated C1-FFLs, in which both A and B need to be present to induce the expression of C, can act to filter out short spurious signals. The enrichment of C1-FFLs in natural TRNs is therefore widely believed by non-evolutionary biologists to be an adaptation for

filtering out short spurious signals that arise due to environmental fluctuations (Mangan, Zaslaver, and Alon 2003).

I developed a sophisticated computational model to simulate the evolution of TRNs under different selection conditions. The model has sufficient mechanistic details so that many biological processes, such as the turnover of individual genes and TF binding sites, can be parameterized directly from experimental data, minimizing the need to guess parameter values. Because we are also curious about whether C1-FFLs evolve due to the demand for filtering out intrinsic noise in gene expression, as opposed to filtering out short spurious signals induced by environmental fluctuations, I also simulate gene expression stochastically to capture random "bursts" of transcription.

I evolved TRNs under selection for filtering out a short spurious signal versus under control selection conditions, and found that functional AND-gated C1-FFLs readily evolve in the former condition but not in the latter. This supports the adaptive origin of AND-gated C1-FFLs in TRNs.

I also found that AND-gated "diamonds" (**Fig. 1B**) evolve as an alternative spurious signal filter. Although diamonds are a known network motif, it was not previously known that they can act as a spurious signal filter. While AND-gated C1-FFLs rely on a short and a long pathway to filtering the spurious signal, AND-gated diamonds rely on the different speeds of gene expression in the two topologically identical pathways (**Fig. 1B**). This agrees with previous findings that the topology of TRNs alone is insufficient to determine the functions of TRNs. AND-gated diamonds can also filter out intrinsic noise in gene expression, while AND-gated C1-FFLs fail to do so, suggesting that intrinsic noise in gene expression can shape the evolution of TRNs.

A third important finding is that non-adaptive network motifs can evolve from adaptive network motifs. Because the binding sequence of a TF is not long, low affinity TF binding sites that are slightly different from the ideal binding sequence arise easily during evolution, adding non-adaptive regulatory interaction to adaptive network motifs (**Fig. 1C**). Because non-adaptive network motifs that evolve in this way can reach high frequency, the enrichment of a network motif in TRNs is not a reliable sign of the adaptive origin of the network motif.

Conclusion

Quality-control mechanisms for gene expression and TRNs represent regulation of the expression of individual genes and of regulatory interactions among genes, respectively. My studies show that the evolution of quality-control mechanisms and of TRNs involve both adaptive and non-adaptive processes. While one research theme in the field of molecular and cellular biology is to clarify the function of various processes that regulate gene expression, non-adaptive processes need to be accounted in order to properly understand the origin and working modes of the regulation of gene expression.

When a trait is hard to explain from the perspective of adaptation, non-adaptive evolution can provide the needed explanation. This is demonstrated by the high transcriptional error rates in the endosymbiotic bacteria, *Buchnera*, which apparently lack a mechanism to reduce the harm from incorporating incorrect nucleotides into mRNAs. It is possible that the high transcriptional error rate in *Buchnera* is mitigated by other mechanisms and/or is even beneficial, but evidence supporting these hypotheses has yet to be discovered. My study notes that mutation tends to degrade the fidelity of the molecular machinery of

transcription, increasing the error rate of transcription. According to theories in population genetics, small populations like *Buchnera* should have very ineffective selection to maintain a beneficial trait, therefore the high transcriptional error rate in *Buchnera* can be the result of mutational bias that overwhelms selection for a low error rate. This is not claiming selection has no role in the evolution of the transcriptional error rate in *Buchnera*; without selection, the transcriptional error rate could be even higher than what is observed.

When there is an apparent adaptive explanation for the origin of a trait, there is often strong resistance against considering an alternative non-adaptive origin -- the topology of TRNs is such a trait. I argue that, in this case, considering non-adaptive evolution is necessary to carrying out careful scientific research. Because it is not independently possible to prove either the adaptive or non-adaptive origin of network motifs, the predictions from the two theories must be tested against each other. By showing that AND-gated C1-FFLs evolve less often when there is no need for filtering out a short spurious signal than when the filter is needed, my study strengthens the hypothesis of the adaptive origin of AND-gated C1-FFLs. While this finding may not surprise adherents to the adaptive origin theory of network motifs, it doesn't mean that similar tests on other network motifs will produce equally unsurprising results. In fact, my simulation does point out that non-adaptive network motifs can evolve easily from adaptive network motifs.

A working hypothesis that balances adaptive and non-adaptive evolution is desired, but it can be difficult to build. The portion of the hypothesis that is about adaptive evolution is usually specific, e.g. trait *X* is an optimized solution for a particular biological problem *Y*, under condition *Z*. However, building the non-adaptive portion of the hypothesis can be tricky because numerous factors could potentially promote the evolution of trait *X*, regardless of selection for solutions to biological problem *Y*. The two computational models in my thesis suggests that considering bias in mutation rates can often reveal non-adaptive traits in evolution.

References

Alon, Uri. 2007. “An Introduction to Systems Biology: Design Principles of Biological Circuits.” *Chapman HallCRC Mathematical and Computational Biology Series*. https://doi.org/citeulike-article-id:1314150.

Artzy-Randrup, Yael, Sarel J Fleishman, Nir Ben-Tal, and Lewi Stone. 2004. “Comment on" Network Motifs: Simple Building Blocks of Complex Networks" and" Superfamilies of Evolved and Designed Networks".” *Science* 305 (5687): 1107.

Bowler, Peter J. 1983. *The Eclipse of Darwinism: Anti-Darwinian Evolution Theories in the Decades Around*. 1st ed. Baltimore: The John Hopkins University Press.

Carroll, Sean B. 2008. “Evo-Devo and an Expanding Evolutionary Synthesis: A Genetic Theory of Morphological Evolution.” *Cell* 134 (1): 25–36. https://doi.org/10.1016/J.CELL.2008.06.030.

Darwin, Charles. 1858. *On the Origin of Species*. Edited by Gillian Beer. New York, NY: Oxford University Press.

———. 1894. *The Variation of Animals and Plants under Domestication*. Vol. 2. D. Appleton.

Fernández, Ariel, and Michael Lynch. 2011. “Non-Adaptive Origins of Interactome Complexity.” *Nature* 474 (7352): 502–5. https://doi.org/10.1038/nature09992.

Fisher, Ronald Aylmer. 1932. *The Genetical Theory of Natural Selection: A Complete Variorum Edition*. Edited by J. H. Bennett. Oxford University Press.

Gilbert, Scott F, John M Opitz, and Rudolf A Raff. 1996. “REVIEW Resynthesizing Evolutionary and Developmental Biology.” *DEVELOPMENTAL BIOLOGY*. Vol. 173. https://ac.els-cdn.com/S0012160696900329/1-s2.0-S0012160696900329-main.pdf?_tid=46ff42ca-e37d-42d4-8285-b9e2952ba473&acdnat=1552500005_b7de7efa8e2b65ddc77c279800fd2531.

Gould, Stephen Jay. 1983. “The Hardening of the Modern Synthesis.” In *Dimensions of Darwinism: Themes and Counterthemes in Twentieth-Century Evolutionary Theory*, edited by Marjorie Grene, 71–93. New York, NY: Cambridge University Press.

Gould, Stephen Jay, and R. C. Lewontin. 1979. “The Spandrels of San Marco and the Panglossian Paradigm: A Critique of the Adaptationist Programme.” *Proceedings of the Royal Society of London. Series B, Containing Papers of a Biological Character. Royal Society (Great Britain)* 205 (1161): 581–98. https://doi.org/10.1098/rspb.1979.0086.

Gout, Jean-Francois, Weiyi Li, Clark Fritsch, Annie Li, Suraiya Haroon, Larry Singh, Ding Hua, et al. 2017. “The Landscape of Transcription Errors in Eukaryotic Cells.” *Science Advances* 3 (10): e1701484.

Graur, Dan, Yichen Zheng, Nicholas Price, Ricardo B R Azevedo, Rebecca a. Zufall, and Eran Elhaik. 2013. “On the Immortality of Television Sets: ‘Function’ in the Human Genome According to the Evolution-Free Gospel of Encode.” *Genome Biology and Evolution* 5 (3): 578–90. https://doi.org/10.1093/gbe/evt028.

Haldane, J.B.S. 1957. “THE COST OF NATURAL SELECTION.” *Journal of Genetics* 55 (3): 511. https://link.springer.com/content/pdf/10.1007%2FBF02984069.pdf.

Huxley, Julian. 1942. *Evolution: The Modern Synthesis*. 3rd ed. London: Allen & Unwin.

Kimura, M. 1968. “Evolutionary Rate at the Molecular Level.” *Nature* 217: 624–26. https://doi.org/10.1038/222385a0.

Laird, Charles D., Betty L. McConaughy, and Brian J. McCarthy. 1969. “Rate of Fixation of Nucleotide Substitutions in Evolution.” *Nature* 224 (5215): 149–54. https://doi.org/10.1038/224149a0.

Lynch, Michael. 2007. “The Evolution of Genetic Networks by Non-Adaptive Processes.” *Nature Reviews. Genetics* 8 (10): 803–13. https://doi.org/10.1038/nrg2192.

———. 2010. “Evolution of the Mutation Rate.” *Trends in Genetics* 26 (8): 345–52. https://doi.org/10.1016/j.tig.2010.05.003.

Lynch, Michael, and John S Conery. 2003. “The Origins of Genome Complexity.” *Science (New York, N.Y.)* 302 (5649): 1401–4. https://doi.org/10.1126/science.1089370.

Lynch, Michael, and Bruce Walsh. 2007. *The Origins of Genome Architecture*. Vol. 98. Sinauer Associates Sunderland (MA).

Mangan, S., a. Zaslaver, and U. Alon. 2003. "The Coherent Feedforward Loop Serves as a Sign-Sensitive Delay Element in Transcription Networks." *Journal of Molecular Biology* 334 (2): 197–204. https://doi.org/10.1016/j.jmb.2003.09.049.

Mayr, Ernst. 1983. "How to Carry Out the Adaptationist Program?" *The American Naturalist* 121 (3): 324–34. https://doi.org/10.1086/284064.

———. 1993. "What Was the Evolutionary Synthesis?" *Trends in Ecology and Evolution* 8 (1): 31–34. https://doi.org/10.1016/0169-5347(93)90128-C.

Mayr, Ernst, and William Provine. 1981. "The Evolutionary Synthesis." *Bulletin of the American Academy of Arts and Sciences*. https://doi.org/10.1126/science.286.5444.1490.

Meer, Kendra M, Paul G Nelson, Kun Xiong, and Joanna Masel. 2019. "Transcriptional Error Rates Vary by Gene Expression Level in E. Coli but Not S. Cerevisiae." *BioRxiv*, 554329.

Müller, Gerd B. 2007. "Evo--Devo: Extending the Evolutionary Synthesis." *Nature Reviews Genetics* 8 (12): 943.

Nei, Masatoshi, Yoshihito Niimura, and Masafumi Nozawa. 2008. "The Evolution of Animal Chemosensory Receptor Gene Repertoires: Roles of Chance and Necessity." *Nature Reviews. Genetics* 9 (12): 951–63. https://doi.org/10.1038/nrg2480.

Ohta, Tomoko. 1973. "Slightly Deleterious Mutant Substitutions in Evolution." *Nature* 246 (5428): 96–98. https://doi.org/10.1038/246096a0.

Ohta, Tomoko, and John H. Gillespie. 1996. "Development of Neutral and Nearly Neutral Theories." *Theoretical Population Biology* 49 (2): 128–42. https://doi.org/10.1006/TPBI.1996.0007.

Ohta, Tomoko, and Motoo Kimura. 1971. "On the Constancy of the Evolutionary Rate of Cistrons." *Journal of Molecular Evolution* 1 (1): 18–25. https://doi.org/10.1007/BF01659391.

Pigliucci, Massimo. 2007. "Do We Need an Extended Evolutionary Synthesis?" *Evolution* 61 (12): 2743–49. https://doi.org/10.1111/j.1558-5646.2007.00246.x.

Provine, William B. 1978. "The Role of Mathematical Population Geneticists in the Evolutionary Synthesis of the 1930s and 1940s." *Studies in History of Biology* 2: 167–92.

———. 1988. "Progress in Evolution and Meaning in Life." In *Evolutionary Progress*, edited by Matthew H. Nitecki, 49–74. Chicago: University of Chicago Press.

Rajon, Etienne, and Joanna Masel. 2011. "Evolution of Molecular Error Rates and the Consequences for Evolvability." *Proceedings of the National Academy of Sciences of the United States of America* 108 (3): 1082–87. https://doi.org/10.1073/pnas.1012918108.

Rokyta, Darin R, Paul Joyce, S Brian Caudle, and Holly A Wichman. 2005. "An Empirical Test of the Mutational Landscape Model of Adaptation Using a Single-Stranded DNA Virus." *Nature Genetics* 37 (4): 441–44. https://doi.org/10.1038/ng1535.

Sansom, Roger. 2003. "Constraining the Adaptationism Debate." *Biology and Philosophy*. Vol. 18. https://link.springer.com/content/pdf/10.1023%2FA%3A1025581622161.pdf.

Simpson, George Gaylord. 1944. *Tempo and Mode in Evolution*. New York, NY: Columbia University Press.

Smith, J. Maynard, R. Burian, S. Kauffman, P. Alberch, J. Campbell, B. Goodwin, R. Lande, D. Raup, and L. Wolpert. 1985. "Developmental Constraints and Evolution: A Perspective from the Mountain Lake Conference on Development and Evolution." *The Quarterly Review of Biology* 60 (3): 265–87. https://doi.org/10.1086/414425.

Smocovitis, V. B. 1992. "Unifying Biology : The Evolutionary Synthesis and Evolutionary Biology." *Journal of the History of Biology* 25 (1): 1–65. https://link.springer.com/content/pdf/10.1007%2FBF01947504.pdf.

Sober, Elliott. 1984. *The Nature of Selection: Evolutionary Theory in Philosophical Focus*. The MIT Press.

Sole, Ricard, and Sergi Valverde. 2006. "Are Network Motifs the Spandrels of Cellular Complexity?" *Trends in Ecology & Evolution* 21 (8): 419–22. https://doi.org/10.1016/j.tree.2006.05.013.

Stoltzfus, Arlin. 2006. “Mutationism and the Dual Causation of Evolutionary Change.” *Evolution and Development*. Wiley/Blackwell (10.1111). https://doi.org/10.1111/j.1525-142X.2006.00101.x.

———. 2015. “The Buffet and the Sushi Conveyor.” 2015. http://www.molevol.org/the-buffet-and-the-sushi-conveyor/.

Sueoka, N. 1988. “Directional Mutation Pressure and Neutral Molecular Evolution.” *Proceedings of the National Academy of Sciences of the United States of America* 85 (8): 2653–57. https://doi.org/10.1073/PNAS.85.8.2653.

Traverse, Charles C., and Howard Ochman. 2016. “Conserved Rates and Patterns of Transcription Errors across Bacterial Growth States and Lifestyles.” *Proceedings of the National Academy of Sciences*, 201525329. https://doi.org/10.1073/pnas.1525329113.

Trut, Lyudmíla, Irina Oskina, and Anastasiya Kharlamova. 2009. “Animal Evolution during Domestication: The Domesticated Fox as a Model.” *BioEssays*. https://doi.org/10.1002/bies.200800070.

Wagner, Andreas. 2003. “Does Selection Mold Molecular Networks?” *Sci. STKE* 2003 (202): pe41--pe41.

Wright, Sewall. 1931. “Evolution in Mendelian Populations.” *Genetics* 16 (2): 97.

Xiong, Kun, Alexander K Lancaster, Mark L Siegal, and Joanna Masel. 2019. “Feed-Forward Regulation Adaptively Evolves via Dynamics Rather than Topology When There Is Intrinsic Noise.” *BioRxiv*, 393884.

Xiong, Kun, Jay P. McEntee, David J. Porfirio, and Joanna Masel. 2017. “Drift Barriers to Quality Control When Genes Are Expressed at Different Levels.” *Genetics* 205 (1): 397–407.

Yampolsky, Lev Y., and Arlin Stoltzfus. 2001. “Bias in the Introduction of Variation as an Orienting Factor in Evolution.” *Evolution and Development* 3 (2): 73–83. https://doi.org/10.1046/j.1525-142x.2001.003002073.x.

Appendix A -- Drift barriers to quality control when genes are expressed at different levels

Genetics Society of America

Founded in 1931, the Genetics Society of America (GSA) is the professional membership organization for scientific researchers, educators, bioengineers, bioinformaticians, and others interested in the field of genetics. Its nearly 5,000 members work to advance knowledge in the basic mechanisms of inheritance, from the molecular to the population level. The GSA is dedicated to promoting research in genetics and to facilitating communication among geneticists worldwide through its conferences, including the biennial conference on Model Organisms to Human Biology, an interdisciplinary meeting on current and cutting-edge topics in genetics research, as well as annual and biennial meetings that focus on the genetics of particular organisms, including *Caenorhabditis elegans, Drosophila*, fungi, mice, yeast, and zebrafish. GSA publishes *GENETICS*, a leading journal in the field, and an online, open-access journal, *G3: Genes|Genomes|Genetics*. For more information about GSA, please visit www.genetics-gsa.org. Also follow GSA on Facebook at facebook.com/GeneticsGSA and on Twitter @GeneticsGSA.

GENETICS (ISSN 0016-6731) is published monthly by the Genetics Society of America, 9650 Rockville Pike, Bethesda, Maryland 20814-3998. For pricing, consortia sales, or a multi-site quotation, please contact Tracey DePellegrin, Executive Editor, at tracey.depellegrin@thegsajournals.org or 412-226-5930.

Correspondence about membership, nonmember subscriptions, and other nonedito-rial matters should be directed to the appropriate address below, according to whether the inquirer is (or would be) a GSA member or institutional or nonmember subscriber.

GSA MEMBERS ONLY:
GSA Administrative Office
9650 Rockville Pike
Bethesda, MD 20814-3998
301-634-7300

INSTITUTIONAL AND NONMEMBER SUBSCRIPTIONS:
Genetics Subscription Office
P.O. Box 11127
Birmingham, AL 35202
Phone: 1-800-633-4931
(205-995-1567 outside the US and Canada)

Back issues of *GENETICS* from 1992 (Volume 130) through 2009 (Volume 183) can be obtained through the nonmember subscriber address above. *GENETICS* is also available in microform from University Microfilms International, 300 North Zeeb Road, Ann Arbor, Michigan 48106; European inquiries may be directed to 30-32 Mortimer Street, Dept. PR, London, W1N 7RA, England.

Produced by Sheridan Journal Services.

Copyright Clearance Center

Confirmation Number: 11800068
Order Date: 03/19/2019

Customer Information

Customer: Kun Xiong
Account Number: 3001422901
Organization: Kun Xiong
Email: xiongkungy@gmail.com
Phone: +1 (520) 245-5935
Payment Method: Invoice

This is not an invoice

Order Details

Genetics

Billing Status: **N/A**

Order detail ID:	71855668
ISSN:	1943-2631
Publication Type:	e-Journal
Volume:	
Issue:	
Start page:	
Publisher:	Genetics Society of America
Author/Editor:	Genetics Society of America

Permission Status: Granted
Permission type: Republish or display content
Type of use: Republish in a thesis/dissertation
Order License Id: 4552690254978

Requestor type	Author of requested content
Format	Electronic
Portion	chapter/article
The requesting person/organization	Kun Xiong
Title or numeric reference of the portion(s)	Drift Barriers to Quality Control When Genes Are Expressed at Different Levels
Title of the article or chapter the portion is from	N/A
Editor of portion(s)	N/A
Author of portion(s)	Kun Xiong, Jay P. McEntee, David J. Porfirio, Joanna Masel
Volume of serial or monograph	205
Issue, if republishing an article from a serial	1
Page range of portion	
Publication date of portion	1/1/2017
Rights for	Main product and any product related to main product
Duration of use	Current edition and up to 5 years
Creation of copies for the disabled	no
With minor editing privileges	no
For distribution to	Worldwide
In the following language(s)	Original language of publication
	no

With incidental promotional use	
Lifetime unit quantity of new product	Up to 499
Title	Adaptive and non-adaptive evolution of the control of gene expression
Institution name	University of Arizona
Expected presentation date	Apr 2019

Note: This item was invoiced separately through our **RightsLink service.** More info **$ 0.00**

Total order items: 1 **Order Total: $0.00**

Drift Barriers to Quality Control When Genes Are Expressed at Different Levels

Kun Xiong,* Jay P. McEntee,† David J. Porfirio,‡ and Joanna Masel†,1

*Department of Molecular and Cellular Biology, †Department of Ecology & Evolutionary Biology, and ‡Department of Computer Science, University of Arizona, Tucson, Arizona 85721

ORCID IDs: 0000-0003-1431-6586 (K.X.); 0000-0002-1213-9734 (J.P.M.); 0000-0001-5383-3266 (D.J.P.); 0000-0002-7398-2127 (J.M.)

ABSTRACT Gene expression is imperfect, sometimes leading to toxic products. Solutions take two forms: globally reducing error rates, or ensuring that the consequences of erroneous expression are relatively harmless. The latter is optimal, but because it must evolve independently at so many loci, it is subject to a stringent "drift barrier"—a limit to how weak the effects of a deleterious mutation s can be, while still being effectively purged by selection, expressed in terms of the population size N of an idealized population such that purging requires $s < -1/N$. In previous work, only large populations evolved the optimal local solution, small populations instead evolved globally low error rates, and intermediate populations were bistable, with either solution possible. Here, we take into consideration the fact that the effectiveness of purging varies among loci, because of variation in gene expression level, and variation in the intrinsic vulnerabilities of different gene products to error. The previously found dichotomy between the two kinds of solution breaks down, replaced by a gradual transition as a function of population size. In the extreme case of a small enough population, selection fails to maintain even the global solution against deleterious mutations, explaining the nonmonotonic relationship between effective population size and transcriptional error rate that was recently observed in experiments on *Escherichia coli*, *Caenorhabditis elegans*, and *Buchnera aphidicola*.

KEYWORDS cryptic genetic variation; stop codon readthrough; robustness; evolvability; transcriptional errors; proofreading

IN classical population genetic models of idealized populations, the probability of fixation of a new mutant depends sharply on the product of the selection coefficient, s, and the population size, N. As s falls below $-1/N$, fixation probabilities drop exponentially, corresponding to efficient selective purging of deleterious mutations. For $s > -1/N$, random genetic drift makes the fate of new mutants less certain. This nonlinear dependence of fixation probability on sN has given rise to the "drift barrier" hypothesis (Lynch 2007), which holds that populations are characterized by a threshold or "barrier" value of the selection coefficient, s, corresponding to the tipping point at which the removal of deleterious mutations switches between effective and ineffective. In idealized populations, described by Wright-Fisher or Moran models, the drift barrier is positioned at $s = \sim -1/N$. Drift barriers also exist, albeit sometimes with less abrupt threshold behavior, in more complex models of evolution in which some assumptions of an idealized population are relaxed (Good and Desai 2014).

The drift barrier theory argues that variation among species in their characteristic threshold values for s, thresholds that are equal by definition to the inverse of the selection effective population size, N_e, can explain why different species have different characteristics, *e.g.*, streamlined *vs.* bloated genomes (Lynch 2007). The simplest interpretation of the drift barrier would seem to imply that large-N_e species show stricter quality control over all biological processes, *e.g.*, higher fidelity in DNA replication, transcription, and translation, than small-N_e species, because molecular defects in quality control mechanisms are less effectively purged in the latter (Lynch 2010; Traverse and Ochman 2016a).

However, the data reveal more complex patterns. Unsurprisingly, *Buchnera aphidicola*, which has exceptionally low N_e (Mira and Moran 2002; Rispe *et al.* 2004), has a higher transcriptional error rate, at 4.67×10^{-5} (Traverse and Ochman 2016b), than the error rate 4.1×10^{-6} previously

doi: 10.1534/genetics.116.192567
Manuscript received June 11, 2016; accepted for publication November 2, 2016; published Early Online November 11, 2016.
Supplemental material is available online at www.genetics.org/lookup/suppl/doi:10.1534/genetics.116.192567/-/DC1.
[1]Corresponding author: Department of Ecology and Evolutionary Biology, University of Arizona, 1041 E. Lowell St., Tucson, AZ 85721. E-mail: masel@emailarizona.edu

reported for *Caenorhabditis elegans* (Gout *et al.* 2013). But, to the surprise of the authors, the error rate in large-N_e *Escherichia coli* is highest of all, at 8.23×10^{-5} (Traverse and Ochman 2016b).

A more refined drift barrier theory can explain these findings. As the fitness burden accumulates from the slightly deleterious mutations that a small-N_e species cannot purge, some forms of quality control may evolve as a second line of defense. The ideal solution is to purge all deleterious mutations, even those of tiny effect; when this first line of defense fails, the second line of defense is to ameliorate the cumulative phenotypic consequences of the deleterious mutations that have accumulated (Frank 2007; Rajon and Masel 2011; Warnecke and Hurst 2011; Lynch 2012; Wu and Hurst 2015). The first line of defense bears no fitness cost (purging is free), but faces a stringent drift barrier; the second line of defense also solves the problem but at a cost. In some circumstances, as described further below, strict quality control can act as a second-line amelioration strategy (Rajon and Masel 2011). The existence of two distinct lines of defense complicates the naive drift barrier logic that large-N_e species should generally exhibit stricter quality control in all molecular processes. The superior performance of large-N_e species in a primary line of defense other than quality control may remove any advantage of strict and costly quality control as a secondary line of defense. This creates a seemingly counter-intuitive pattern in quality control, in which small-N_e species can evolve more faithful processes than large-N_e species such as *E. coli*.

The existence of two substantively different strategies was first proposed by Krakauer and Plotkin (2002), who contrasted "redundancy" (robustness to the consequences of mutational errors) with "antiredundancy" (hypersensitivity to mutations). By positing that the redundancy strategy is costly, they find that only small-N_e species suffer from a large enough drift load (Kimura *et al.* 1963) to make this cost, and hence redundancy, worthwhile. Large N_e species not burdened by drift load are able to adopt the alternative antiredundancy strategy, which bears no cost, and hence allows the population to achieve higher fitness.

A related argument was made by Rajon and Masel (2011) in the context of mitigating the harms threatened by errors in molecular processes such as translation. Rajon and Masel (2011) distinguished between "local" solutions, where a separate solution is required at each locus, and "global" solutions that can deal with problems at many loci simultaneously. The evolution of extensive quality control mechanisms was deemed a global solution because a single mutation impacting general quality control mechanisms can affect the prevention of gene expression errors at many loci. Note that quality control includes not only mechanisms such as proofreading for preventing errors from happening in the first place, but also mechanisms that reduce downstream damage from errors, *e.g.*, degradation of mRNA molecules that seem faulty. Global quality control should come with a cost in time or energy.

Rajon and Masel's (2011) alternative, local solution is to have a benign rather than a strongly deleterious "cryptic genetic sequence" at each locus at which expression errors might occur, making the consequence of an error at that locus relatively harmless. In contrast to the global solution, these local solutions bear no direct fitness cost, but because selection at any one locus is weak, they are more difficult to maintain than global solutions. The local solution corresponds to a low number of mutations, k, in Krakauer and Plotkin (2002).

Both the quality control of Rajon and Masel (2011) and the redundancy of Krakauer and Plotkin (2002) to the consequences of mutations are global across loci, and also costly. Meantime, both the local solutions of Rajon and Masel (2011) and the reduction in the number of mutations, k, that accompanies the antiredundancy of Krakauer and Plotkin (2002) carry no true fitness cost, but instead require a large-N_e drift barrier as a limit to their adaptation. A mutation disrupting a solution specific to a single locus requires a large value of N_e for its purging, whereas a mutation disrupting a global quality control mechanism will have large fitness consequences and so be easier to purge. As a consequence, only large N_e populations evolve the higher-fitness local solution, while it is the small N_e populations that evolve global solutions such as extensive (and costly) quality control.

Selection to achieve the local solution by purging deleterious mutations to cryptic sequences (leaving in place genotypes whose cryptic genetic sequences are benign) may be difficult and hence restricted to high-N_e populations. There are, however, reasons to believe that it is not impossible. For example, when the error in question is reading through a stop codon, the local cryptic genetic sequence is the 3′UTR, which is read by the ribosome. One option for a more benign form of this cryptic sequence is the presence of a "backup" stop codon that provides the ribosome with a second and relatively early chance to terminate translation. Such backup stops are common at the first position past the stop in prokaryotes (Nichols 1970). In *Saccharomyces cerevisiae*, there is also an abundance of stop codons at the third codon position past the stop (Williams *et al.* 2004). Moreover, conservation at this position depends strongly on whether or not the codon is a stop, and the overrepresentation of stops at this position is greater in more highly expressed genes (Liang *et al.* 2005). In some ciliates, where the genetic code has been reassigned, so that UAA and UAG correspond to glutamine, this overrepresentation is much more pronounced (Adachi and Cavalcanti 2009). As with the consequences of erroneous readthrough, selective pressure on erroneous amino acid misincorporation and/or misfolding (Drummond and Wilke 2008), and on erroneous protein–protein interactions (Brettner and Masel 2012), are also strong enough to shape protein expression and interaction patterns. In the case of transcriptional errors, while both *E. coli* and *B. aphidicola* have high error rates, only *E. coli* shows signs of having evolved a first line of defense in the form of a decreased frequency, with which observed transcriptional errors translate into nonsynonymous changes relative to randomly sampled transcriptional errors (Traverse and Ochman 2016a).

Rajon and Masel (2011) found that, for intermediate values of N_e that correspond strikingly well to many multicellular species of interest, the evolutionary dynamics of the system were bistable, with either the global or the local solution possible. This is a natural consequence of a positive feedback loop; in the presence of a strict global quality control mechanism, specialized solutions at particular loci are unnecessary, and mutations destroying them pass through the drift barrier (we use the expression "pass through the drift barrier" to mean that $0 > s > -1/N$), with their subsequent absence increasing the demand for quality control. Similarly, when specialized solutions predominate, the advantage to quality control is lessened, and resulting higher error rates further increase selection for many locally specialized solutions. If true, this bistability suggests that historical contingency, rather than the current value of N_e, determines which processes are error-prone *vs.* high-fidelity for populations at intermediate N_e.

In the current work, we note that the model of Rajon and Masel (2011) contained an unrealistic symmetry, namely that the fitness consequence of a molecular error at one locus was exactly equal to that at any other loci. Here, we find that, with reasonable amounts of variation among loci (*e.g.*, in their expression level or the per-molecule damage from their misfolded form), the bistability disappears. Intermediate solutions evolve instead, where cryptic deleterious sequences are purged only in more highly expressed genes, and quality control evolves to intermediate levels. Variation among loci does not change the previous finding that evolvability tracks the proportion of loci that contain a benign rather than a deleterious cryptic sequence.

The high rate of transcriptional error in *B. aphidicola* can be explained by adding a second bias toward deleterious mutations (in error rate), and hence a second drift barrier to our model. *B. aphidicola* and *E. coli* have high error rates for different reasons; high-fidelity quality control is redundant and unnecessarily expensive in *E. coli*, but unattainable in *B. aphidicola*, leading to similarly high transcriptional error rates.

Methods

Fitness

We follow the additive model of Rajon and Masel (2011), as outlined below, with a few important modifications to accommodate variation in gene expression levels. The model's canonical example is the risk that a ribosome reads through a stop codon during translation.

The global mitigation strategy is to improve quality control of this gene expression subprocess. We assume that additional quality control that reduces the error rate, ρ, by some proportion, consumes a certain amount of time or comparable resource. Relative to a generation time of 1 in the absence of quality control costs, this gives generation time $1 + \delta\ln(1/\rho)$, where δ scales the amount of resources that could have been used in reproduction, but are redistributed to quality control. Malthusian fitness is the inverse of generation time, giving

$$w_{QC} = \frac{1}{1 + \delta\ln(1/\rho)} \quad (1)$$

Following Rajon and Masel (2011), we set $\delta = 10^{-2.5}$, such that reducing ρ from 10^{-2} to 10^{-3} corresponds to a 0.7% reduction in fitness.

When a readthrough error happens, with frequency ρ, the consequences for fitness depend on the nature of the "cryptic sequence" that lies beyond the stop codon in the 3′UTR. The consequences of mistakes, mutational or otherwise, have a bimodal distribution, being either strongly deleterious (often lethal), or relatively benign, but rarely in between (Eyre-Walker and Keightley 2007; Fudala and Korona 2009). For example, a strongly deleterious variant of a protein might misfold in a dangerous manner, while a benign variant might fold correctly, although with reduced activity. We assume that alternative alleles of "cryptic genetic sequences" can be categorized according to a benign/deleterious dichotomy.

The local mitigation strategy, the alternative to global quality control, is thus for each cryptic sequence to evolve away from "deleterious" options and toward "benign" options. The local strategy of benign cryptic sequences has no direct fitness cost, but it is nevertheless difficult to evolve at so many loci at once. In contrast, expressing deleterious cryptic sequences has an appreciable cost. This cost scales both with the base rate of expression of the gene, and the proportion, ρ, of gene products that include the cryptic sequence.

Let the expression of gene i be E_i. We assign the concentration E_i of protein molecules of type i by sampling values of E_i from a $\log_2$-normal distribution with standard deviation (SD) σ_E. We define D to be the total frequency of protein expression that would be highly deleterious if expressed in error:

$$D = \frac{\sum_{i\in loci\_with\_del\_crypt\_seq} E_i}{\sum_{i\in loci} E_i} \quad (2)$$

where the numerator sums only over loci that are deleterious, and the denominator sums over all loci. This normalization cancels out the effect of the mean value of E_i. We assume the costs of deleterious readthrough are additive across genes, based on the concept that misfolded proteins (Thomas *et al.* 1995) may aggregate in a nonspecific and harmful manner with other proteins and/or membranes (Kourie and Henry 2002), or may simply be expensive to dispose of (Goldberg 2003). After the stop codon is read through, translation will usually end at a backup stop codon within the 3′UTR. Under the assumption of additivity, readthrough events will reduce fitness by $c\rho D$, where c represents the strength of selection against misfolded proteins. Geiler-Samerotte *et al.* (2011) found that an increase in misfolded proteins of ∼0.1% of total cellular protein molecules per cell imposed a cost of about 2% to relative growth rate. This gives an estimate of $c = 0.02/0.1\% = 20$.

Readthrough involving benign cryptic sequences does not incur this cost. However, when all cryptic sequences are benign (*i.e.*, $D = 0$), nothing stops ρ from increasing to unreasonably large values, *i.e.*, $\rho > 0.5$, which makes "erroneous" expression into the majority (and hence the "new normal") form. This represents the antiredundancy solution of Krakauer and Plotkin (2002), in which any mutation has an extremely deleterious effect; indeed, as their per-locus penalty s (analogous to our ρcE) approaches 1, the fitness of their $k = 0$ genotype (analogous to our $D = 0$) approaches infinity. To avoid this scenario in our model of quality control, we add a cost in fitness $c\rho^2(1-D)$, whose impact is felt only at high values of ρ. One possible biological interpretation of this second order term is that, with probability ρ^2, readthrough occurs not just through the regular stop codon, but also through the backup stop codon at the end of the benign cryptic genetic sequence. To reflect the effects of the double-error scenario under this interpretation, we therefore multiplied the second order term by the probability $\mu_{del}/(\mu_{del} + \mu_{ben})$ that a neutrally evolving cryptic sequence will be deleterious, where μ_{del} is the rate of deleterious-to-benign mutations, and μ_{ben} the reverse rate. Other double-error interpretations might involve different constants. In our case, the fitness component representing the cost of misfolded proteins is given by

$$w_{misfolding} = \max\left(0, 1 - c\rho D - c\rho^2(1-D)\frac{\mu_{del}}{\mu_{del} + \mu_{ben}}\right) \tag{3}$$

Equation 3 is a natural extension of the additive model of Rajon and Masel (2011), generalizing to the case of variation in the degree of importance of cryptic loci. Where previous work referred to the number, L_{del}, of loci having the deleterious rather than benign form, we now distinguish between two measures, L_{del} and D, the latter reporting the proportion of gene product molecules rather than the number of gene loci.

Rajon and Masel (2011) also obtained near-identical results using a very different, multiplicative model. While this suggests that the exact function form of Equation 3 is unimportant, we chose the additive Equation 3 model as the more reasonable of the two options. The multiplicative model is premised on loss-of-function of the wild-type proteins, which likely has negligible impact for small losses of a protein whose activity is already close to saturation. In contrast, the additive model is premised on gain-of-negative-function effects of misfolded proteins. These plausibly constitute a major burden on fitness, through a combination of toxicity, disposal costs, and resources spent to replace a faulty molecule with a normal one.

To study evolvability, let a subset of K (typically 50) out of the L (typically ≥600) loci affect a quantitative trait, x, selection on which creates a third fitness component. Error-free expression of locus, k, occurring with frequency $1-\rho$, has quantitative effect α_k, while expression that involves a benign version of the cryptic sequence has quantitative effect $\alpha_k + \beta_k$. Expression that involves a deleterious version of the cryptic sequence is assumed to result in a misfolded protein that has no effect on the quantitative trait. We assume that expression level, E_k, is constant and already factored into values of α_k and β_k. This gives

$$x = \sum_{k}^{K}[(1-\rho)\alpha_k + \rho B_k(\alpha_k + \beta_k)] \tag{4}$$

where $B_k = 1$ indicates a benign cryptic sequence, and $B_k = 0$ a deleterious one. As in Rajon and Masel (2011), we impose Gaussian selection on x relative to an optimal value x_{opt}

$$w_{trait}(x) = e^{\frac{-(x-x_{opt})^2}{2\sigma_f^2}} \tag{5}$$

where $\sigma_f = 0.5$.

Putting the three fitness components together, the relative fitness of a genotype is given by the product

$$w = w_{QC} \times w_{misfolding} \times w_{trait}. \tag{6}$$

Variance in expression levels

We estimated the variance in expression σ_E^2 from PaxDB (Wang *et al.* 2012, 2015), which is based on data released by the Global Proteome Machines (GMP) and other sources. We inferred σ_E equal to 2.24 (based on GMP 2012 release) or 3.31 (GMP 2014 release), for *S. cerevisiae*, and 2.93 (GMP 2014 release) for *Schizosaccharomyces pombe*. Note that, while our quantitative estimate of σ_E comes from variation in the expression levels of different proteins, consideration of variation along other lines might make a SD of 2.25 into a conservative underestimate of the extent of variation. See Supplemental Material, Figure B in File S1 for an exploration of this parameter value.

Mutation

There are six kinds of mutation: (1) conversion of a deleterious cryptic sequence to a benign form, (2) conversion from benign to deleterious, (3) change to the error rate, ρ, (4) change in the α value of one of the K quantitative trait genes, (5) change in the β value of one of those K genes, and (6) the co-option of a cryptic sequence to become constitutive, replacing the value of replacing α_k with that of $\alpha_k + \beta_k$ and reinitializing B_k and β_k.

It is this sixth kind of mutation that is responsible for the evolvability advantage of the local solution of benign cryptic sequences, providing more mutational raw material by which x might approach x_{opt} (Rajon and Masel 2011, 2013). The mutational co-option of a deleterious sequence ($B = 0$) is too strongly deleterious to be favored, even when replacing α_k and β_k might be advantageous. In other words, only benign cryptic sequences are available for mutational co-option. We use the term co-option of a 3′UTR readthrough sequence to refer to the case when a stop codon is lost by mutation, and not just read through by the ribosome (Giacomelli *et al.* 2007; Vakhrusheva *et al.* 2011; Andreatta *et al.* 2015). Mutational co-option for mimicking the consequences of errors other

than stop codon readthrough might involve mutations that change expression timing to make a rare protein–protein interaction common, or switch a protein's affinity preference between two alternative partners.

Because we use an origin-fixation approach to simulate evolution (see below), only relative and not absolute mutation rates matter for our outcomes, with the absolute rates setting only the timescale—our rates are therefore effectively unitless. We use the same mutation rates as Rajon and Masel (2011), reduced 10-fold for convenience. Each locus with a benign cryptic sequence mutates to deleterious at rate $\mu_{del} = 2.4 \times 10^{-8}$, while deleterious loci mutate to benign less often, at rate $\mu_{ben} = 6 \times 10^{-9}$. Changes to the error rate ρ occur at rate, $\mu_\rho = 10^{-6}$, while the α and β values of quantitative loci each change with rates $\mu_\alpha = 3 \times 10^{-7}$ and $\mu_\beta = 3 \times 10^{-8}$, respectively. Mutational co-option occurs at each quantitative locus at rate $\mu_{coopt} = 2.56 \times 10^{-9}$.

Each mutation to ρ increases $\log_{10}\rho$ by an amount sampled from Normal(ρ_{bias}, ${\sigma_\rho}^2$). By default, we set $\rho_{bias} = 0$ and $\sigma_\rho = 0.2$. To study extremely small populations with drift barriers to evolving even a global solution, we set $\rho_{bias} = 0.256$ and 0.465, corresponding to ratios of ρ-increasing mutations: ρ-decreasing mutations of 9:1 and 99:1, respectively.

A similar scheme for α and β might create, in the global solution case of relaxed selection, a probability distribution of β whose variance increases in an unbounded manner over time (Lande 1975; Lynch and Gabriel 1983). Following previous work (Rajon and Masel 2011, 2013), we therefore let mutations alter α and β by an increment drawn from a normal distribution with mean $-\alpha/a$ or $-\beta/a$, with a set to 750, and with SD of σ_m/K in both cases, with σ_m set to 0.5. In the case of neutrality, this mutational process eventually reaches a stationary distribution with mean 0 and SD as calculated in Equation S3 of Rajon and Masel (2011):

$$V(a,K,\sigma_m) = \frac{(\sigma_m/K)^2}{1-((a-1)/a)^2} \tag{7}$$

A co-option at gene k changes the gene's quantitative effect to

$$(1-\rho)(\alpha_k+\beta_k) + \rho B_k^{'}\left(\alpha_k+\beta_k+\beta_k^{'}\right) \tag{8}$$

where $B_k^{'}$ and $\beta_k^{'}$ are the state and the quantitative effect of a new cryptic sequence created by co-option. Following a co-option mutation at locus k, we set the new B_k equal to 1 or 0, with probabilities proportional to μ_{ben} and μ_{del}, and resample the value of β_k from Normal[0, $V(a, K, \sigma_m)$].

Evolutionary simulations by origin-fixation

We model evolution using an approach known as "weak mutation" (Gillespie 1983), or "origin-fixation" (McCandlish and Stoltzfus 2014). This approximation of population genetics is accurate in the limit where the waiting time until the appearance of the next mutation destined to fix is substantially longer than its subsequent fixation time. The population can then be approximated as genetically homogeneous in any moment in time. While unrealistic for higher mutation rates and larger population sizes, origin-fixation models are computationally convenient. Still more importantly, origin-fixation models, unlike more realistic models with segregating variation, allow the location of the drift barrier to be set externally in the form of the value of the parameter, N, rather than having the location of the drift barrier emerge from complicated linkage phenomena within the model. Fortunately, for quantitative traits affected by multiple cryptic loci, most evolvability arises from diversity of the effects of co-option of different loci, rather than among the diversity of the effects of co-option from different starting genotypes (Rajon and Masel 2013). This allows us to study evolvability [in the population sense of Wagner (2008)], even in the absence of genetic diversity that is imposed by the origin-fixation formulation.

Our computationally efficient implementation of origin-fixation dynamics is described in detail in File S1, simulating a series of mutations that successively fix, and the waiting times between each.

Initialization and convergence

We initialized the trait optimum at $x_{opt} = 0$. We could have initialized all values of α_k and β_k at zero. However, at steady state, variance in $\sum_1^K \alpha_k$ and $\sum_1^K \beta_k$ is far lower than would be expected from variance in α_k and β_k—this emerges through a process of compensatory evolution (Rajon and Masel 2013). Allowing a realistic steady state to emerge in this way is computationally slow under origin-fixation dynamics, especially when N is large. We instead sampled the initial values of α_k and β_k from Normal[0, $V(a, K, \sigma_m)$], where $V(a, K, \sigma_m)$ is defined by Equation 7, and then subtracted $\overline{\alpha}$ from α_k, and $\overline{\beta}$ from β_k, where $\overline{\alpha}$ and $\overline{\beta}$ are the means of a genotype across each of its quantitative loci, k. This process initializes α_k and β_k to have variances equal to those of the stationary distributions, while the overall trait value is initialized at the optimal value, zero. This procedure greatly reduces the burn-in computation time needed to achieve a somewhat subtle state of negative within-genotype among-loci correlations. We confirmed that subsequent convergence of the variance of $\sum_1^K \alpha_k$ was fast, occurring in <1000 steps, where a "step" is defined to be the fixation of one mutation. We expect $\log_{10}\rho$, D, and variance in β_k, to converge even faster than variance in α_k.

For the low-ρ initial conditions, ρ was initialized at 10^{-5}, and we initialized the benign *vs.* deleterious status of cryptic sequences at the neutral mutational equilibrium, choosing exactly $L \times \mu_{del}/(\mu_{del} + \mu_{ben})$ (rounded to the nearest integer) to be deleterious, independently of their different values of E. For the high-ρ initial conditions, we set ρ to 10^{-1}, and made all cryptic sequences benign.

We ran simulations for 10^5 steps, recording information at fixed times (measured in terms of waiting times), corresponding to approximately every 1000 steps on average, and hence yielding about 100 timepoints. To summarize the evolutionary outcome, we calculated the arithmetic means of $\log_{10}\rho$, of L_{del}, and of D among the last 20 timepoints, *i.e.*, approximating steps $0.8 \times 10^5 - 1 \times 10^5$.

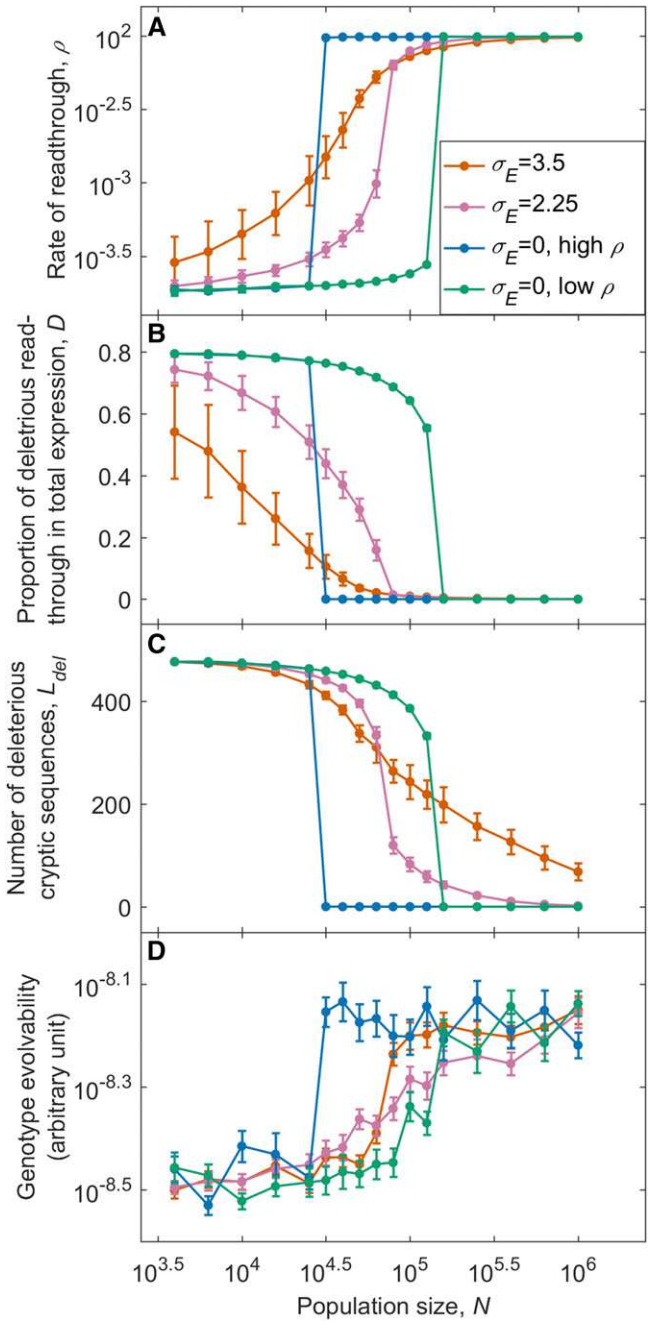

Figure 1 Evolutionary dynamics are bistable in the absence of variation in gene expression (σ_E = 0), but not with variation in gene expression (σ_E = 2.25–3.5). We calculated the average values of ρ, D, and L_{del} toward the end of the simulations, and then measured the genotype evolvability after changing the optimal trait value (see *Methods* for details). For each value of N, 20 simulations were initialized at high-ρ conditions, and 15 at low-ρ conditions. For σ_E = 2.25–3.5, simulations from the two initial conditions reached indistinguishable endpoints (Figure A in File S1), so the results were pooled. The increment in N is $10^{0.1}$ between $10^{4.4}$ and $10^{5.2}$ to increase resolution, and is $10^{0.2}$ elsewhere. At σ_E = 0, D is indistinguishable from zero for $N \geq 10^{5.2}$ under high-ρ conditions, and for $N \geq 10^{4.7}$ under low-ρ conditions, corresponding to L_{del} being effectively zero. In contrast, when σ_E = 2.25 or 3.5, because the weakness of selection on low-expression genes prevents L_{del} from falling all the way to zero, D never quite reaches zero either, despite appearing superimposable in B. For (A–C), data are shown as mean ±SD. For evolvability (D), data are shown as mean ±SE. For (A) and (D), these apply to log-transformed values. Evolvability is based on time to fitness recovery; see Figure C in File S1 for similar results based on time to trait recovery. L = 600.

Evolvability

After adaptation to a trait optimum of x_{opt} = 0 had run to convergence (*i.e.*, after 10^5 steps), we changed x_{opt} to 2, forcing the quantitative trait to evolve rapidly. This allows the co-option of benign cryptic sequences an opportunity to increase evolvability. We measured evolvability in two ways: as the inverse of the waiting time before trait x exceeded 1, and the inverse of the waiting time before the population recovered half of the fitness it lost after x_{opt} changed. By default, we present results showing evolvability as time to fitness recovery; evolvability as time to trait recovery is shown only in Figure C in File S1.

We want our measures of evolvability to reflect a genotype's potential to generate beneficial mutations, but this goal was complicated by population size. A large population finds a given beneficial mutation faster than does a small population, inflating the total fixation flux $\sum_{i \in beneficial\_mutation} \mu_i N P_{fix}(i)$, where $\mu_i N$ is the influx of mutations of beneficial type i and P_{fix} is their probability of fixation (the latter described by Equation 9 in File S1), in direct proportion to population size. We therefore divided our evolvability measures by the population size to correct for this effect. This normalization converts the population-level evolvability measure into a measure of the population-size-independent evolvability of a single individual that has the genotype of interest.

Data availability

Source code for the simulations is available at https://github.com/MaselLab/. All simulations were run with Matlab (R2014a).

Results

Recall that, in the absence of variation in expression among genes, there are two solutions to handle erroneous expression due to stop codon readthrough: at high population size N, the local solution purges all deleterious cryptic sequences, making high rates of readthrough harmless, while, at low N, the global solution reduces the rate of readthrough, allowing deleterious cryptic sequences to accumulate near-neutrally. At intermediate N, we see bistability, with either solution possible, depending on starting conditions (Figure 1, σ_E = 0). It is important to note that we use the word "bistability" loosely. Strictly speaking, bistability means that the system has two stable steady states (here a state is defined by readthrough rate and the exact property of each cryptic sequence), *i.e.*, two attractors. But, in a stochastic model, there are no attractors in the strict sense of the word, only a stationary distribution of states. We use the term bistability to refer to the case where the stationary distributions of states have two modes. Transitions between the two modes are rare, therefore the two modes can be loosely interpreted as the two attractors of the system.

Our results qualitatively reproduce the bistability reported by Rajon and Masel (2011) for the case where there is no expression variation among genes, though the range of values of N leading to bistability is smaller than that found in Rajon and Masel (2011), in which a full Wright-Fisher simulation is used. The smaller range of bistability in our model could be caused by the ease with which long-term evolution is captured using an origin-fixation framework, or by other subtle differences between the approaches, *e.g.*, the greater ease of compensatory evolution under Wright-Fisher dynamics than under origin-fixation. We chose origin-fixation mainly to reduce the computational burden, which for our study was increased by the need to track individual loci, in contrast to previous work that needed only to track the number of loci with deleterious cryptic sequence, without distinguishing their identities (Rajon and Masel 2011, 2013).

However, bistability vanishes with variation in expression among genes (Figure 1, $\sigma_E = 2.25$ and $\sigma_E = 3.5$). To understand why, consider a population initialized at low readthrough rate (ρ) and many deleterious cryptic sequences. Because the strength of selection against a deleterious cryptic sequence at locus i is proportional to ρE_i (the effect of a locus i on D in Equation 3 is proportional to E_i), purging works at the most highly expressed loci, even when ρ is low. This lowers the proportion D of readthrough events that are deleterious, which relaxes selection for high fidelity, leading to an increase in ρ. As ρ increases, loci with lower E_i become subject to effective purging, which further reduces D, which feeds back to increase ρ further. Because E_i is log-normally distributed, but contributes linearly to selection via D, each round of the feedback loop involves smaller changes than the last. Eventually, the changes are too small for selection on them to overcome mutation bias in favor of deleterious sequences. Similarly, when a population is initialized at high ρ, mutational degradation begins at low E_i sites, and arrests when selection is strong enough to kick in. The point of balance between mutation bias and selection defines a single intermediate attractor for $\sigma_E \geq 2.25$, instead of the bistable pair of attractors found for uniform E_i ($\sigma_E = 0$). For $\sigma_E < 2.25$, bistability is still found, but for a narrower range of population sizes than in the absence of variation (Figure B in File S1).

Even though bistability is not found for $\sigma_E = 2.25$, there is still a fairly sharp dichotomy, with solutions being either local (high ρ and low L_{del}) or global (low ρ and high L_{del}), and intermediate solutions found only for a very restrictive range of N, following a sigmoidal curve (Figure 1, A and C). Increasing variation in expression among genes blurs the boundary between the local solution and the global solution. Intermediate solutions are found for broader ranges of N as expression variance σ_E increases to 3.5. The trend, as expression variance σ_E increases from 0, is to first replace bistability with a limited range of intermediate solutions ($\sigma_E = 2.25$), and then for the intermediate solutions to become more prevalent, with extreme local and global solutions becoming less attainable as $\sigma_E > 2.25$.

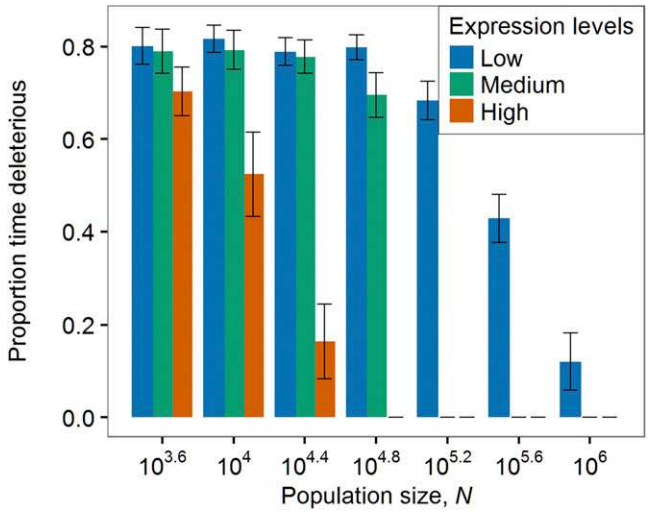

Figure 2 The effectiveness of purging a cryptic sequence of deleterious mutations depends on its expression level. We examined the states of the cryptic sequences of the loci with the 10 highest, the 10 lowest, and the 10 median expression levels among the 600 loci in each of the simulations shown in Figure 1 ($\sigma_E = 2.25$). We counted how often each locus contained a deleterious cryptic sequence among the last 20 timepoints we had collected from that simulation. Bars represent the proportion of time that each of the 10 loci carried a deleterious cryptic sequence, averaged over 20 replicates, and shown as mean ±SD. Simulations were initialized at low-ρ conditions.

The breakdown of the local solution begins with intermediate values of L_{del}, while the breakdown of the global solution begins with intermediate values of ρ and D (Figure 1, A–C). The breakdown of global solutions involves high-expression loci (Figure 2), which affect D more than L_{del}. In contrast, the breakdown of local solutions involves low-expression loci (Figure 2), which affect L_{del} more than D. Because ρ is better described as coevolving with D than with L_{del}, as explained earlier, intermediate values of ρ are seen more in the breakdown of global than local solutions.

A primary motivation behind characterizing the two solutions is that the local solution was found to have dramatically higher evolvability than the global solution (Rajon and Masel 2011). We therefore check whether this conclusion still broadly stands in the presence of variation in expression levels. The local solution promotes evolvability by making benign cryptic sequences available for co-option. Differences in evolvability between genotypes should therefore be largely determined by the fraction of quantitative trait loci that carry benign, rather than deleterious, cryptic sequences. In agreement with this, evolvability inversely mirrors L_{del}, as a function of population size, *i.e.*, evolvability (Figure 1D) resembles L_{del} (Figure 1C) far more than it resembles ρ (Figure 1A) or D (Figure 1B).

The distinction between global and local solutions becomes more extreme when the mutation bias toward deleterious rather than benign cryptic sequences is increased from a 4:1 ratio to a 99:1 ratio, but persists even when the mutation bias is eliminated in favor of a 1:1 ratio (Figure 3). In the absence of

mutation bias, there is less evolvability to be gained by the local relative to the global solution, since half the quantitative loci are available for co-option regardless (Figure 3C). Nevertheless, a small evolvability advantage to the local solution can still be observed (Figure 3D). In any case, assuming mutation bias toward deleterious options is biologically reasonable, and Figure 3 shows that results are not sensitive to the quantitative strength of our assumption on this count.

When we also account for mutation bias that tends to increase rather than decrease the error rate ρ, our model can explain the previously puzzling observation that the rate of transcriptional errors in small-N_e endosymbiont bacteria *Buchnera* is so much higher than that of *C. elegans*, and almost as high as that of large-N_e *E. coli* (McCandlish and Plotkin 2016; Traverse and Ochman 2016b). In extremely small populations, even the global solution is subject to a drift barrier, making ρ higher than its optimal value. For N so small such that most ρ-increasing mutations pass through the drift barrier, ρ can be almost as large as that in large populations (Figure 4A). Despite their high error rates, these extremely small populations also carry heavy drift loads of deleterious cryptic products (Figure 4, B and C), consistent with the fact that in *B. aphidicola*, unlike *E. coli*, selection is unable to reduce the fraction of nonsynonymous transcriptional errors that are nonsynonymous (Traverse and Ochman 2016a). High ρ shows the absence of a global solution, while high D and L_{del} show the absence of a local solution; neither solution is found for a sufficiently small population. Similar error rates in large and small populations can also be found, given bias in mutations to ρ, when there is no variation in expression levels (Figure E in File S1).

The parameters in our model can be classified into three groups, and the exploration of their values is summarized in Table A in File S1. The first group controls selection coefficients relevant to the global *vs.* local solution outcome: the variance in expression levels (σ_E^2), the number of loci (L, Figure D in File S1), the cost of misfolded protein molecules (c), and the cost of quality control (δ, Figure F in File S1). The second group controls mutation bias relevant to the global *vs.* local solution outcome: the frequency with which mutations turn deleterious cryptic sequences benign *vs.* the reverse (μ_{ben}:μ_{del}), whether mutations to ρ tend to increase or decrease it ($P_{+\rho}$:$P_{-\rho}$), and variance in the magnitude of mutations to ρ (σ_ρ^2, Figure G in File S1). The third group contains all the parameters that control the evolution of quantitative traits encoded by a minority of loci relevant to the evolvability properties. Because our focus in this manuscript is on the evolution of global *vs.* local solutions, not on the precise details of the relationship between local solutions and evolvability, these parameter values were explored less.

The influence of σ_E^2 dominates our results. Its effect in eliminating bistability holds, with the one exception that very "cheap" quality control could partially restore bistability (Figure F in File S1). Otherwise, we found that three parameters—c, δ, and μ_{ben}:μ_{del}—are the main determinants of the population size at which the transition between global

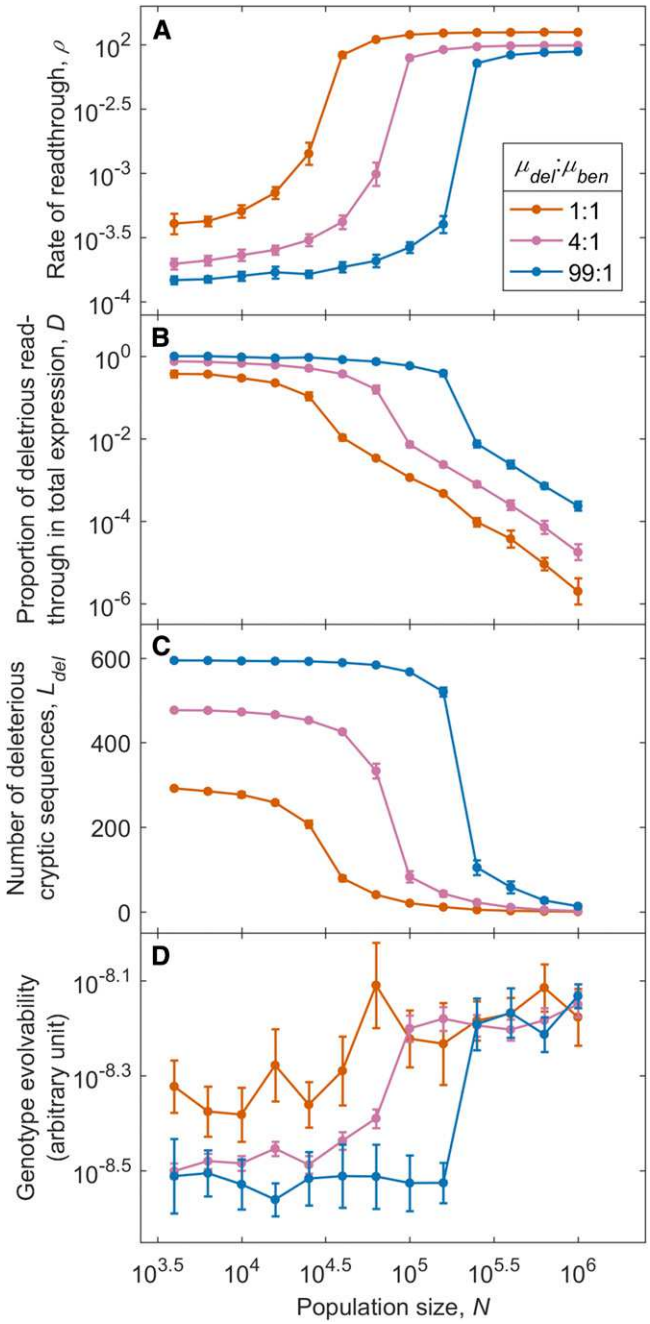

Figure 3 Results become more extreme when the mutation bias in the state of a cryptic sequence is increased from a 4:1 ratio to a 99:1 ratio, but do not disappear completely when the mutation bias is eliminated in favor of a 1:1 ratio. The location of the drift barrier shifts as a function of mutation bias, but the dichotomy between local and global solutions (as seen in values of ρ and D) is not sensitive to relaxing the mutation bias. The advantage of the local solution with respect to evolvability [as seen in (D) and mirrored in L_{del} (C)] is more sensitive to lack of mutation bias, but is still visible even with a 1:1 ratio. To compare results across different mutation biases, we kept the sum of the two mutation rates constant. For the low-ρ initial conditions, the number of deleterious cryptic sequences was initialized at the neutral mutational equilibrium of $L \times \mu_{del}/(\mu_{del} + \mu_{ben})$ (rounded to the nearest integer). For μ_{del}:μ_{ben} = 4:1, we reused the results shown in Figure 1. For the other ratios, five replicates were run for each initial condition, and pooled. For (A–C), data are shown as mean ±SD. For (D), data are shown as mean ±SE. For (A) and (D), these apply to log-transformed values. L = 600 and σ_E = 2.25.

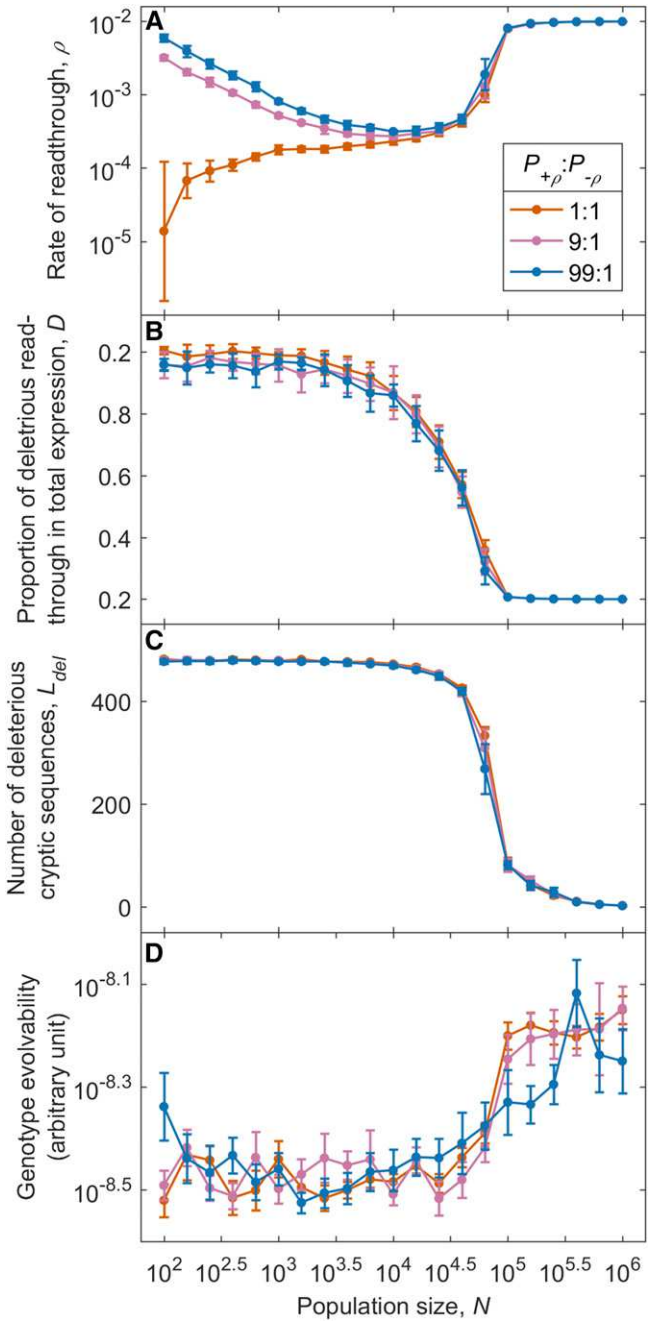

Figure 4 Mutation bias tends to increase ρ, such that even the global solution breaks down in sufficiently small populations. $P_{+\rho}$ is the probability that a mutation increases ρ, and $P_{-\rho}$ is the probability of a decrease. Each data point, (except those taken from Figure 1 with $P_{+\rho}$:$P_{-\rho}$ = 1:1 and $N = 10^{3.6}$–$10^{6.0}$), is pooled from five replicates of high-ρ initial conditions and five replicates of low-ρ initial conditions. Because we assume multiplicative mutational effects to ρ, its value converges even for extremely small N. *i.e.*, as ρ increases, the additive effect size $\Delta\rho$ of a typical mutation also increases, preventing it from passing through the drift barrier. For (A–C), data are shown as mean ±SD. For (D), data are shown as mean ±SE. For (A) and (D), these apply to log-transformed values. $L = 600$ and $\sigma_E = 2.25$.

and local solutions takes place, and of the exact error rate that evolves for global and local solutions (Table A in File S1). The other parameters in the first and second groups have little or no influence on the evolutionary outcomes that we study. In general, parameters in the first group, controlling selection, have stronger effects than the second group, controlling mutation bias.

Discussion

When genes vary in their expression levels, the dichotomy between the local and global solutions is replaced by a continuous transition. Very large populations still resemble the local solution, although mutations making cryptic sequences deleterious still pass through the drift barrier in the occasional low-expression gene. Very small populations still resemble the global solution, although mutations making cryptic sequences deleterious may still be effectively purged in a few high-expression genes; because their high expression disproportionately affects the burden from misexpression, this relaxes expression for high fidelity, leading to less strict quality control.

In agreement with drift barrier theory, large-N_e *E. coli* exhibits a local solution—a tendency for transcription errors to have synonymous effects—while small-N_e *B. aphidicola* does not (Traverse and Ochman 2016a). While, as predicted, the global solution of low transcriptional error rates does not obey the naïve drift barrier expectation of being higher in *B. aphidicola* than in *E. coli* (Traverse and Ochman 2016a), nor are transcription error rates drastically lower in *B. aphidicola* as predicted by previous theory on the interplay between global and local solutions (Rajon and Masel 2011; McCandlish and Plotkin 2016). This significantly lower rate relative to *E. coli* is, however, found in intermediate-N_e *C. elegans*. Where previous work (Rajon and Masel 2011) explained only the relative rates for *E. coli* and *C. elegans*, here we also explain the high error rate of *B. aphidicola* by taking into account a drift barrier on the global solution of low error rates. This drift barrier is significant because of mutation bias toward higher error rates. Small *B. aphidicola* populations have higher error rates than *C. elegans* because it is the best that evolution at low N_e can manage, despite the deleterious consequences; large *E. coli* populations have similarly high error rates because, with the worst consequences of error already purged, they do not need to incur the cost that quality control entails.

With small amounts of variation in expression among genes, the range of intermediate values of N_e for which bistability is found shrinks. With more variation, bistability vanishes in favor of a sigmoidal transition between global and local solutions. With still more, the sigmoid is smoothed out, and intermediate solutions are found for most values of N_e.

To interpret our results correctly, we must therefore estimate the degree to which genes vary. The results presented here focus on two estimates of the variance in log-expression in yeast, namely σ_E of 2.25 and 3.5. However, variation among genes in the deleterious consequences of misfolding, in addition to variation in expression levels, might make larger σ_E a better model of reality, further supporting a continuum of

intermediate solutions. In other words, the value of c in Equation 3 may vary among genes. Note that apart from the second-order ρ^2 term, the cost of a deleterious misfolded protein i depends only on the product of c_i and expression level E_i. Given log-normal distributions of c_i and expression level E_i, the variance of the log-product is equal to the sum of the two log-variances, so we can transform this scenario into one where c is constant, and σ_E^2 is equal to this sum. This can be done because changing c_i and E_i only affects $w_{misfolding}$, and not other factors such as the magnitude of a locus's influence on the quantitative trait. In other words, adding variation to c is almost equivalent to increasing the variance in expression levels.

The values of μ_{del} and μ_{ben} may also vary among genes. Drift barrier effects operate via the effect of population size on the fate of deleterious not beneficial mutations—if purging is efficient, then the beneficial mutation rate does not matter, because a single beneficial mutation is enough. We therefore focus on μ_{del}. The inclusion of a benign-to-deleterious mutation M_i at locus i depends on the product of μ_{del} at locus i and M_i's probability of fixation. It seems likely that variation among genes in the probability that a deleterious cryptic sequence becomes fixed will swamp variation in the deleterious mutation rate—variation in expression levels causes the former to vary over orders of magnitude. Note that, as for the case of variation in c, it is possible to construct a manipulation of E_i that has the same effect on the relevant product, via the probability of fixation, as would occur given a change in μ_{del}. While this case is less neat than for the product c_iE_i, it illustrates that a model of variation in expression levels can reflect, to some extent, the effect of variation in μ_{del}.

Our model makes three critical assumptions, which must be understood for the results to be interpreted appropriately. First, a "locus" in our model consists of one regular and one cryptic sequence. The primary example that we used to parameterize the simulations posits an entire protein-coding gene as the regular sequence, and the extended polypeptide resulting from stop codon readthrough as the cryptic alternative. In the example of transcriptional errors, a locus is a single codon, with its corresponding amino acid being the regular sequence, and the most common consequence of a transcriptional error as the cryptic. The case of one regular sequence and many alternative cryptic ones has not been modeled. Similarly, proteins may each have a regular fold or binding partner, and our model considers the contrast between this state and a single cryptic alternative.

Second, we assume that the rate of gene expression errors is set globally, across all loci. In reality, individual context may also affect the error rate, giving error rates a local solution aspect as well. A model of three rather than two interacting solutions—global error rates, local error rates, and local robustness to the consequences of error—remains for future work. Perhaps highly expressed genes will have both more benign cryptic sequences and lower rates of error, or perhaps the evolution of one kind of local solution will alleviate the need for another. Testing this empirically requires data on site-specific error rates, and on a credible marker for the benign status of members of an identifiable class of cryptic sequences. Such tools are now becoming available, and indeed we recently found a positive correlation between a large number of readthrough errors at a particular stop codon and the benign status of the readthrough translation product (L. J. Kosinski *et al.* unpublished results). We also reanalyzed the data of Traverse and Ochman (2016a) to find that highly expressed transcripts have lower transcriptional error rates (K. Meer *et al.* unpublished results).

Finally, we assume that the consequences of errors have a bimodal distribution: either highly deleterious or largely benign, but rarely in between. In other words, we assume that a basic phenomenon in biology is that changes tend to either break something, or to tinker with it. There are a variety of lines of evidence supporting this intuitively reasonable assumption (Fudala and Korona 2009; Wylie and Shakhnovich 2011).

Acknowledgments

We thank Lilach Hadany, Yoav Ram, and other members of the Hadany group for helpful discussions that prompted us to explore variation in expression. We thank Paul Nelson for developing the idea of local error rates as an expansion of our model, Ben Wilson for help with R, and Etienne Rajon, Yoav Ram, Tobias Warnecke, and one anonymous reviewer, for helpful comments on the manuscript. We also thank Charles Traverse and Howard Ochman for sharing their data on transcriptional errors. An allocation of computer time from the University of Arizona Research Computing High Performance Computing (HPC) and High Throughput Computing (HTC) at the University of Arizona is gratefully acknowledged. This work was supported by the John Templeton Foundation [grant number 39667]. D.J.P. was also funded by the Undergraduate Biology Research Program at the University of Arizona.

Literature Cited

Adachi, M., and A. R. O. Cavalcanti, 2009 Tandem stop codons in ciliates that reassign stop codons. J. Mol. Evol. 68: 424–431.

Andreatta, M. E., J. A. Levine, S. G. Foy, L. D. Guzman, L. J. Kosinski *et al.*, 2015 The recent de novo origin of protein C-termini. Genome Biol. Evol. 7: 1686–1701.

Brettner, L. M., and J. Masel, 2012 Protein stickiness, rather than number of functional protein-protein interactions, predicts expression noise and plasticity in yeast. BMC Syst. Biol. 6: 128.

Drummond, D. A., and C. O. Wilke, 2008 Mistranslation-induced protein misfolding as a dominant constraint on coding-sequence evolution. Cell 134: 341–352.

Eyre-Walker, A., and P. D. Keightley, 2007 The distribution of fitness effects of new mutations. Nat. Rev. Genet. 8: 610–618.

Frank, S. A., 2007 Maladaptation and the paradox of robustness in evolution. PLoS One 2: e1021.

Fudala, A., and R. Korona, 2009 Low frequency of mutations with strongly deleterious but nonlethal fitness effects. Evolution 63: 2164–2171.

Geiler-Samerotte, K. A., M. F. Dion, B. A. Budnik, S. M. Wang, D. L. Hartl *et al.*, 2011 Misfolded proteins impose a dosage-dependent fitness cost and trigger a cytosolic unfolded protein response in yeast. Proc. Natl. Acad. Sci. USA 108: 680–685.

Giacomelli, M. G., A. S. Hancock, and J. Masel, 2007 The conversion of 3′ UTRs into coding regions. Mol. Biol. Evol. 24: 457–464.

Gillespie, J. H., 1983 Some properties of finite populations experiencing strong selection and weak mutation. Am. Nat. 121: 691–708.

Goldberg, A. L., 2003 Protein degradation and protection against misfolded or damaged proteins. Nature 426: 895–899.

Good, B. H., and M. M. Desai, 2014 Deleterious passengers in adapting populations. Genetics 198: 1183–1208.

Gout, J.-F., W. K. Thomas, Z. Smith, K. Okamoto, and M. Lynch, 2013 Large-scale detection of in vivo transcription errors. Proc. Natl. Acad. Sci. USA 110: 18584–18589.

Kimura, M., T. Maruyama, and J. F. Crow, 1963 The mutation load in small populations. Genetics 48: 1303–1312.

Kourie, J. I., and C. L. Henry, 2002 Ion channel formation and membrane-linked pathologies of misfolded hydrophobic proteins: the role of dangerous unchaperoned molecules. Clin. Exp. Pharmacol. Physiol. 29: 741–753.

Krakauer, D. C., and J. B. Plotkin, 2002 Redundancy, antiredundancy, and the robustness of genomes. Proc. Natl. Acad. Sci. USA 99: 1405–1409.

Lande, R., 1975 The maintenance of genetic variability by mutation in a polygenic character with linked loci. Genet. Res. 26: 221–235.

Liang, H., A. R. O. Cavalcanti, and L. F. Landweber, 2005 Conservation of tandem stop codons in yeasts. Genome Biol. 6: R31.

Lynch, M., 2007 *The origins Of Genome Architecture*. Sinauer Associates, Sunderland, MA.

Lynch, M., 2010 Evolution of the mutation rate. Trends Genet. 26: 345–352.

Lynch, M., 2012 Evolutionary layering and the limits to cellular perfection. Proc. Natl. Acad. Sci. USA 109: 18851–18856.

Lynch, M., and W. Gabriel, 1983 Phenotypic evolution and parthenogenesis. Am. Nat. 122: 745–764.

McCandlish, D. M., and A. Stoltzfus, 2014 Modeling evolution using the probability of fixation: history and implications. Q. Rev. Biol. 89: 225–252.

McCandlish, D. M., and J. B. Plotkin, 2016 Transcriptional errors and the drift barrier. Proc. Natl. Acad. Sci. USA 113: 3136–3138.

Mira, A., and N. A. Moran, 2002 Estimating population size and transmission bottlenecks in maternally transmitted endosymbiotic bacteria. Microb. Ecol. 44: 137–143.

Nichols, J. L., 1970 Nucleotide sequence from the polypeptide chain termination region of the coat protein cistron in bacteriophage R17 RNA. Nature 225: 147–151.

Rajon, E., and J. Masel, 2011 The evolution of molecular error rates and the consequences for evolvability. Proc. Natl. Acad. Sci. USA 108: 1082–1087.

Rajon, E., and J. Masel, 2013 Compensatory evolution and the origins of innovations. Genetics 193: 1209–1220.

Rispe, C., F. Delmotte, R. C. H. J. van Ham, and A. Moya, 2004 Mutational and selective pressures on codon and amino acid usage in buchnera, endosymbiotic bacteria of aphids. Genome Res. 14: 44–53.

Thomas, P. J., B.-H. Qu, and P. L. Pedersen, 1995 Defective protein folding as a basis of human disease. Trends Biochem. Sci. 20: 456–459.

Traverse, C. C., and H. Ochman, 2016a Conserved rates and patterns of transcription errors across bacterial growth states and lifestyles. Proc. Natl. Acad. Sci. USA 113: 3311–3316.

Traverse, C. C., and H. Ochman, 2016b Correction for Traverse and Ochman, conserved rates and patterns of transcription errors across bacterial growth states and lifestyles. Proc. Natl. Acad. Sci. USA 113: E4257–E4258.

Vakhrusheva, A., M. Kazanov, A. Mironov, and G. Bazykin, 2011 Evolution of prokaryotic genes by shift of stop codons. J. Mol. Evol. 72: 138–146.

Wagner, A., 2008 Robustness and evolvability: a paradox resolved. Proc. Biol. Sci. 275: 91–100.

Wang, M., M. Weiss, M. Simonovic, G. Haertinger, S. P. Schrimpf *et al.*, 2012 PaxDb, a database of protein abundance averages across all three domains of life. Mol. Cell. Proteomics 11: 492–500.

Wang, M., C. J. Herrmann, M. Simonovic, D. Szklarczyk, and C. von Mering, 2015 Version 4.0 of PaxDb: protein abundance data, integrated across model organisms, tissues, and cell-lines. Proteomics 15: 3163–3168.

Warnecke, T., and L. D. Hurst, 2011 Error prevention and mitigation as forces in the evolution of genes and genomes. Nat. Rev. Genet. 12: 875–881.

Williams, I., J. Richardson, A. Starkey, and I. Stansfield, 2004 Genome-wide prediction of stop codon readthrough during translation in the yeast *Saccharomyces cerevisiae*. Nucleic Acids Res. 32: 6605–6616.

Wu, X., and L. D. Hurst, 2015 Why selection might be stronger when populations are small: intron size and density predict within and between-species usage of exonic splice associated cis-Motifs. Mol. Biol. Evol. 32: 1847–1861.

Wylie, C. S., and E. I. Shakhnovich, 2011 A biophysical protein folding model accounts for most mutational fitness effects in viruses. Proc. Natl. Acad. Sci. USA 108: 9916–9921.

Communicating editor: J. Hermisson

Supplemental material for the manuscript

"Drift barriers to quality control when genes are expressed at different levels"

Xiong K, McEntee JP, Porfirio DJ, Masel J

Implementation of origin-fixation simulations

Origin-fixation models are often implemented via a crude rejection algorithm; large numbers of mutations are simulated, and each is accepted as a successful fixation event if and only if a random number sample from the uniform [0, 1] distribution falls below its (fairly low) fixation probability. For large *N*, this method is computationally slow when significant numbers of nearly neutral mutations must be sampled before one fixes with probability ~1/*N*. Given that our model posits only a relatively small range of possible mutations, we instead sampled only mutations that go on to become fixed, by sampling according to the relative values of "fixation flux", proportional to mutation rate × fixation probability for each of our six categories of mutation. In other words, we used a form of the Gillespie (1977) algorithm.

In a haploid population of size *N*, the probability of fixation of a new mutant into a resident population is given by

$$P_{fix} = \frac{1-e^{-s}}{1-e^{-Ns}} \quad (9)$$

where $s = w_{mutant}/w_{resident}-1$. It is then straightforward to calculate fixation flux values for all possible switches between benign and deleterious states:

$$f_{del\_to\_ben} = N\mu_{ben} \sum_{i \in loci\_with\_del\_crypt\_seq} P_{fix}(del\_to\_ben\_at\_i) \quad (10)$$

$$f_{ben\_to\_del} = N\mu_{del} \sum_{i \in loci\_with\_ben\_crypt\_seq} P_{fix}(ben\_to\_del\_at\_i) \quad (11)$$

Matters are slightly more complicated for quantitative mutations to α, β and ρ, because we must integrate the fixation flux over all possible sizes ($\Delta\alpha_k$, $\Delta\beta_k$, and $\Delta\log_{10}\rho$) for a mutation at a given locus, prior to summing across loci to arrive at the fixation flux for an entire mutational category:

$$f_\alpha = N\mu_\alpha \sum_k^K \int P_{fix}(\Delta\alpha_k) P(\Delta\alpha_k) d\Delta\alpha_k \quad (12)$$

$$f_\beta = N\mu_\beta \sum_k^K \int P_{fix}(\Delta\beta_k) P(\Delta\beta_k) d\Delta\beta_k \quad (13)$$

$$f_\rho = N\mu_\rho \int P_{fix}(\Delta\log_{10}\rho) P(\Delta\log_{10}\rho) d\Delta log_{10}\rho \quad (14)$$

where $P(\Delta\alpha_k)$, $P(\Delta\beta_k)$, and $P(\Delta\log_{10}\rho)$ are the probability densities for the magnitude of a given kind of mutation.

We use the quadrature method to calculate the integral over these possibilities, using a grid of 2000, limited for $\Delta\alpha_k$ to the interval $[-\alpha_k/\alpha - 5\sigma_m/K, -\alpha_k/\alpha + 5\sigma_m/K]$, for $\Delta\beta_k$ to the interval $[-\beta_k/\alpha - 5\sigma_m/K, -\beta_k/\alpha + 5\sigma_m/K]$, and for $\Delta\log_{10}\rho$, to the interval $[-10\sigma_\rho, \min(10\sigma_\rho, -\log_{10}\rho)]$. In the latter case, the number of grid intervals is reduced proportional to any truncation of the interval at $-\log_{10}\rho$.

For mutational co-options of benign cryptic sequences, the effect of replacing the value of α_k with that of $\alpha_k+\beta_k$ is fixed, but there is also a stochastic range of effects of initializing a new β_k and a new B_k (Eq. 15). Let $P(\beta_k')$ be the probability density of a new β_k given by Normal(0, $V(a, K, \sigma_m)$), and $P(B_k' = 1) = 1 - P(B_k' = 0)$ be the probability that a new B_k equals to 1, and hence the new β_k affects the trait value. The fixation flux associated with cooption mutations we obtained numerically by integration over the range [$-5\sigma_m/K$, $5\sigma_m/K$]:

$$f_{coopt} = N\mu_{coopt} \sum_{k \in loci\_with\_ben\_crypt\_seq}^{K} \begin{pmatrix} P(B_k' = 1) \int P_{fix}(\beta_k', B_k' = 1) P(\beta_k') d\beta_k' \\ +P(B_k' = 0) P_{fix}(B_k' = 0) \end{pmatrix} \quad (15)$$

The expected waiting time before the current genotype is replaced by another is

$$\text{waiting time} = \frac{1}{\text{total fixation flux over all six categories}} \quad (16)$$

A standard Gillespie (1977) algorithm would calculate the realized waiting time as a random number drawn from an exponential distribution with this mean. Since we are only interested in the outcome of evolution, and not the variation in its timecourse, we used the expected waiting time instead, decreasing our computation time. The waiting time can be interpreted as the time it takes for a mutation destined for fixation to appear, neglecting the time taken during the process of fixation itself. Using this interpretation, we specify waiting times in terms of numbers of generations, based on our assumptions about absolute mutation rates.

We assign the identity of the next fixation event among the six categories according to probabilities proportional to their relative fixation fluxes, then we assign the identity within the category. For switches between benign and deleterious states, allocating a fixation event within a category according to the relative values of fixation fluxes is straightforward. For mutations to ρ, α, and β, and mutational co-option, we relax the granularity and cutoff assumptions of the grid-integration method when choosing a mutation within the category. Instead, we sample a mutational value of $\Delta\log_{10}\rho$ from Normal(ρ_{bias}, σ_ρ^2). We reject and resample $\Delta\log_{10}\rho$ if $\Delta\log_{10}\rho \geq -\log_{10}\rho$. Otherwise, we accept vs. reject-resample according to the fixation probability of that exact mutation, by comparing this probability to a random number uniformly distributed at [0, 1.1×the maximum fixation probability across the grid points previously calculated for $\Delta\log_{10}\rho$ during our grid calculation]. For $\Delta\alpha$ (or $\Delta\beta$), the procedure is conceptually similar but has a more complicated implementation. We first sample from Normal(0, $(\sigma_m/K)^2$). We then add the random number to each of the values of $-\alpha_k/a$, and calculate the sum of corresponding fixation probabilities across all loci k. We accept vs. reject-resample the mutation by comparing this sum to a random sample from a uniform distribution at [0, 1.1×the maximum corresponding fixation probability sum calculated during our grid calculation]. If the mutation is accepted, we allocate it to a locus k with probability proportional to their relative fixation probabilities. For mutational co-option of a benign cryptic sequence, the main effect is to replace α_k with $\alpha_k+\beta_k$, but there are also subtler effects arising from the reinitialization of the new cryptic sequence. Any of the k loci for which $B = 1$ are eligible for co-option, the new value of B may be either 0 to 1, and the new β_k may take a range of values. Each combination of k and new B has its own fitness flux, and the first choice is among these {k, B} pairs. Next we sample

β_k from Normal(0, $(\sigma_m/K)^2$); for a new B equal to 0 we always accept the result, and for new B equal to 1, we accept vs. reject-resample β_k by comparing its probability of fixation to a random sample from a uniform distribution at [0, 1.1×the maximum corresponding fixation probability sum calculated during our grid calculation].

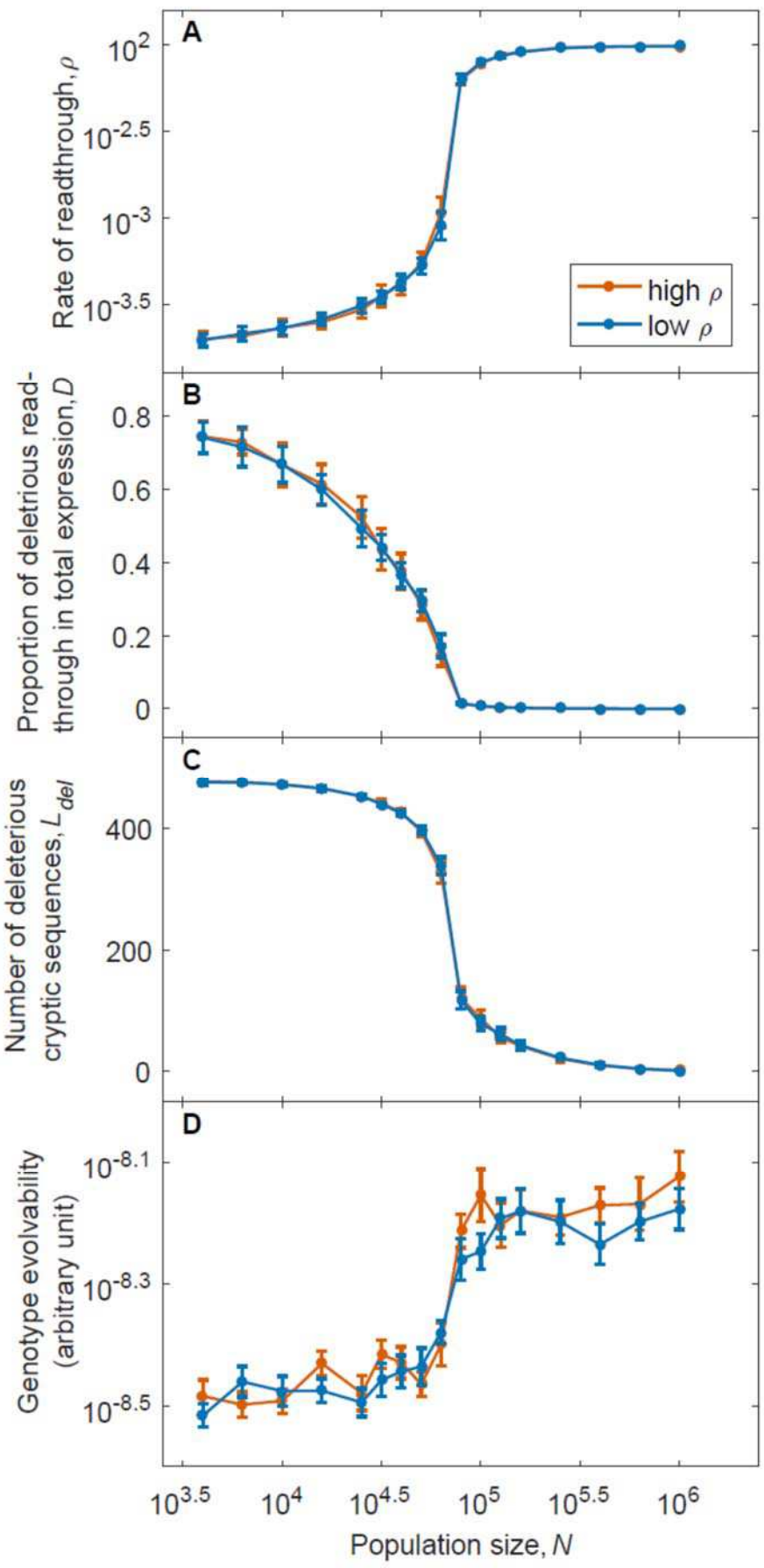

Figure A: At σ_E = 2.25, the final state of the evolutionary simulation does not depend on the initial conditions. The data shown here is the same as that shown pooled in Fig. 1.

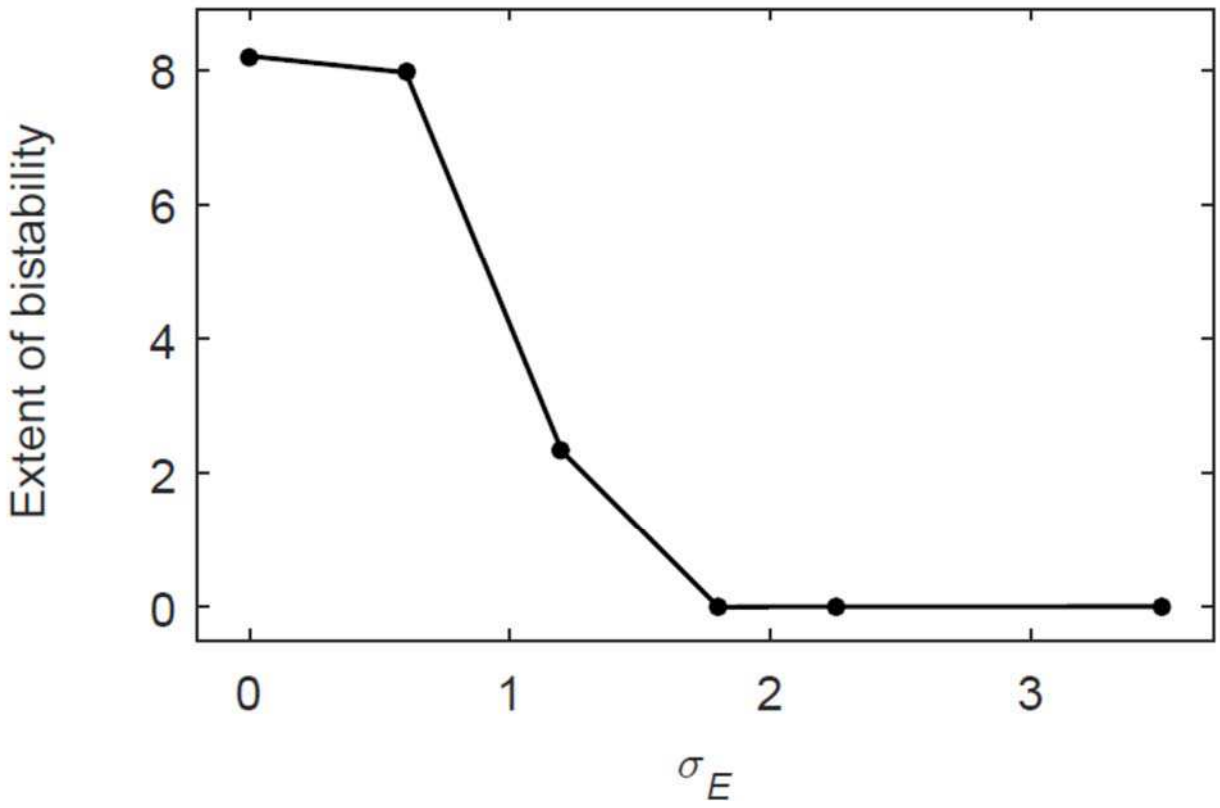

Figure B: The range of population sizes that exhibit significant bistability drops dramatically even for σ_E < 2.25. We used average values of ρ towards the end of the simulations as a measure of the solution found by each replicate. For each initial condition, we averaged over five replicates (except for σ_E = 0, 2.25, and 3.5, where we reused the 20 replicates of Fig. 1), and over each of the values of N between $10^{3.6}$ to 10^{6}, with an increment of $10^{0.2}$. The extent of bistability was assessed as $\sum_N(\log_{10}\bar{\rho}_{init\_low} - \log_{10}\bar{\rho}_{init\_high})^2$. L = 600.

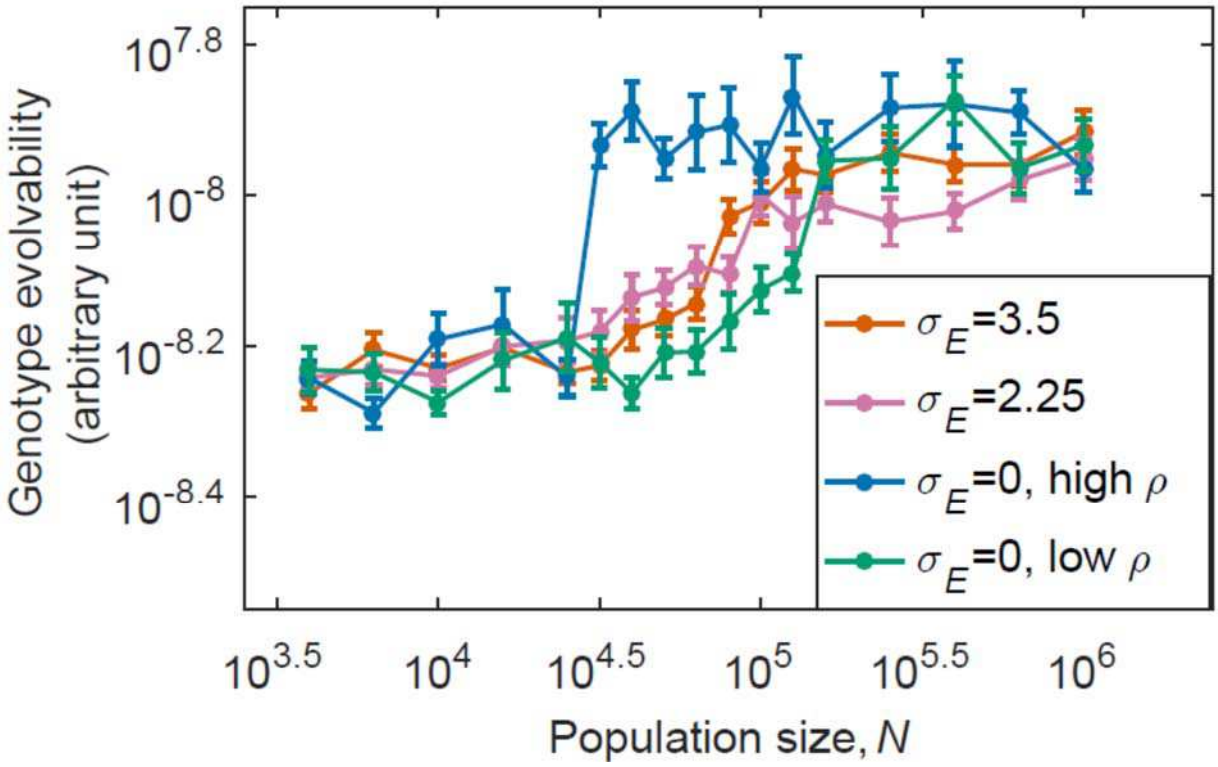

Figure C: The time taken for the trait to approach the new value of x_{opt} behaves similarly to the recovery time of fitness shown in Fig. 1**D**. The same simulations were used as in Fig. 1. At σ_E = 2.25 and σ_E = 3.5, we pooled the results from high-ρ and low-ρ conditions. Evolvability is shown as mean$\pm$SE of the log-transformed values. L = 600.

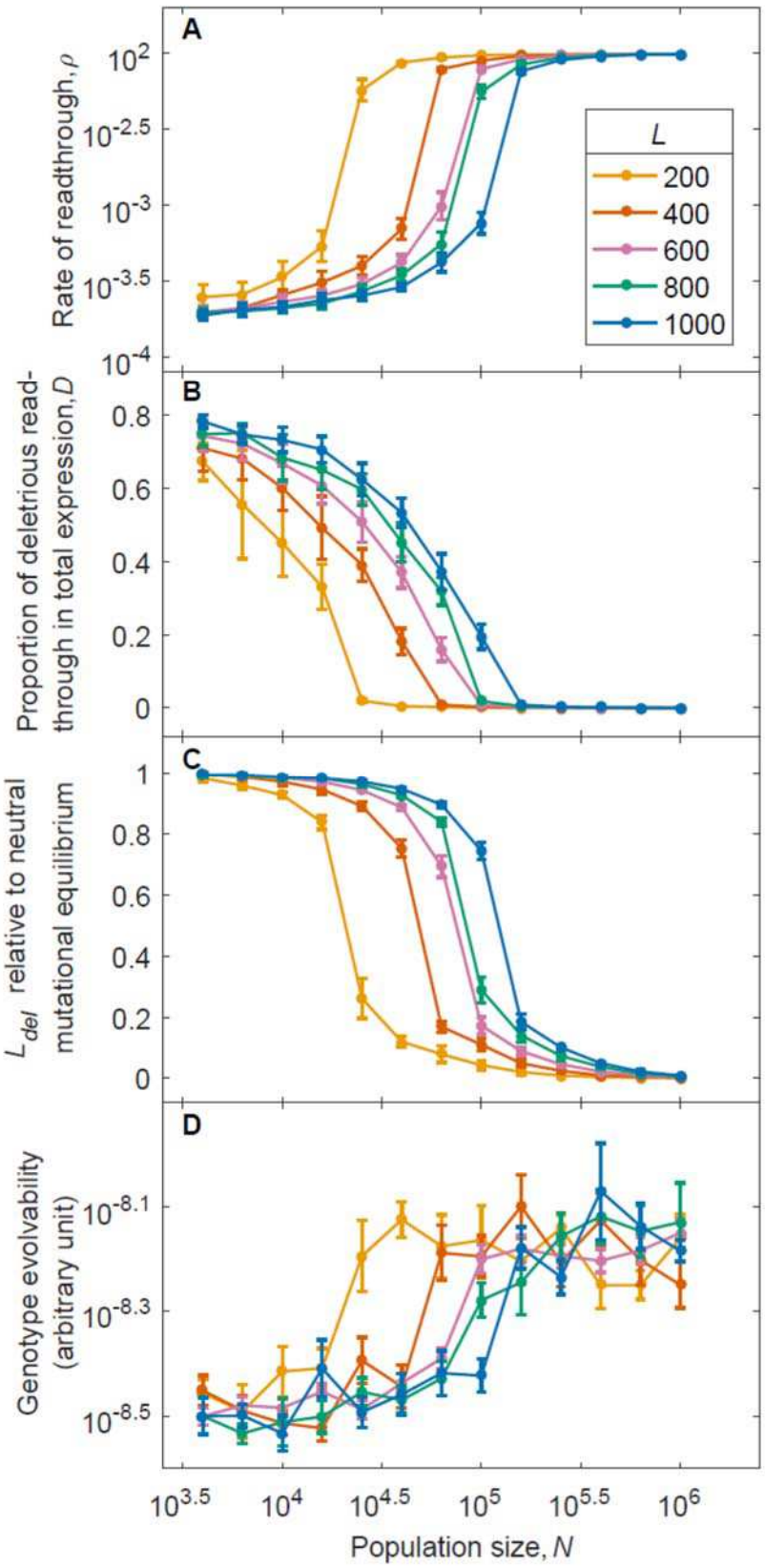

Figure D: Changing the number of loci does not qualitatively change our results. Quantitatively, fewer loci favor more local solutions. Changing *L* alters the average contribution of each locus to *D*. This alters the average strength of selection on each locus, independent of population size. Therefore, the same solutions, characterized by the values of ρ and *D*, are "shifted" to small values of *N* as *L* decreases. While *L* changed, we held the number of quantitative trait loci constant at 50. For *L* = 600, we reused the results shown in Fig. 1. For other values of *L*, five replicates were run for each of the two initial conditions. We pooled results from both initial conditions across all values of *L*. We normalized L_{del} to the neutral mutational equilibrium of $L \times \mu_{del}/(\mu_{del}+\mu_{ben})$. For panels **A** to **C**, data is shown as mean$\pm$SD. For **D**, data is shown as mean$\pm$SE. For **A** and **D**, these apply to log-transformed values. $\sigma_E = 2.25$.

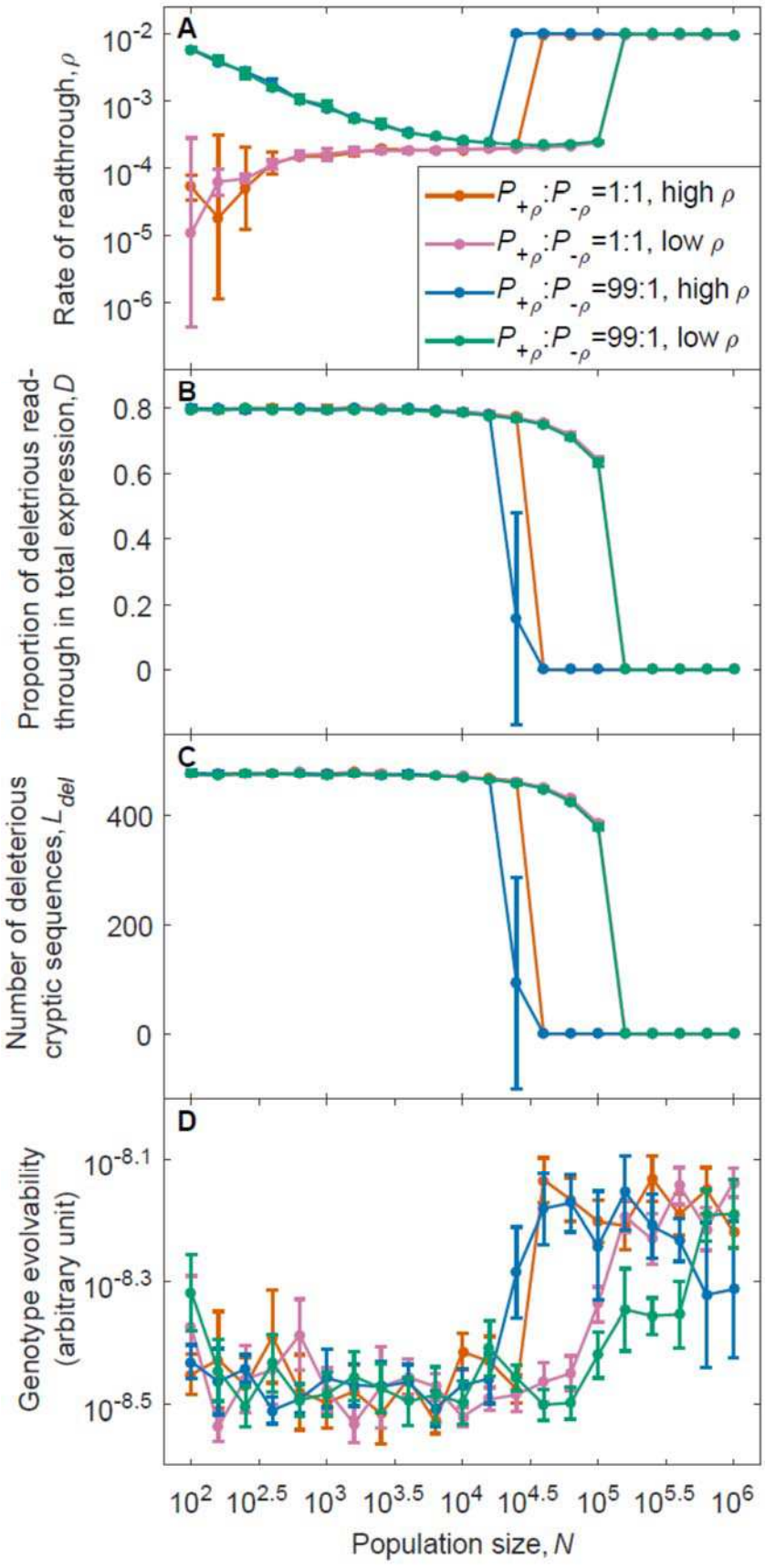

Figure E: Fig. 4 results (that the global solution breaks down in sufficiently small populations) remain true in the absence of variation of expression levels. Data points between $N = 10^{3.6}$ to $N = 10^{6.0}$ and $P_{+\rho}:P_{-\rho} = 1:1$, are reused from Fig. 1; for the others, we performed 5 replicates for each condition. For panels **A** to **C**, data is shown as mean$\pm$SD. For **D**, data is shown as mean$\pm$SE. For **A** and **D**, these apply to log-transformed values. $L = 600$.

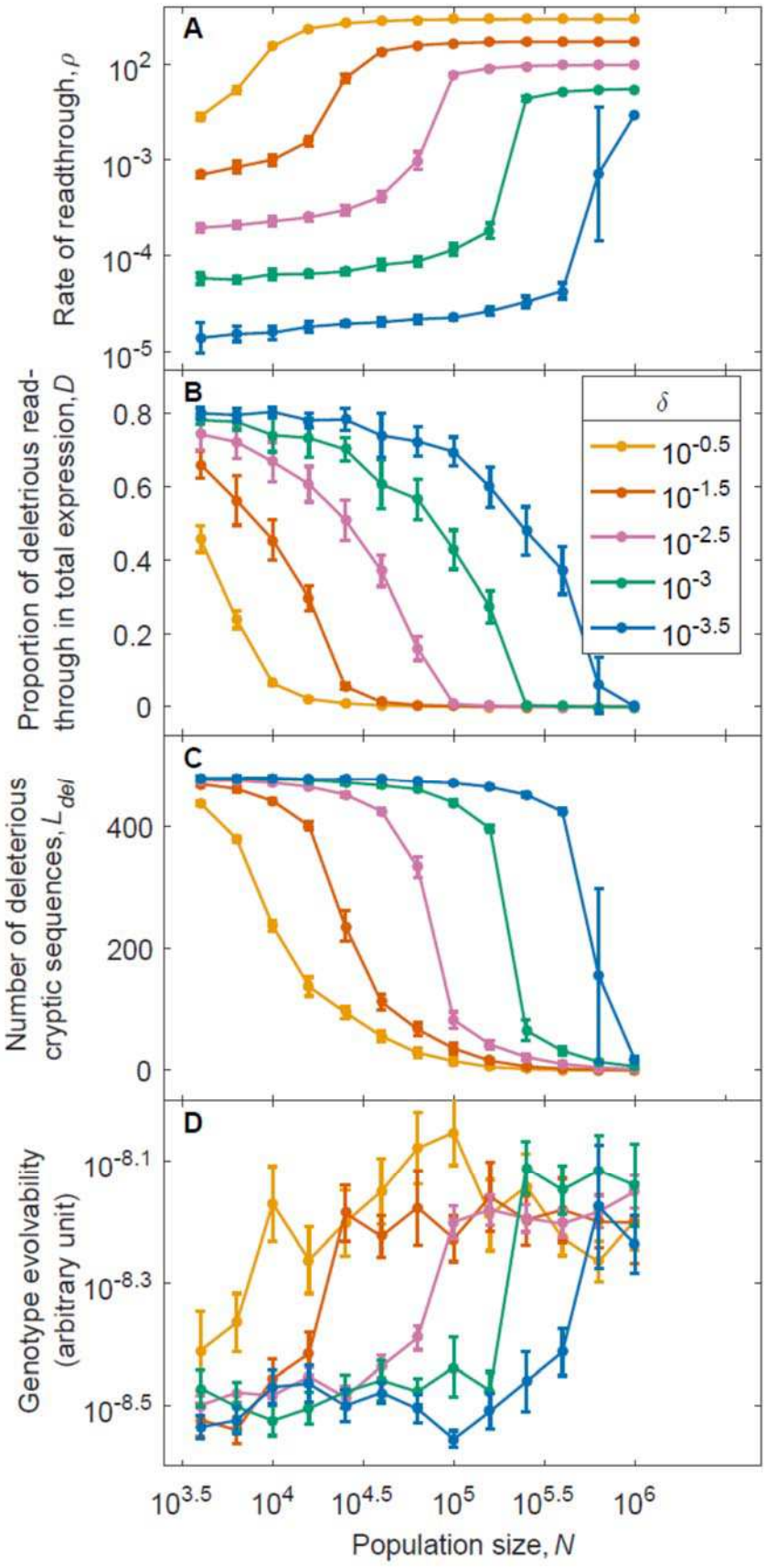

Figure F: Increasing the cost of quality control δ expands global solutions to smaller populations and reduces the differences in error rates as a function of population size. For $\delta = 10^{-2.5}$, we reused the data from Fig. 1; for each of the other values of δ, we ran 5 replicates from the high-ρ initial condition and 5 from the low-ρ initial condition. Each data point represents the pooled results from the two initial conditions. For panels **A** to **C**, data is shown as mean$\pm$SD. For **D**, data is based on time to fitness recovery and is shown as mean$\pm$SE. For **A** and **D**, the mean, SD and SE are calculated on log-transformed values. The large error bars at $N = 10^{5.8}$ under $\delta = 10^{-3.5}$ across all panels are due to different initial conditions, which is a sign of bistability. $L = 600$, $\sigma_E = 2.25$.

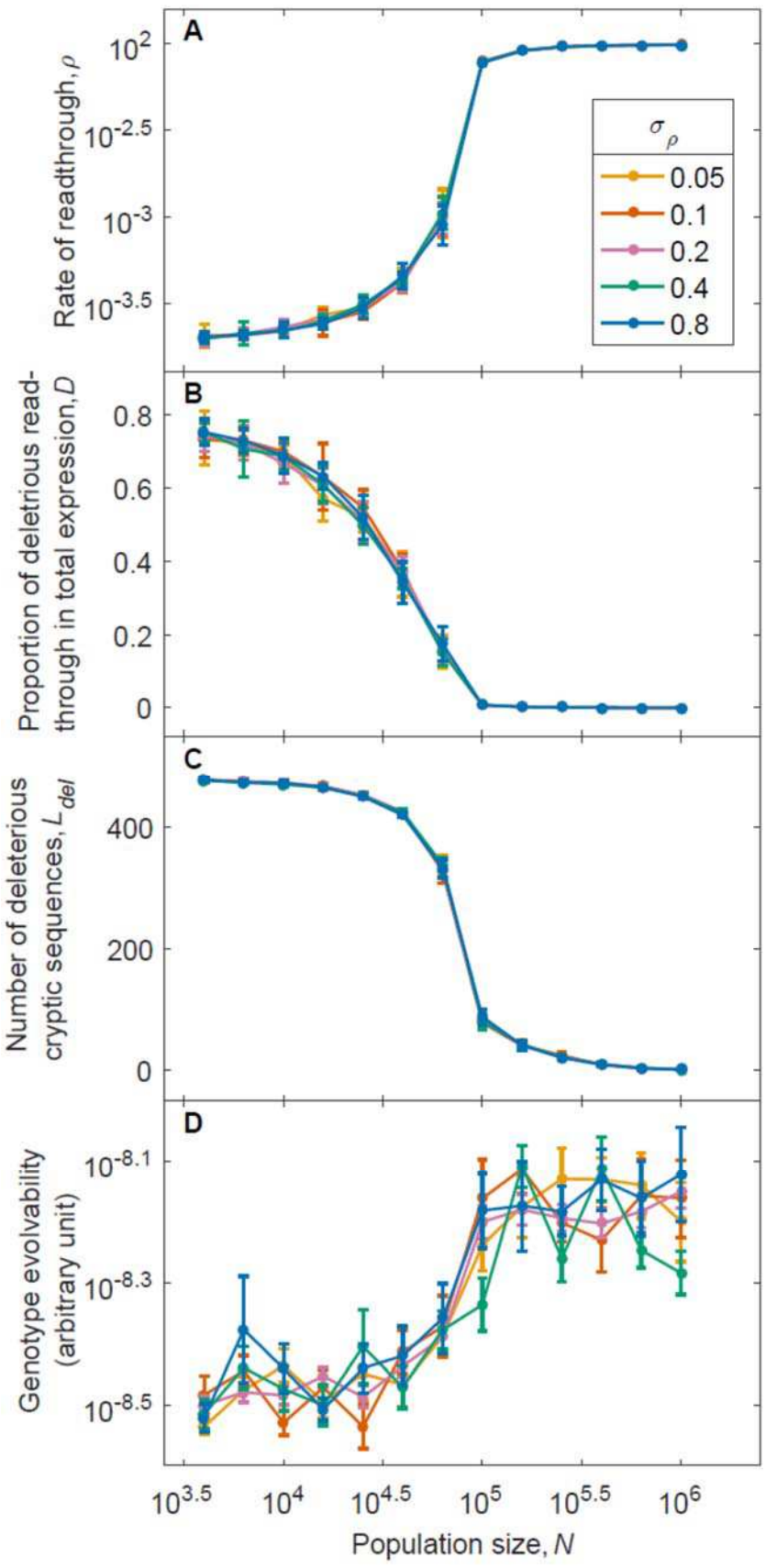

Figure G: The variance in the magnitude of mutations to ρ does not affect a population's solution to error or evolvability. For $\sigma_\rho = 0.2$, we reused the data from Fig. 1; for each of the other values of σ_ρ, we ran 5 replicates from each of the two initial conditions. We pooled results from the two initial conditions for each data point. For panels **A** to **C**, data is shown as mean$\pm$SD. For **D**, data is based on time to fitness recovery and is shown as mean$\pm$SE. For **A** and **D**, these apply to log-transformed values. $L = 600$, $\sigma_E = 2.25$.

Table A: Summary of model parameters

Group	Parameter	Biological meaning	Exploration	Parameter values in model[1]	Influence on global v. local solutions
Selection for local vs. global solution	σ_E^2	Variance of $\log_2$ expression among loci	Fig. 1, Fig. S2	5.1 (0-12.3)	Central finding: lower σ_E^2 promotes dichotomy
	c	Cost of misfolding	Fig. S3[2]	20 (7-28[2])	Large c makes ρ smaller, with a slightly larger impact on global solutions, and expands the bistable region to smaller populations.
	δ	Scaling of quality control costs	Fig. S6	$10^{-2.5}$ ($10^{-0.5}$-$10^{-3.5}$)	Higher cost makes ρ larger, with a larger impact on global solutions, and expands global solutions to smaller populations
	L	Total number of loci	Fig. S4, Fig. S2[2]	600 (200-1000)	Lower L shift the transition between local and global solutions to smaller populations, but maintain the shape of the transition
Mutation bias for local vs. global solution	μ_{del}	Rate of benign-to-deleterious mutations	Fig. 3	μ_{del}:μ_{ben} = 4:1 (1:1-99:1)	Stronger mutation bias lowers ρ and shifts the transition between local and global solutions to larger populations
	μ_{ben}	Rate of deleterious-to-benign mutations			
	$P_{+\rho}\times\mu_\rho$	Rate of mutations that increase ρ	Fig. 4, Fig. S5	$P_{+\rho}$:$P_{-\rho}$ = 1:1 (1:1-99:1)	Mutation bias prevents extremely small populations from reducing ρ
	$P_{-\rho}\times\mu_\rho$	Rate of mutations that decrease ρ			
	σ_ρ^2	var(mutations to ρ)	Fig. S7	0.04 (2.5×10^{-3}-0.64)	No apparent influence
Relevant only for quantitative effects and evolvability (of peripheral interest to our central findings)	K	Number of quantitative trait loci	Fig. S7[2]	50 (5-50[2])	-
	α	Speed that α and β revert to mean	Fig. S10[2]	750 (250-2000[2])	
	μ_{coopt}	Rate of co-option mutations	-	2.56×10^{-9}	
	μ_α	Rate of mutations to α	-	3×10^{-7}	
	μ_β	Rate of mutations to β	-	3×10^{-8}	
	σ_m^2	σ_m^2/K = var(mutations to α and β)	Fig. S8[2]	0.25 (0.04-1[2])	
	σ_f	Strength of selection on trait	No loss of generality when σ_m^2 only is explored	0.2	

[1] The numbers outside parentheses are the default values and the numbers inside indicate the parameter range explored.
[2] Rajon and Masel (2011)

Supplementary References:

Rajon, E., and J. Masel, 2011 The evolution of molecular error rates and the consequences for evolvability. Proc. Natl. Acad. Sci. U.S.A. 108**:** 1082-1087.

Appendix B -- Feed-forward regulation adaptively evolves via dynamics rather than topology when there is intrinsic noise

Feed-forward regulation adaptively evolves via dynamics rather than topology when there is intrinsic noise

Short title: Adaptive evolution of feed-forward regulation

Kun Xiong[1], Alex K. Lancaster[2], Mark L. Siegal[3], Joanna Masel[4*]

[1] Department of Molecular and Cellular Biology, University of Arizona, Tucson, Arizona, United States of America

[2] Ronin Institute, Montclair, New Jersey, United States of America

[3] Center for Genomics and Systems Biology, Department of Biology, New York University, New York, New York, United States of America

[4] Department of Ecology and Evolutionary Biology, University of Arizona, Tucson, Arizona, United States of America

* Corresponding author

Email: masel@email.arizona.edu

Abstract

We develop a null model of the evolution of transcriptional regulatory networks, and use it to support an adaptive origin for a canonical “motif”, a 3-node feed-forward loop (FFL) hypothesized to filter out short spurious signals by integrating information from a fast and a slow pathway. Our mutational model captures the intrinsically high prevalence of weak affinity transcription factor binding sites. We also capture stochasticity and delays in gene expression that distort external signals and intrinsically generate noise. Functional FFLs evolve readily under selection for the hypothesized function, but not in negative controls. Interestingly, a 4-node “diamond” motif also emerged as a short spurious signal filter. The diamond uses expression dynamics rather than path length to provide fast and slow pathways. When there is no external spurious signal to filter out, but only internally generated noise, only the diamond and not the FFL evolves.

Introduction

Transcriptional regulatory networks (TRNs) are integral to development and physiology, and underlie all complex traits. An intriguing finding about TRNs is that certain topological "motifs" of interconnected transcription factors (TFs) are over-represented relative to random re-wirings that preserve the frequency distribution of connections. The significance of this finding remains open to debate.

The canonical example is the feed-forward loop (FFL), in which TF A regulates a target C both directly, and indirectly via TF B, and no regulatory connections exist in the opposite direction[1-3]. Each of the three regulatory interactions in a FFL can be either activating or repressing, so there are eight distinct kinds of FFLs (**Fig. S1**)[4]. Given the eight frequencies expected from the ratio of activators to repressors, two of these kinds of FFLs are significantly over-represented[4]. In this paper, we focus on one of these two over-represented types, namely the type 1 coherent FFL (C1-FFL), in which all three links are activating rather than repressing (**Fig. S1**, top left). C1-FFL motifs are an active part of systems biology research today, e.g. they are used to infer the function of specific regulatory pathways[5, 6].

The over-representation of FFLs in observed TRNs is normally explained in terms of selection favoring a function of FFLs. Specifically, the most common adaptive hypothesis is that cells often benefit from ignoring short-lived signals and responding only to durable signals[3, 4, 7]. Evidence that C1-FFLs can perform this function comes from the behavior both of theoretical models[4] and of *in vivo* gene circuits[7]. A C1-FFL can achieve this function when its regulatory logic is that of an "AND" gate, i.e. both the direct path from A to C and the indirect path from A to B to C must be

activated before the response is triggered. In this case, the response will only be triggered if, by the time the signal trickles through the longer path, it is still active on the shorter path as well. This yields a response to long-lived signals but not short-lived signals.

However, just because a behavior is observed, we cannot conclude that the behavior is a historical consequence of past selection favoring that behavior[8, 9]. The explanatory power of this adaptive hypothesis of filtering out short-lived and spurious signals needs to be compared to that of alternative, non-adaptive hypotheses[10]. The over-representation of C1-FFLs might be a byproduct of some other behavior that was the true target of selection[11]. Alternatively, it might be an intrinsic property of TRNs generated by mutational processes – gene duplication patterns have been found to enrich for FFLs in general[12], although not yet C1-FFLs in particular. Adaptationist claims about TRN organization have been accused of being just-so stories, with adaptive hypotheses still in need of testing against an appropriate null model of network evolution[13-23].

Here we develop such a computational null model of TRN evolution, and apply it to the case of C1-FFL over-representation. We include sufficient realism in our model of cis-regulatory evolution to capture the non-adaptive effects of mutation in shaping TRNs. In particular, we consider "weak" TF binding sites (TFBSs) that can easily appear *de novo* by chance alone, and from there be selected to bind a TF more strongly, as well as simulating mutations that duplicate and delete genes.

We also capture the stochasticity of gene expression, which causes the number of mRNAs and hence proteins to fluctuate[24, 25]. This is important, because demand for spurious signal filtering

and hence C1-FFL function may arise not just from external signals, but also from internal fluctuations. Stochasticity in gene expression also shapes how external spurious signals are propagated. Stochasticity is a constraint on what TRNs can achieve, but it can also be adaptively co-opted in evolution[26]; either way, it might underlie the evolution of certain motifs. Most other computational models of TRN evolution that consider gene expression as the major phenotype do not simulate stochasticity in gene expression (but see three notable exceptions[27-29]).

Here we ask whether AND-gated C1-FFLs evolve as a response to selection for filtering out short and spurious external signals. Our new model allows us to compare the frequencies of network motifs arising in the presence of this hypothesized evolutionary cause to motif frequencies arising under non-adaptive control simulations, i.e. evolution under conditions that lack short spurious external signals while controlling both for mutational biases and for less specific forms of selection. We also ask whether other network motifs evolve to filter out short spurious signals, and if so, whether different conditions favor the appearance of different motifs during evolution.

Model overview

We simulate the dynamics of TRNs as the TFs activate and repress one another's transcription over developmental time, to generate gene expression phenotypes on which selection then acts over longer evolutionary timescales. For each moment in developmental time, we simulate the numbers of nuclear and cytoplasmic mRNAs in a cell, the protein concentrations, and the chromatin state of each gene in a haploid genome. Transitions between three possible chromatin states -- Repressed, Intermediate, and Active -- are a stochastic function of TF

binding, and transcription initiation from the Active state is also stochastic. An overview of the model is shown in **Fig. 1**. The pattern of TF binding affects chromatin, which affects transcription rates, eventually feeding back to affect the concentration of TFs and hence their binding. The genotype is specified by a set of cis-regulatory sequences that contain TFBSs to which TFs may bind, by which consensus sequence each TF recognizes and with what affinity, and by 5 gene-specific parameters that control gene expression as a function of TF binding: mean duration of transcriptional bursts, mRNA degradation, protein production, and protein degradation rates, and gene length (which affects delays in transcription and translation). An external signal (**Fig. 1A red**) is treated like another TF, and the concentration of an effector gene (**Fig. 1A blue**) in response is a primary determinant of fitness, combined with a cost associated with gene expression (**Fig. 1B**). Mutants replace resident genotypes as a function of the difference in estimated fitness (**Fig. 1C**). Parameter values, taken as far as possible from *Saccharomyces cerevisiae*, are summarized in **Table S1**. Source code in C is available at https://github.com/MaselLab/network-evolution-simulator.

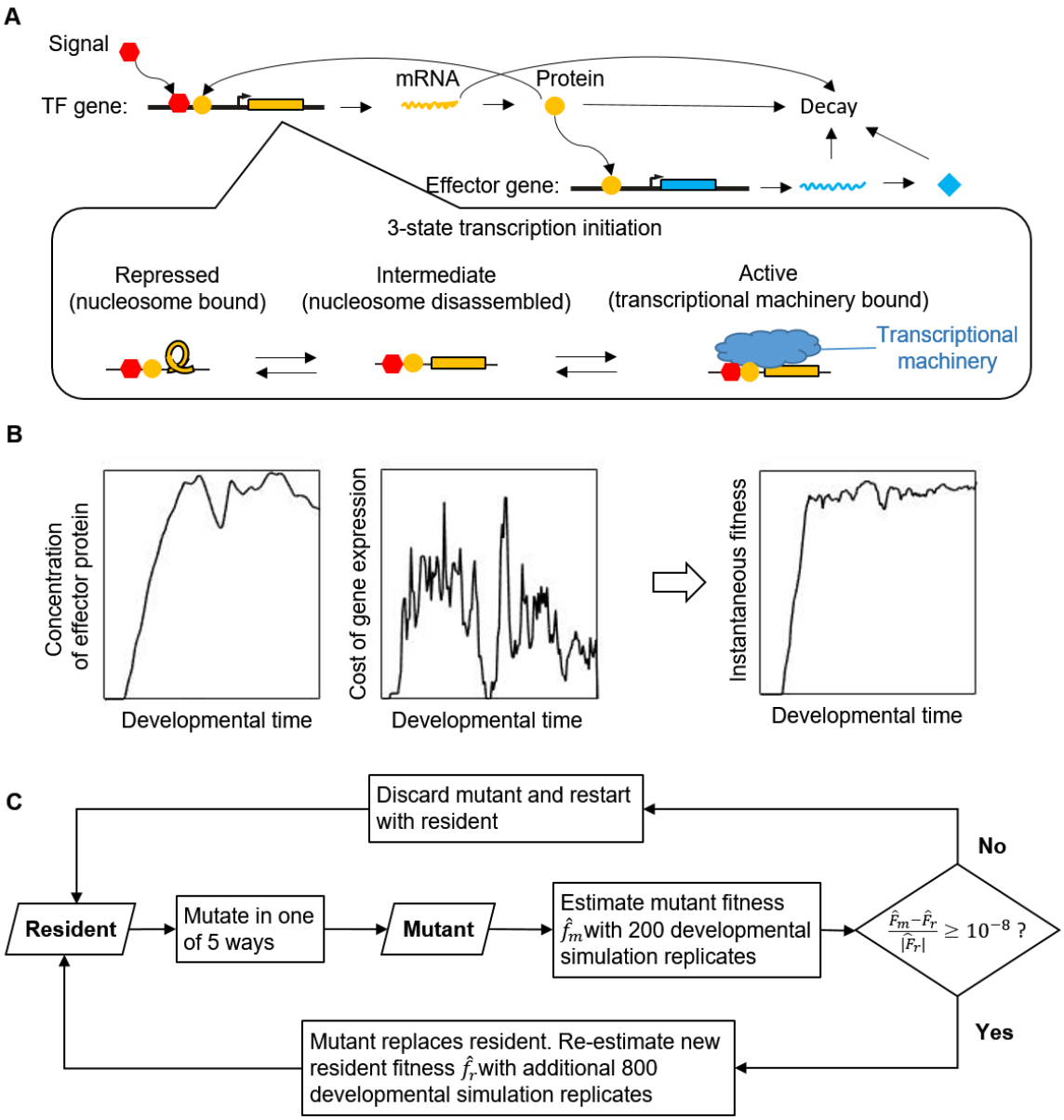

Figure 1. Overview of the model. (A) Simulation of gene expression phenotypes. We show a simple TRN with one TF (yellow) and one effector gene (blue), with arrows for major biological processes simulated in the model. **(B) Phenotype-fitness relationship.** Fitness is primarily determined by the concentration of an effector protein (here shown as beneficial as in Eq. 1, but potentially deleterious in a different environment as in Eq. 2), with a secondary component coming from the cost of gene expression (proportional to the rate of protein production), combined to give an instantaneous fitness at each moment in developmental time. **(C) Evolutionary simulation.** A single resident genotype is replaced when a mutant's estimated fitness is high enough. Stochastic gene expression adds uncertainty to the estimated fitness, allowing less fit mutants to occasionally replace the resident, capturing the flavor of genetic drift.

Transcription factor binding

Transcription of each gene is controlled by TFBSs present within a 150-bp cis-regulatory region. When bound, a TF occupies a stretch of DNA 14 bp long. In the center of this stretch, each TF recognizes an 8-bp consensus sequence, and binds to it with a TF-specific (and mutable) dissociation constant $K_d(0)$. TFs also bind somewhat specifically when there are one or two mismatches, with $K_d(1)$ and $K_d(2)$ values calculated from $K_d(0)$ according to a model of approximately additive binding energy per base pair. With three mismatches, binding occurs at the same background affinity as to any 14 bp stretch of DNA. We model competition between a smaller number of specific higher-affinity binding sites and the much larger number of non-specific binding sites, the latter corresponding to the total amount of nucleosome-free sequence in *S. cerevisiae*. Competition with non-specific binding can be approximated by using an effective dissociation constant $\widehat{K}_d = 10K_d$. See Supplementary Text Section 1 for justification and details of these model choices.

Each TF is either an activator or a repressor. The algorithm for obtaining the probability distribution for *A* activators and *R* repressors being bound to a given cis-regulatory region at a given moment in developmental time is described in Supplementary Text Section 2.

Transcriptional regulation

Activation of the effector gene requires at least two TFBSs to be occupied by activators – not necessarily different activators. The requirement for two activators makes the effector gene capable of evolving an AND-gate via a configuration of TFBSs in which the only way to have two

TFs bound is for them to be different TFs (**Fig. 2**). All other genes are AND-gate-incapable, meaning that their activation requires only one TFBS to be occupied by an activator. P_A denotes the probability of having at least one activator bound for an AND-gate-incapable gene, or two for an AND-gate-capable gene. P_R denotes the probability of having at least one repressor bound.

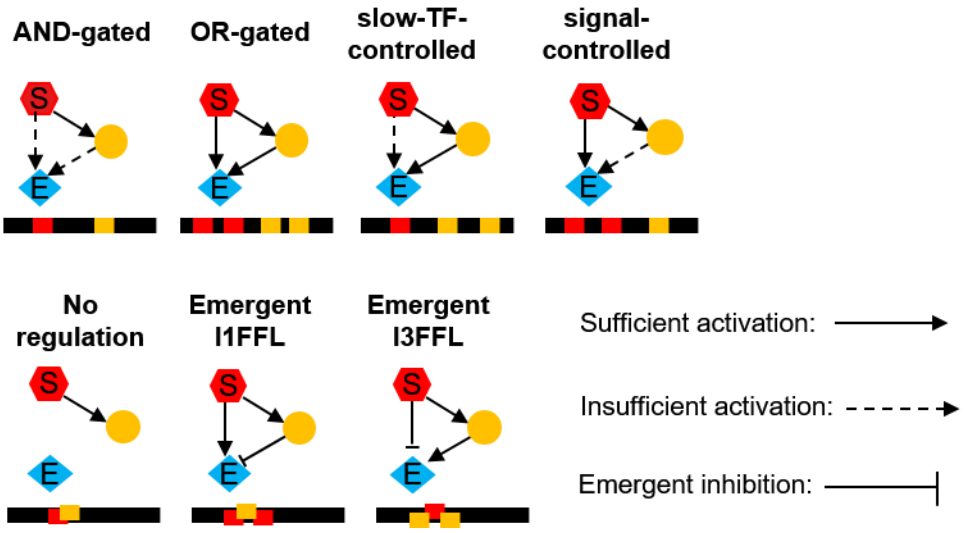

Figure 2. The numbers of TFBSs, and any hindrance between them, determine the regulatory logic of effector expression. We use the pattern of TFBSs (red and yellow bars along black cis-regulatory sequences) to classify the regulatory logic of the effector gene. C1-FFLs are classified first by whether or not they are capable of simultaneously binding the signal and the TF (top vs bottom). Further classification is based on whether either the signal or the TF has multiple non-overlapping TFBSs, allowing it to activate the effector without help from the other (solid arrow). The three subtypes on the bottom (where the signal and TF cannot bind simultaneously) are rarely seen; they are unless otherwise indicated included in "Any logic" and "non-AND-gated" tallies, but are not analyzed separately. Two of them involve emergent repression, creating "incoherent" feed-forward loops (see **Fig. S1** for full FFL naming scheme). Emergent repression occurs when the binding of one activator to its only TFBS prevents the other activator from binding to either of its two TFBSs, hence preventing simultaneous binding of two activators.

Noise in yeast gene expression is well described by a two step process of transcriptional activation[30, 31], e.g. nucleosome disassembly followed by transcription machinery assembly. We denote the three corresponding possible states of the transcription start site as Repressed, Intermediate, and Active (**Fig. 1A**). Transitions between the states depend on the numbers of activator and repressor TFs bound (e.g. via recruitment of histone-modifying enzymes[32, 33]). We make conversion from Repressed to Intermediate a linear function of P_A, ranging from the background rate 0.15 min^{-1} of histone acetylation[34] (presumed to be followed by nucleosome disassembly), to the rate of nucleosome disassembly 0.92 min^{-1} for the constitutively active PHO5 promoter[30]:

$$r_{Rep\_to\_Int} = 0.92P_A + 0.15(1 - P_A).$$

We make conversion from Intermediate to Repressed a linear function of P_R, ranging from a background histone de-acetylation rate of 0.67 min^{-1} [34], up to a maximum of 4.11 min^{-1} (the latter chosen so as to keep a similar maximum:basal rate ratio as that of $r_{Rep\_to\_Int}$):

$$r_{Int\_to\_Rep} = 4.11P_R + 0.67(1 - P_R).$$

We assume that repressors disrupt the assembly of transcription machinery[35] to such a degree that conversion from Intermediate to Active does not occur if even a single repressor is bound. In the absence of repressors, activators facilitate the assembly of transcription machinery[36]. Brown et al.[30] reported that the rate of transcription machinery assembly is 3.3 min^{-1} for a constitutively active PHO5 promoter, and 0.025 min^{-1} when the Pho4 activator of the PHO5 promoter is knocked out. We use this range to set

$$r_{Int\_to\_Act} = 3.3P_{A\_no\_R} + 0.025P_{notA\_no\_R}$$

where $P_{A\_no\_R}$ is the probability of having no repressors and either one (for an AND-gate-incapable gene) or two (for an AND-gate-capable gene) activators bound, and $P_{notA\_no\_R}$ is the probability of having no TFs bound (for AND-gate-incapable genes) or having no repressors and not more than one activator bound (for AND-gate-capable genes).

The promoter sequence not only determines which specific TFBSs are present, but also influences non-specific components of the transcriptional machinery[37, 38]. We capture this via gene-specific but TF-binding-independent rates $r_{Act\_to\_Int}$ with which the machinery disassembles and a burst of transcription ends. In other words, we let TF binding regulate the frequency of "bursts" of transcription, while other properties of the cis-regulatory region regulate their duration. For example, the yeast transcription factor Pho4 regulates the frequency but not duration of bursts of PHO5 expression, by regulating the rates of nucleosome removal and of transition to but not from a transcriptionally active state[30]. Parameterization of $r_{Act\_to\_Int}$ is described in Supplementary Text Section 3.

mRNA and protein dynamics

All genes in the Active state initiate new transcripts stochastically at rate $r_{max\_transc\_init}$ = 6.75 mRNA/min[30], while the time for completing transcription depends on gene length (see Supplementary Text Section 4 for parameterization of gene length and associated delay times). We model a second delay before a newly completed transcript produces the first protein, which

we assume is dominated by translation initiation (length-independent) plus elongation (length-dependent) and not splicing or mRNA export (see Supplementary Text Section 5). After the second delay, we model protein production as continuous at a gene-specific rate $r_{protein\_syn}$ (see Supplementary Text Section 5).

Protein transport into the nucleus is rapid[39] and is approximated as instantaneous and complete, so that the newly produced protein molecules immediately increase the probability of TF binding. Each gene has its own mRNA and protein decay rates, initialized from distributions taken from data (see Supplementary Text Section 6).

All the rates regarding transcription and translation are listed in **Table S1**, including distributions estimated from data, and hard bounds imposed to prevent unrealistic values arising during evolutionary simulations.

Developmental simulation

Our algorithm is part stochastic, part deterministic. We use a Gillespie algorithm[40] to simulate stochastic transitions between Repressed, Intermediate, and Active chromatin states, and to simulate transcription initiation and mRNA decay events. Fixed (i.e. deterministic) delay times are simulated between transcription initiation and completion, and between transcript completion and the production of the first protein. Protein production and degradation are described deterministically with ODEs, and updated frequently in order to recalculate TF concentrations and hence chromatin transition rates. Details of our simulation algorithm are

given in the Supplementary Text Section 7. We initialize developmental simulations with no mRNA or protein, and all genes in the Repressed state.

Selection

Filtering out short spurious signals is a special case of signal recognition. In environment 1, expressing the effector is beneficial, and in environment 2 it is deleterious. We select for TRNs that take information from the signal and correctly decide whether to express the effector. Fitness is a weighted average across separate developmental simulations in the two environments, one with a signal and one without. In both cases, we begin each developmental simulation with no signal. To ensure that gene expression changes in response to the signal, and not via an internal timer, we simulate a burn-in phase with duration drawn from an exponential distributed truncated at 30 minutes, with un-truncated mean of 10 minutes. By having no fitness effects of gene expression during the burn-in, we eliminate a significant source of noise in fitness estimation due to variable burn-in duration. In our control condition, at the end of the burn-in, the signal suddenly switches to a constant "on" level in environment 1, and remains off in environment 2. In our test condition (**Fig. 3**), the signal is turned on in the same way in environment 1 but is also briefly turned on (for the first 10 minutes after the burn-in) in environment 2 – selection is to ignore this short spurious signal. The signal is treated as though it were an activating TF whose concentration is controlled externally, with an "off" concentration of zero and an "on" concentration of 1,000 molecules per cell, which is the typical per-cell number of a yeast TF[41].

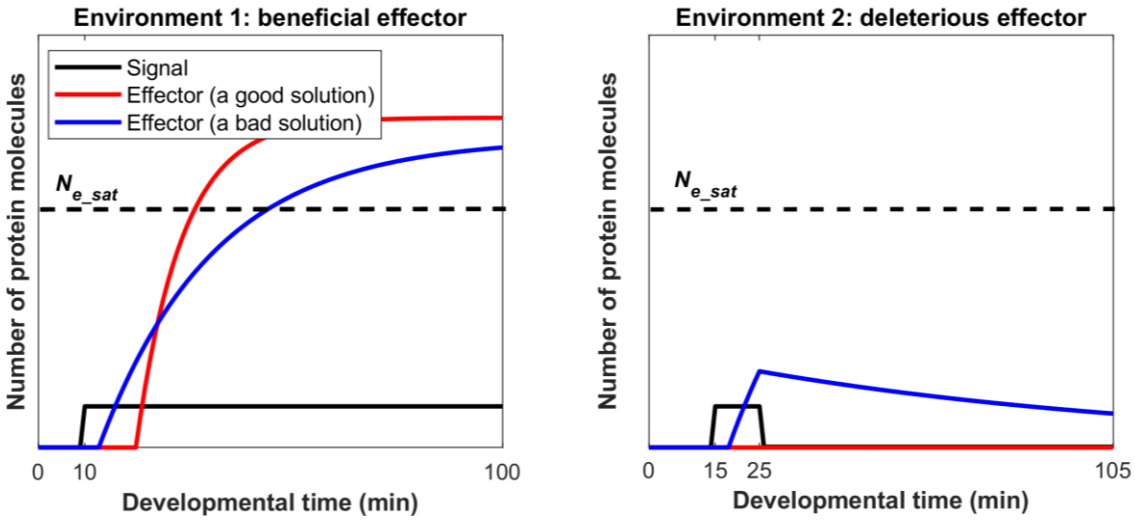

Figure 3. Selection for filtering out short spurious signals. Each selection condition averages fitness across simulations in two environments. The effectors have different fitness effects in the two environments, and the signal also behaves differently in the two environments. Simulations begin with zero mRNA and protein, and all genes at the Repressed state. Each simulation is burned in for a randomly sampled length of time in the absence of signal (shown here as 10 minutes in environment 1, and 15 minutes in environment 2), and continues for another 90 minutes after the burn-in. The signal is shown in black. Red illustrates a good solution in which the effector responds appropriately in each of the environments, while blue shows an inferior solution. See **Fig. S2** for examples of high-fitness and low-fitness evolved phenotypes, where, as shown in this schematic, high-fitness solutions have longer delays followed by more rapid responses thereafter.

We make fitness quantitative in terms of a "benefit" $B(t)$ as a function of the amount of effector protein $N_e(t)$ at developmental time t. Our motivation is a scenario in which the effector protein is responsible for directing resources from a metabolic program favored in environment

2 to a metabolic program favored in environment 1. In environment 1, where the effector produces benefits,

$$B(t) = \begin{cases} b_{max} \frac{N_e(t)}{N_{e\_sat}}, & N_e(t) < N_{e\_sat} \\ b_{max}, & N_e(t) \geq N_{e\_sat} \end{cases}, \quad (1)$$

where b_{max} is the maximum benefit if all resources were redirected, and N_{e_sat} is the minimum amount of effector protein needed to achieve this. Similarly, in environment 2

$$B(t) = \begin{cases} b_{max} - b_{max} \frac{N_e(t)}{N_{e_{sat}}}, & N_e(t) < N_{e_{sat}} \\ 0, & N_e(t) \geq N_{e_{sat}} \end{cases}. \quad (2)$$

We set N_{e_sat} to 10,000 molecules, which is about the average number of molecules of a metabolism-associated protein per cell in yeast[41]. Without loss of generality given that fitness is relative, we set b_{max} to 1.

A second contribution to fitness comes from the cost of gene expression $C(t)$ (**Fig. 1B, middle**). We make this cost proportional to the total protein production rate. We estimate a fitness cost of gene expression of 2×10^{-6} per protein molecule translated per minute, based on the cost of expressing a non-toxic protein in yeast[42] (see Supplementary Text Section 7 for details).

We simulate gene expression for 90 minutes plus the duration of the burn-in (**Fig. 3**). A "cellular fitness" in a given environment is calculated as the average instantaneous fitness $B(t)$-$C(t)$ over the 90 minutes. We consider environment 2 to be twice as common as environment 1 (a

"signal" should be for an uncommon event rather than the default), and take the corresponding weighted average.

Evolutionary simulation

We simulate a novel version of origin-fixation (weak-mutation-strong-selection) evolutionary dynamics, i.e. the population contains only one resident genotype at any time, and mutant genotypes are either rejected or chosen to be the next resident (Fig. 1C). Despite the fact that our mutant acceptance rule (see below) was chosen to maximize computational efficiency, our model usually takes 10 CPUs 1-3 days to complete an evolutionary simulation; modeling a heterogeneous population is clearly out of the question. We note that genetic homogeneity entails ignoring some important population genetic phenomena. First, if there were recombination, heterogeneity would favor mutations that combine well with a range of other genotypes. Second, clonal interference would shift evolution toward beneficial mutations of larger effect[43] (an effect we can mimic by modifying the value 10^{-8} in the equation below). Third, polymorphic populations would evolve mutational robustness[44]. None of these three effects seems *a priori* likely to change our conclusions, although the possibility cannot be ruled out.

Estimators $\hat{F}$ of genotype fitness are averages of the cellular fitness values of 200 developmental replicates per environment in the case of the mutant, plus an additional 800 should it be chosen to be the next resident. The mutant replaces the resident if

$$\frac{\hat{F}_{mutant} - \hat{F}_{resident}}{|\hat{F}_{resident}|} \geq 10^{-8}.$$

This differs from Kimura's[45] equation for fixation probability, but captures the flavor of genetic drift. Genetic drift allows slightly deleterious mutations to occasionally fix, and beneficial mutations to sometimes fail to do so, even as the probability of fixation is monotonic with fitness. This is also achieved by our procedure, because of stochastic deviations of $\hat{F}$ from true genotype fitness. The number of developmental replicates captures the flavor of effective population size.

Note that it is possible, especially at the beginning of an evolutionary simulation, for relative fitness to be paradoxically negative. This occurs when a randomly initialized genotype does not express the effector (garnering no fitness benefit), but does express other genes (accruing a cost of expression); this combination makes fitness negative. In this rare case, for simplicity, we use the absolute value of $\hat{F}$ on the denominator.

If 2,000 successive mutants are all rejected, the simulation is terminated; upon inspection, we found that these resident genotypes had evolved to not express the effector in either environment. We refer to each change in resident genotype as an evolutionary step. We stop the simulation after 50,000 evolutionary steps; at this time, most replicate simulations seem to have reached a fitness plateau (**Fig. S3**); we analyze all replicates except those terminated early. To reduce the frequency of early termination in the case where the signal was not allowed to directly regulate the effector, we used a burn-in phase selecting on a more accessible intermediate phenotype (see Supplementary Text Section 10). In this case, burn-in occurred for 1,000 evolutionary steps, followed by the usual 50,000 evolutionary steps with selection for the phenotype of interest (**Fig. S3**, right panels). Most replicates found a stable fitness plateau

within 10,000 evolutionary steps, although some replicates were temporarily trapped at a low fitness plateau (**Fig. S3**).

Genotype Initialization

We initialize genotypes with 3 activator genes, 3 repressor genes, and 1 effector gene. Cis-regulatory sequences and consensus binding sequences contain As, Cs, Gs, and Ts sampled with equal probability. Rate constants associated with the expression of each gene are sampled from the distributions summarized in **Table S1**.

Mutation

A genotype is subjected to 5 broad classes of mutation, at rates summarized in **Table S2** and justified in Supplementary Text Section 9. First are single nucleotide substitutions in the cis-regulatory sequence; the resident nucleotide mutates into one of the other three types of nucleotides with equal probability. Second are single nucleotide changes to the consensus binding sequence of a TF, with the resident nucleotide mutated into recognizing one of the other three types with equal probability. Both of these types of mutation can affect the number and strength of TFBSs.

Third are gene duplications or deletions. Because computational cost scales steeply (and non-linearly) with network size, we do not allow effector genes to duplicate once there are 5 copies, nor TF genes to duplicate once the total number of TF gene copies is 19. We also do not allow the signal, the last effector gene, nor the last TF gene to be deleted.

Fourth are mutations to gene-specific expression parameters. Most of these (L, $r_{Act\_to\_Int}$, $r_{protein\_syn}$, r_{mRNA_deg}, and $r_{protein\_deg}$) apply to both TFs and effector genes, while mutations to the gene-specific values of $K_d(0)$ apply only to TFs. Each mutation to L increases or decreases it by 1 codon, with equal probability unless L is at the upper or lower bound. Effect sizes of mutations to the other five parameters are modeled in such a way that mutation would maintain specified log-normal stationary distributions for these values, in the absence of selection or arbitrary bounds (see Supplementary Text Section 9 for details). Upper and lower bounds (Supplementary Text Section 9) are used to ensure that selection never drives these parameters to unrealistic values.

Fifth is conversion of a TF from being an activator to being a repressor, and vice versa. The signal is always an activator, and does not evolve.

Importantly, this scheme allows for divergence following gene duplication. When duplicates differ due only to mutations of class 4, i.e. protein function is unchanged, we refer to them as "copies" of the same gene, encoding "protein variants". Mutations in classes 2 and 5 can create a new protein.

Table S3 summarizes the tendencies of different mutation types to be accepted, and to contribute to evolution. Acceptance rates are high, indicative of substantial nearly neutral evolution, in which slightly deleterious mutations are fixed and subsequently compensated for.

Results

Functional AND-gated C1-FFLs evolve readily under selection for filtering out a short spurious signal

We begin by simulating the easiest case we can devise to allow the evolution of C1-FFLs for their purported function of filtering out short spurious signals. The signal is allowed to act directly on the effector, after which all that needs to evolve is a single activating TF between the two, as well as AND-logic for the effector (**Fig. 2**, top left; see "Transcriptional regulation" in the Model Overview for how AND-logic evolution is handled). We score network motifs at the end of a set period of evolution (see Supplemental Text Section 11 for details), further classifying evolved C1-FFLs into subtypes based on the presence of non-overlapping TFBSs (**Fig. 2**). The adaptive hypothesis predicts the evolution of the C1-FFL subtype with AND-regulatory logic, which requires the effector to be stimulated both by the signal and by the slow TF. While all evolutionary replicates show large increases in fitness, the extent of improvement varies dramatically, indicating whether or not the replicate was successful at evolving the phenotype of interest rather than becoming stuck at an alternative locally optimal phenotype (**Fig. 4A**). AND-gated C1-FFLs frequently evolve in replicates that reach high fitness outcomes, but not replicates that reach lower fitness (**Fig. 4B**).

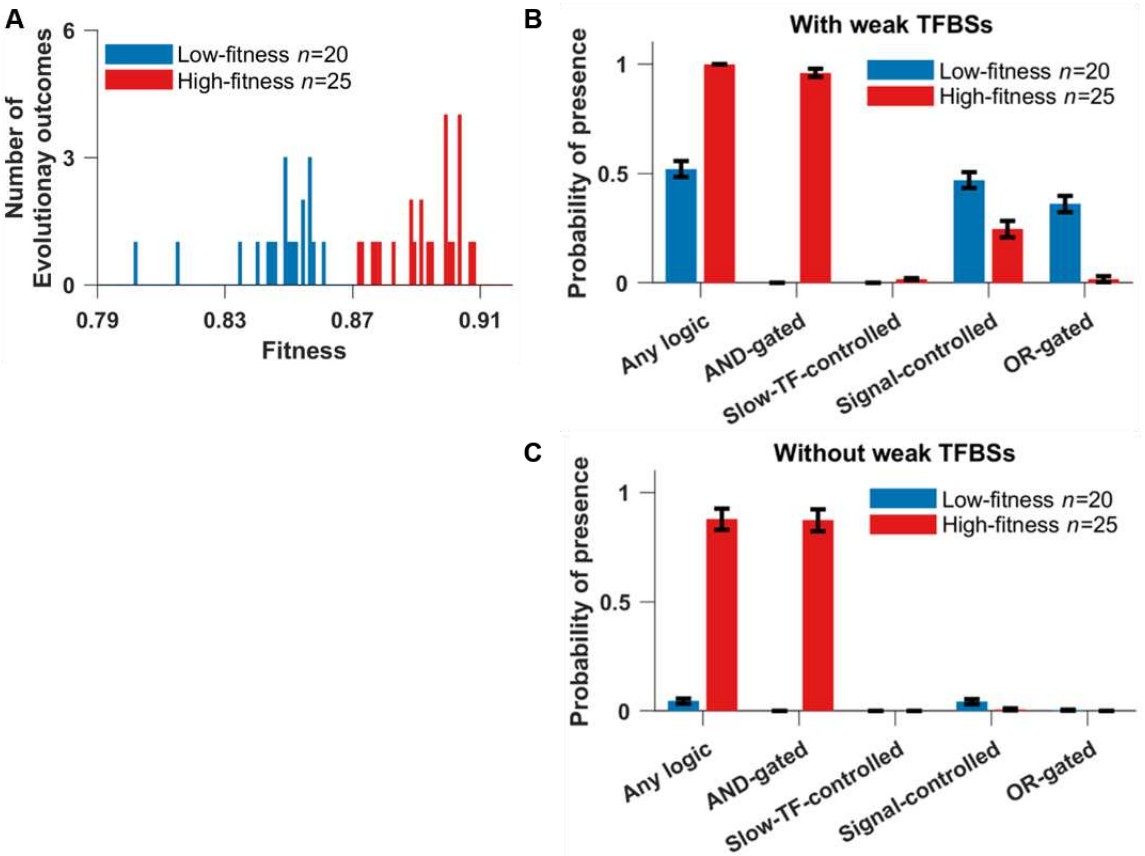

Figure 4. AND-gated C1-FFLs are associated with a successful response to selection for filtering out short spurious signals. (A) Distribution of fitness outcomes across replicate simulations, calculated as the average fitness over the last 10,000 steps of the evolutionary simulation. We divide genotypes into a low-fitness group (blue) and a high-fitness group (red) using as a threshold an observed gap in the distribution. **(B)** High fitness replicates are characterized by the presence of an AND-gated C1-FFL. "Any logic" counts the presence of any of the seven subtypes shown in **Fig. 2B**. Because one TRN can contain multiple C1-FFLs of different subtypes, each of which are scored, the sum of the occurrences of all seven subtypes will generally be more than "Any logic". See Supplementary Text Section 11 for details on the calculation of the y-axis. **(C)** The over-representation of AND-gated C1-FFLs becomes even more pronounced relative to alternative logic-gating when weak (two-mismatch) TFBSs are excluded while scoring motifs. Data are shown as mean±SE of the occurrence over replicate evolution simulations.

We also see C1-FFLs that, contrary to expectations, are not AND-gated. Non-AND-gated motifs are found more often in low fitness than high fitness replicates (**Fig. 4B**), indicating that the preference for AND-gates is associated with adaptation rather than mutation bias. However, some non-AND-gated motifs are still found even in the high fitness replicates. This is because motifs and their logic gates are scored on the basis of all TFBSs, even those with two mismatches and hence low binding affinity. Unless these weak TFBSs are deleterious, they will appear quite often by chance alone. A random 8-bp sequence has probability $\binom{8}{2} \times 0.25^6 \times 0.75^2 = 0.0038$ of being a two-mismatch binding site for a given TF. In our model, a TF has the potential to recognize 137 different sites in a 150-bp cis-regulatory sequence (taking into account steric hindrance at the edges), each with 2 orientations. Thus, by chance alone a given TF will have $0.0038 \times 137 \times 2 \approx 1$ two-mismatch binding sites in a given cis-regulatory sequence (ignoring palindromes for simplicity), compared to only ~0.1 one-mismatch TFBSs. Non-AND-gated C1-FFLs mostly disappear when two-mismatch TFBSs are excluded, but the AND-gated C1-FFLs found in high fitness replicates do not (**Fig. 4C**).

To confirm the functionality of these AND-gated C1-FFLs, we mutated the evolved genotype in two different ways (**Fig. 5A**) to remove the AND regulatory logic. As expected, this lowers fitness in the presence of the short spurious signal but increases fitness in the presence of constant signal, with a net reduction in fitness (**Fig. 5B**). This is consistent with AND-gated C1-FFLs representing a tradeoff, by which a more rapid response to a true signal is sacrificed in favor of the greater reliability of filtering out short spurious signals.

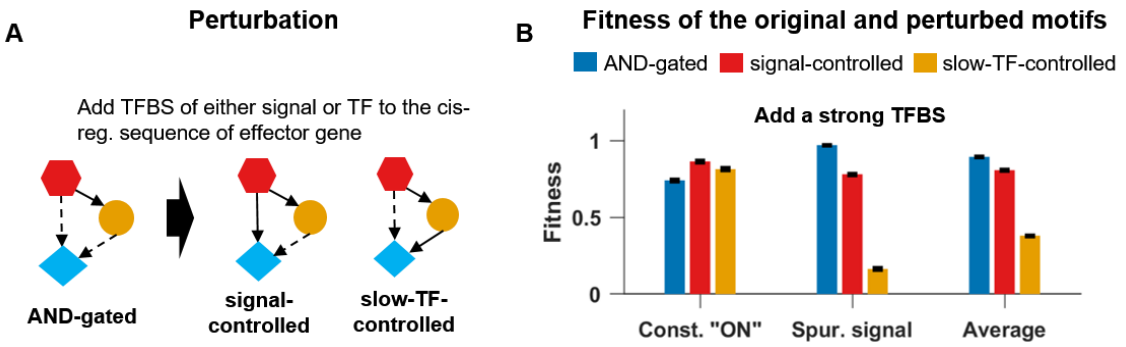

Figure 5. Destroying the AND-logic of a C1-FFL removes its ability to filter out short spurious signals. (**A**) For each of the *n* = 25 replicates in the high fitness group in **Fig. 4**, we perturbed the AND-logic in two ways, by adding one binding site of either the signal or the slow TF to the cis-regulatory sequence of the effector gene. **(B)** For each replicate, the fitness of the original motif (blue) or of the perturbed motif (red or orange) was averaged across the subset of evolutionary steps with an AND-gated C1-FFL and lacking other potentially confounding motifs (see Supplementary Text Section 11 for details). Destroying the AND-logic slightly increases the ability to respond to the signal, but leads to a larger loss of fitness when short spurious signals are responded to. Fitness is shown as mean±SE over replicate evolutionary simulations.

Adaptive motifs are constrained not only in their topology and regulatory logic, but also in the parameter space of their component genes. In particular, there is selection for rapid synthesis of both effector and TF proteins, as well as rapid degradation of effector mRNA and protein (**Table S4**). Fast effector degradation reduces the transient expression induced by the short spurious signal (**Fig. S2**).

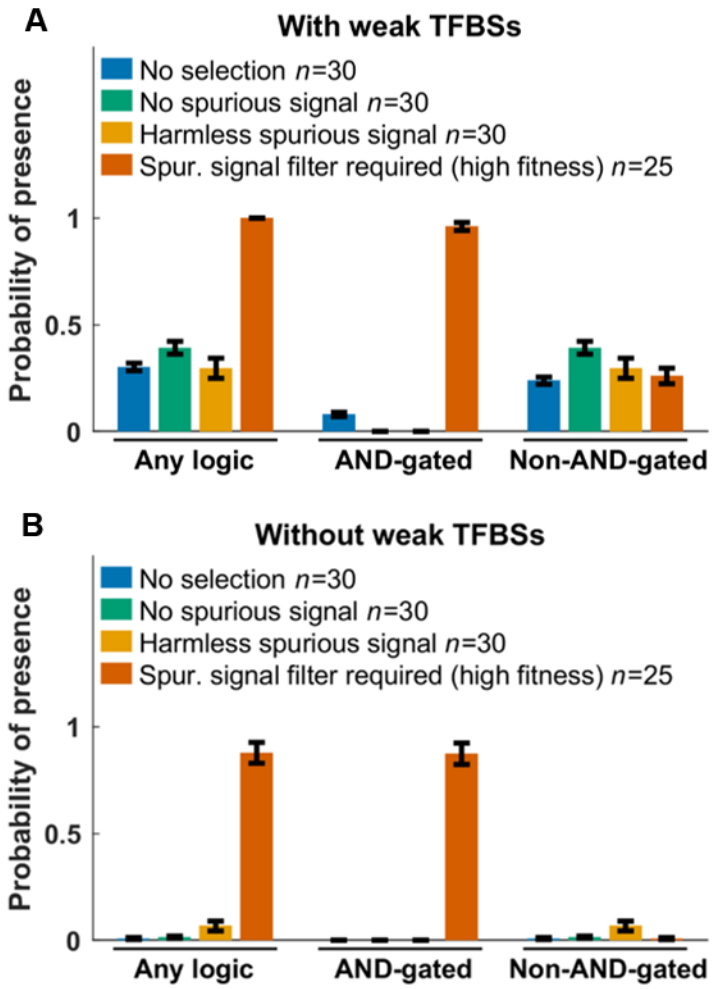

Figure 6. Selection for filtering out short spurious signals is the primary cause of C1-FFLs. TRNs are evolved under different selection conditions, and we score the probability that at least one C1-FFL is present (Supplementary Text Section 11). Weak (two-mismatch) TFBSs are included **(A)** or excluded **(B)** during motif scoring. Data are shown as mean±SE over evolutionary replicates. C1-FFL occurrence is similar for high-fitness and low-fitness outcomes in control selective conditions (**Fig. S4**), and so all evolutionary outcomes were combined. "Spurious signal filter required (high fitness)" uses the same data as in **Fig. 4**.

To test the extent to which AND-gated C1-FFLs are a specific response to selection to filter out short spurious signals, we simulated evolution under three negative control conditions: 1) no

selection, i.e. all mutations are accepted to become the new resident genotype; 2) no spurious signal, i.e. selection to express the effector under a constant "ON" signal and not under a constant "OFF" signal; 3) harmless spurious signal, i.e. selection to express the effector under a constant "ON" environment whereas effector expression in the "OFF" environment with short spurious signals is neither punished nor rewarded beyond the cost of unnecessary gene expression. AND-gated C1-FFLs evolve much less often under all three negative control conditions (**Fig. 6**), showing that their prevalence is a consequence of selection for filtering out short spurious signals, rather than a consequence of mutational bias and/or simpler forms of selection. C1-FFLs that do evolve under control conditions tend not to be AND-gated (**Fig. 6A**), and mostly disappear when weak TFBSs are excluded during motif scoring (**Fig. 6B**).

Diamond motifs are an alternative adaptation in more complex networks

In real biological situations, sometimes the source signal will not be able to directly regulate an effector, and must instead operate via a longer regulatory pathway involving intermediate TFs[46]. In this case, even if the signal itself takes the idealized form shown in **Fig. 3**, its shape after propagation may become distorted by the intrinsic processes of transcription. Motifs are under selection to handle this distortion.

To enforce indirect regulation, we ran simulations in which the signal was only allowed to bind to the cis-regulatory sequences of TFs and not of effector genes. The fitness distribution of the evolutionary replicates has no obvious gaps (**Fig. S5**), so we compared the highest fitness, lowest fitness, and median fitness replicates. In agreement with results when direct regulation is

allowed, genotypes of low and medium fitness contain few AND-gated C1-FFLs, while high fitness genotypes contain many more (**Fig. 7B, left and right**).

While visually examining the network context of these C1-FFLs, we discovered that many were embedded within AND-gated "diamonds". In a diamond, the signal activates the expression of two genes that encode different TFs, and the two TFs activate the expression of an effector gene (**Fig. 7A middle**). When one of the two TF genes activates the other, then a C1-FFL is also present among the same set of genes; we call this topology a "FFL-in-diamond" (**Fig. 7A right**), and the prevalence of this configuration drew our attention toward diamonds. This led us to discover that AND-gated diamonds also occurred frequently without AND-gated C1-FFLs, in the configuration we call "isolated diamonds" (**Fig. 7A middle**). Note that it is in theory possible, but in practice uncommon, for diamonds to be part of more complex conjugates. Systematically scoring the AND-gated isolated diamond motif confirmed its high occurrence (**Fig. 7B and C, middle**).

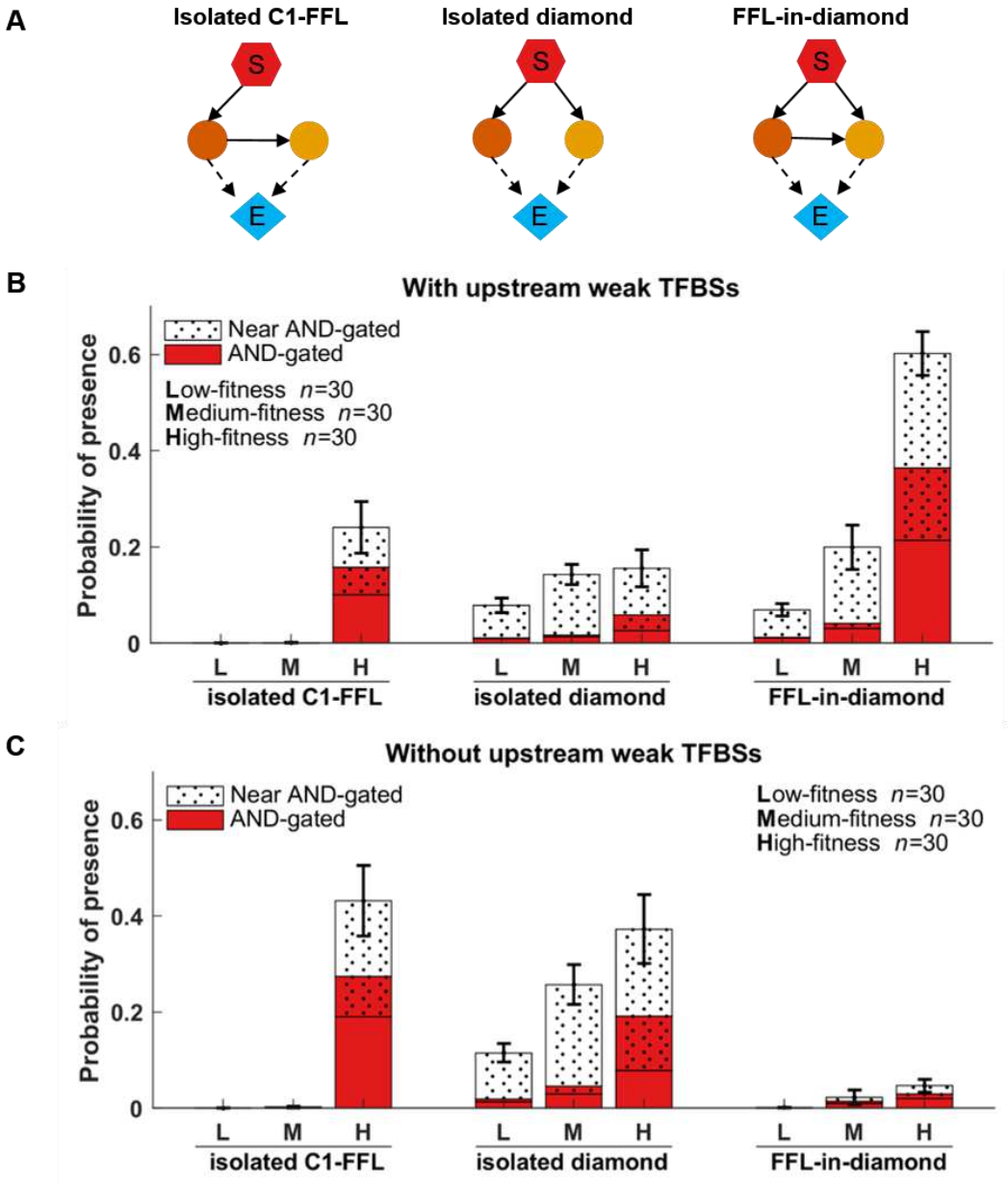

Figure 7. Both AND-gated C1-FFLs and AND-gated diamonds (A) are associated with high fitness in complex networks under selection to filter out short spurious signals. Out of 160 simulations (**Fig. S5**), we took the 30 with the highest fitness (H), the 30 with the lowest fitness (L), and 30 of around median fitness (M). AND-gated motifs are scored while including weak TFBSs in the effectors' cis-regulatory regions, near-AND-gated motifs are those scored only when these weak TFBSs are excluded. It is possible for the same genotype to contain one of each, resulting in overlap between the red AND-gated columns and the dotted near-AND-gated columns. Weak TFBSs upstream in the TRN, i.e. not in the effector, are shown both included (**B**) and excluded (**C**). See Supplementary Text Section 11 for y-axis calculation details. Error bars show mean±SE of the proportion of evolutionary steps containing the motif in question, across replicate evolutionary simulations.

An AND-gated C1-FFL integrates information from a short/fast regulatory pathway with information from a long/slow pathway, in order to filter out short spurious signals. A diamond achieves the same end of integrating fast and slowly transmitted information via differences in the gene expression dynamics of the two regulatory pathways, rather than via topological length (**Fig. 8**). The fast and slow pathways could be distinguished in a number of ways, e.g. by the slope at which the transcription factor concentration increases or the time at which it exceeds a threshold or plateaus. We found it convenient to identify the "fast TF" as the one with the higher protein degradation rate. Specifically, we use the geometric mean of the protein degradation rate over gene copies of a TF in order to differentiate the two TFs. The parameter values of the fast TF are more evolutionarily constrained than those of the slow TF (**Table S5**). In particular, there is selection for rapid degradation of the fast TF protein and mRNA (**Table S5**). Isolated AND-gated C1-FFLs also show pronounced selection for the TF in the fast pathway to have rapid protein degradation (**Table S6**).

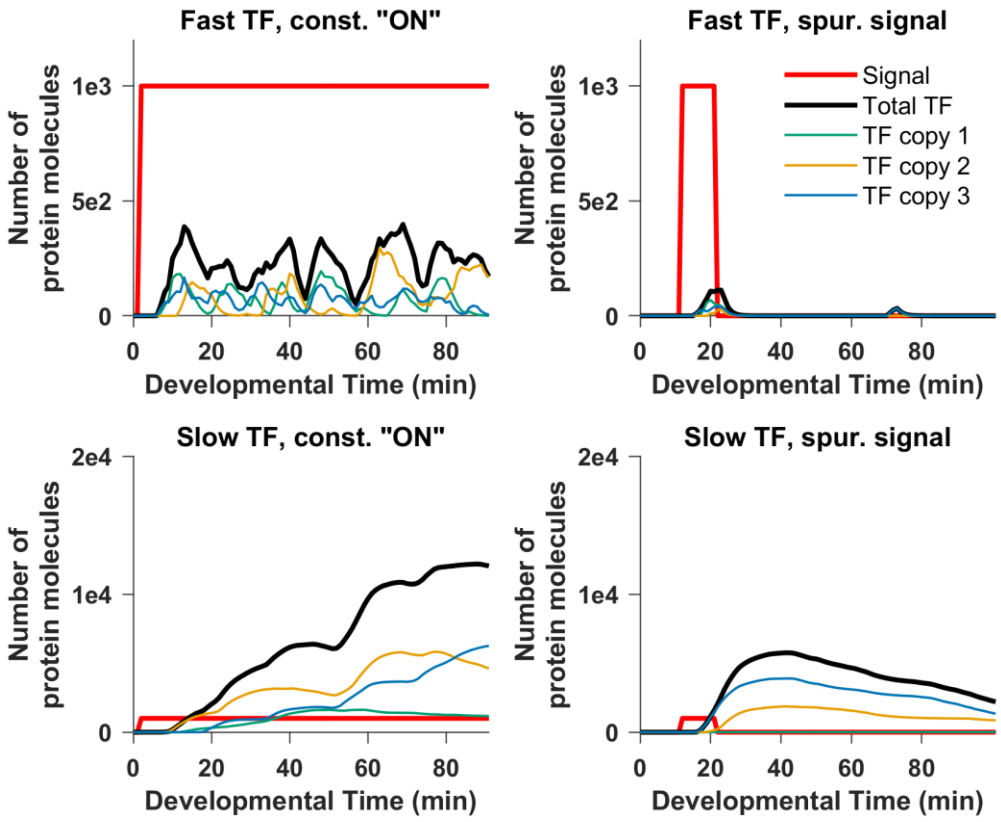

Figure 8. The two intermediate TFs in an AND-gated "diamond" motif have different expression dynamics and propagate the signal at different speeds. Expression of the two TFs in one representative genotype from the one high-fitness evolutionary replicate in **Fig. 7B** that evolved an AND-gated isolated diamond is shown. Each TF is a different protein, and each is encoded by 3 gene copies, shown separately in color, with the total in thick black. The expression of one TF plateaus faster than that of the other; this is characteristic of the AND-gated diamond motif, and leads to the same functionality as the AND-gated C1-FFL.

But mutational biases make it difficult to evolve very fast-degrading mRNA and protein. And even when they do evolve, fast degradation keeps the fast TF at low concentrations. To compensate, the fast TF must overcome mutational bias to also evolve high binding affinity and rapid protein synthesis (**Table S5**, **Table S6**).

Note that a simple transcriptional cascade, signal -> TF -> effector, has also been found experimentally to filter out short spurious signals when the intermediate TF is rapidly degraded, dampening the effect of a brief signal[47]. Two such transcriptional cascades involving different intermediate TFs form a diamond, so the utility of a single cascade is a potential explanation for the high prevalence of double-cascade diamonds. However, in this case we would have no reason to expect marked differences in expression dynamics between the two TFs, as illustrated in **Fig. 8** and **Table S5**. Enrichment for AND-gates (**Fig. 7**) indicates selection to integrate information from the two cascades. On the other hand, we do find some non-AND-gated diamonds, and these might best be considered as cascades. Inspection of their parameter values reveals that in these diamonds, both TFs have fast-degrading mRNAs and proteins so that both TFs shut down rapidly once signal is turned off. This makes such diamonds less vulnerable to spurious signals, reducing the need for the AND gate. The difficulty of evolving not just one but two fast-degrading high-affinity TFs likely explains why non-AND-gated diamonds are rare. As we will see in the next section, these non-AND-gated diamonds are nevertheless scored as AND-gated when weak TFBSs are excluded.

Weak TFBSs can change how adaptive motifs are scored even when they do not change function

Results depend on whether we include weak TFBSs when scoring motifs. Weak TFBSs can either be in the effector's cis-regulatory region, affecting how the regulatory logic is scored, or in TFs upstream in the TRN, affecting only the presence or absence of motifs. When a motif is scored as AND-gated only when two-mismatch TFBSs in the effector are excluded, we call it a "near-

AND-gated" motif. Recall from **Fig. 2** that effector expression requires two TFs to be bound, with only one TFBS of each type creating an AND-gate. When a second, two-mismatch TFBS of the same type is present, we have a near-AND-gate. TFs may bind so rarely to this weak affinity TFBS that its presence changes little, making the regulatory logic still effectively AND-gated. A near-AND-gated motif may therefore evolve for the same adaptive reasons as an AND-gated one. **Fig. 7B** and **C** shows that both AND-gated and near-AND-gated motifs are enriched in the higher fitness genotypes.

When we exclude upstream weak TFBSs while scoring motifs, FFL-in-diamonds are no longer found, while the occurrence of isolated C1-FFLs and diamonds increases (**Fig. 7C**). This makes sense, because adding one weak TFBS, which can easily happen by chance alone, can convert an isolated diamond or C1-FFL into a FFL-in-diamond (added between intermediate TFs, or from signal to slow TF, respectively).

AND-gated isolated C1-FFLs appear mainly in the highest fitness outcomes, while AND-gated isolated diamonds appear in all fitness groups (**Fig. 7C**), suggesting that diamonds are easier to evolve. 25 out of 30 high-fitness evolutionary replicates are scored as having a putatively adaptive AND-gated or near-AND-gated motif in at least 50% of their evolutionary steps when upstream weak TFBSs are ignored (close to addition of bars in **Fig. 7C**, because these two AND-gated motifs rarely coexist in a high-fitness genotype).

Just as for the AND-gated C1-FFLs evolved under direct regulation and analyzed in **Fig. 5**, perturbation analysis supports an adaptive function for AND-gated C1-FFLs and diamonds evolved under indirect regulation (**Fig. 9A.i, 9B.i**). Breaking the AND-gate logic of these motifs by

adding a (strong) TFBS to the effector cis-regulatory region reduces the fitness under the spurious signal but increases it under the constant “ON” beneficial signal, resulting in a net decrease in the overall fitness.

If we add a weak (two-mismatch) TFBS instead, this converts an AND-gated motif to a near-AND-gated motif. This lowers fitness only when the extra link is from the slow TF to the effector, and not when the extra link is from the fast TF to the effector (**Fig. 9A.ii, 9B.ii)**.

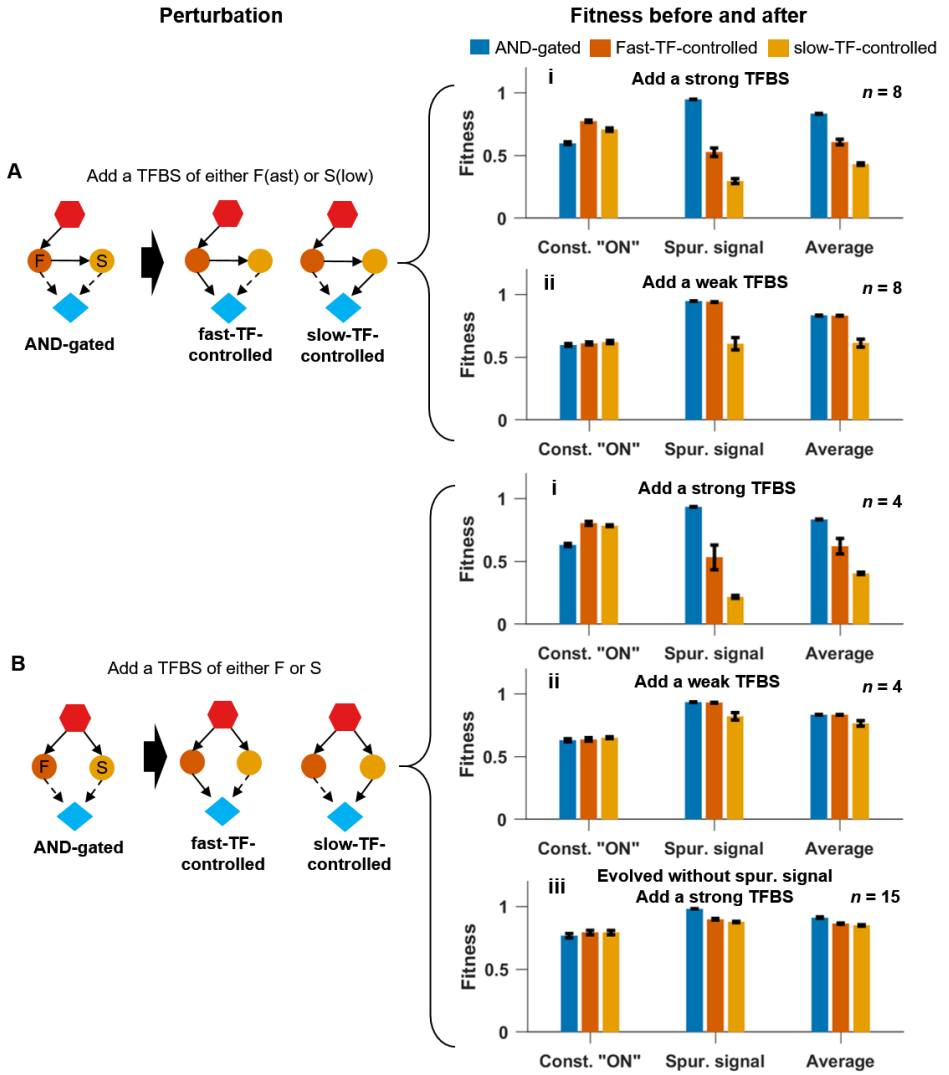

Figure 9. Perturbation analysis shows that AND-gated C1-FFLs (A) and diamonds (B) filter out short spurious signals. We add a strong TFBS **(i)** or a two-mismatch TFBS **(ii)** or **(iii)**; the latter creates near-AND-gated motifs. Allowing the effector to respond to the slow TF alone slightly increases the ability to respond to the signal, but leads to a larger loss of fitness when effector expression is undesirable. Allowing the effector to respond to the fast TF alone does so only when the conversion uses a strong TFBS not a two-mismatch TFBS. **(A)** We perform the perturbation on 8 of the 18 high-fitness replicates from **Fig.7B** that evolved an AND-gated C1-FFL. **(B)** (**i**) and (**ii**) are based on 4 of the 26 high-fitness replicates that evolved an AND-gated diamond in **Fig. 7B**, (**iii**) is based on 15 of the 37 replicates that evolved an AND-gated diamond in response to selection for signal recognition in the absence of an external spurious signal (**Fig. 10B**). Replicate exclusion was based on the co-occurrence of other motifs with the potential to confound results (see Supplementary Text Section 12 for details). Fitness is shown as mean±SE of over replicate evolutionary simulations, calculated as described for **Fig. 5**.

Indeed, these extra links are tolerated during evolution too. If we take the 16 high-fitness replicates that contain a near-AND-gated C1-FFL in at least 1% of the evolutionary steps, then for 15 replicates of the 16, at least 88% of the near-AND-gated C1-FFLs in each of the 15 replicates are only near-AND-gated because of extra weak TFBSs for the fast TF. In the remaining 1 replicate, 93% of the near-AND-gated C1-FFLs have extra weak TFBSs specific for each of the TFs (and are therefore scored as OR-gated). In this last replicate, the two TFs in these OR-gated C1-FFLs have high and similar protein degradation rates, reducing the need for an AND gate for reasons discussed earlier. We similarly examine high-fitness replicates that, when upstream weak TFBSs are excluded, contain a near-AND-gated diamond in at least 1% of the evolutionary steps. In 15 of these 24 evolutionary replicates, the near-AND regulatory logic is in most evolutionary steps due to an extra weak TFBS of the fast TF, in 8 replicates (all of them OR-gated, like the OR-gated C1-FFL already discussed) it is due to weak TFBSs for each of the TFs, and in only 1 replicate is it due to an extra TFBS for the slow TF. For the latter two categories, both TFs in near-AND-gated diamonds have high and similar protein degradation rates. By chance alone, fast and slow TF should be equally likely to contribute the weak TFBS that makes a motif near-AND-gated rather than AND-gated. This expected 50:50 ratio can be rejected from our observed 15:0 and 15:1 ratios with $p = 3 \times 10^{-5}$ and $p = 3 \times 10^{-4}$, respectively (cumulative binomial distribution, one-sided test). This non-random occurrence of weak TFBSs creating near-AND-gates illustrates how even weak TFBSs can be shaped by selection against some (but not all) motif-breaking links.

AND-gated isolated diamonds also evolve in the absence of external spurious signals

We simulated evolution under the same three control conditions as before, this time without allowing the signal to directly regulate the effector. In the "no spurious signal" and "harmless spurious signal" control conditions, motif frequencies are similar between low and high fitness genotypes (**Fig. S6, Fig. S7)**, and so our analysis includes all evolutionary replicates. When weak (two-mismatch) TFBSs are excluded, AND-gated isolated C1-FFLs are seen only after selection for filtering out a spurious signal, and not under other selection conditions (**Fig. 10A**). However, AND-gated isolated diamonds also evolve in the absence of spurious signals, indeed at even higher frequency (**Fig. 10B**). Results including weak TFBSs are similar (**Fig. S8**).

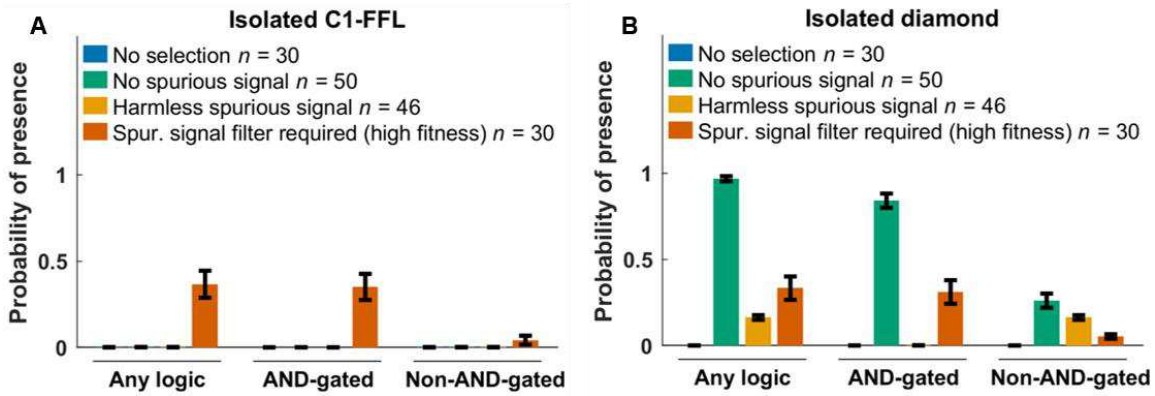

Figure 10. Selection for filtering out a short spurious signal is the primary way to evolve AND-gated isolated C1-FFLs (A), but AND-gated isolated diamonds also evolve in the absence of spurious signals (B). The selection conditions are the same as in **Fig. 6**, but we do not allow the signal to directly regulate the effector. When scoring motifs, we exclude all two-mismatch TFBSs; more comprehensive results are shown in **Fig. S8**. Many non-AND-gated diamonds have the "no regulation" logic in **Fig. 2**, perhaps as an artifact created by the duplication and divergence of intermediate TFs; we excluded them from the "Any logic" and "Non-AND-gated" tallies in (B). See Supplementary Text Section 11 for the calculation of y-axis. Data are shown as mean±SE over evolutionary replicates. We reused data from **Fig. 7** for "Spurious signal filter required (high fitness)".

Perturbing the AND-gate logic in these isolated diamonds reduces fitness via effects in the environment where expressing the effector is deleterious (**Fig. 9B.iii**). Even in the absence of external short spurious signals, the stochastic expression of intermediate TFs might effectively create short spurious signals when the external signal is set to "OFF". It seems that AND-gated diamonds evolve to mitigate this risk, but that AND-gated C1-FFLs do not. The duration of internally generated spurious signals has an exponential distribution, which means that the optimal filter would be one that does not delay gene expression[48]. The two TFs in an AND-gated diamond can be activated simultaneously, but they must be activated sequentially in an AND-gated C1-FFL; the shorter delays possible with AND-gated diamonds might explain why only diamonds and not FFLs evolve to filter out intrinsic noise in gene expression.

Discussion

Adaptive nature of AND-gated C1-FFLs

There has never been sufficient evidence to satisfy evolutionary biologists that motifs in TRNs represent adaptations for particular functions. Critiques by evolutionary biologists to this effect[13-23] have been neglected, rather than answered, until now. While C1-FFLs can be conserved across different species[49-52], this does not imply that specific "just-so" stories about their function are correct. In this work, we study the evolution of AND-gated C1-FFLs, which are hypothesized to be adaptations for filtering out short spurious signals[3]. Using a novel and more mechanistic computational model to simulate TRN evolution, we found that AND-gated C1-FFLs evolve readily under selection for filtering out a short spurious signal, and not under control conditions. Our results support the adaptive hypothesis about C1-FFLs.

AND-gated C1-FFLs express an effector after a noise-filtering delay when the signal is turned on, but shut down expression immediately when the signal is turned off, giving rise to a "sign-sensitive delay"[3, 7]. Rapidly switching off has been hypothesized to be part of their selective advantage, above and beyond the function of filtering out short spurious signals[48]. We intended to select only for filtering out a short spurious signal, and not for fast turn-off; specifically, we expected effector expression to evolve a delay equal to the duration of the spurious signal. However, evolved solutions still expressed the effector in the presence of short spurious signals (**Fig. S2**), and thus benefitted from rapidly turning off this spurious expression. In other words, we effectively selected for both delayed turn-on and rapid turn-off, despite our intent to only select for the former.

It is difficult to distinguish adaptations from "spandrels"[8]. Standard procedure is to look for motifs that are more frequent than expected from some randomized version of a TRN[2, 53]. For this method to work, this randomization must control for all confounding factors that are non-adaptive with respect to the function in question, from patterns of mutation to a general tendency to hierarchy – a near-impossible task. Our approach to a null model is not to randomize, but to evolve with and without selection for the specific function of interest. This meets the standards of evolutionary biology for inferring the adaptive nature of a motif[13-23].

Technical lessons learned

Previous studies have also attempted to evolve adaptive motifs in a computational TRN, successfully under selection for circadian rhythm and for multiple steady states[54], and

unsuccessfully under selection to produce a sine wave in response to a periodic pulse[23]. Other studies have evolved adaptive motifs in a mixed network of transcriptional regulation and protein-protein interaction[55-57]. Our successful simulation might offer some methodological lessons, especially a focus on high-fitness evolutionary replicates, which was done by us and by Burda et al.[54] but not by Knabe et al.[23].

Knabe et al.[23] suggested that including a cost for gene expression may suppress unnecessary links and thus make it easier to score motifs. However, when we removed the cost of gene expression term ($C(t) = 0$ in Supplementary Section 8), AND-gated C1-FFLs still evolved in the high-fitness genotypes under selection for filtering out a spurious signal (**Fig. S9**). In our model, removing the cost of gene expression did not, via permitting unnecessary links, conceal motifs.

While simplified relative to reality, our model is undeniably complicated. An important question is which complications are important for what. One complication is our nucleotide-sequence-level model of cis-regulatory sequences. This has the advantage of capturing weak TFBSs, realistic turnover, and other mutational biases. The disadvantage is that calculating the probabilities of TF binding is computationally expensive and scales badly with network size. Future work might design a more schematic model of cis-regulatory sequences to improve computation while still capturing realistic mutation biases. A second complication of our approach is the stochastic simulation of gene expression. This is essential for our question, because intrinsic noise in gene expression can mimic the effects of a spurious signal, but may be less important in other scenarios, e.g. where the focus is on steady state behavior.

The ubiquity of weak TFBSs complicates motif scoring

Our model, while complex for a model and hence capable of capturing intrinsic noise, is inevitably less complex than the biological reality. However, we hope to have captured key phenomena, albeit in simplified form. One key phenomenon is that TFBSs are not simply present vs. absent but can be strong or weak, i.e. the TRN is not just a directed graph, but its connections vary in strength. Our model, like that of Burda et al.[54] in the context of circadian rhythms, captures this fact by basing TF binding affinity on the number of mismatch deviations from a consensus TFBS sequence. While in reality, the strength of TF binding is determined by additional factors, such as broader nucleic context and cooperative behavior between TFs (reviewed in Inukai et al.[58]), these complications are unlikely to change the basic dynamics of frequent appearance of weak TFBSs and greater mutational accessibility of strong TFBSs from weak TFBSs than de novo. Similarly, AND-gating can be quantitative rather than qualitative[59], a phenomenon that weak TFBSs in our model provide a simplified version of.

Core links in adaptive motifs almost always involve strong not weak TFBSs. However, weak (two-mismatch) TFBSs can create additional links that prevent an adaptive motif from being scored as such. Some potential additional links are neutral while others are deleterious; the observed links are thus shaped by this selective filter, without being adaptive. Note that there have been experimental reports that even weak TFBSs can be functionally important[60, 61]; these might, however, better correspond to 1-mismatch TFBSs in our model than two-mismatch TFBSs. Ramos et al.[61] and Crocker et al.[60] identified their “weak” TFBSs in comparison to the strongest possible TFBS, not in comparison to the weakest still showing affinity above baseline.

Different solutions for filtering out short spurious signals

A striking and unexpected finding of our study was that AND-gated diamonds evolved as an alternative motif for filtering out short spurious external signals, and that these, unlike FFLs, were also effective at filtering out intrinsic noise. Multiple motifs have previously been found capable of generating the same steady state expression pattern[21]; here we find multiple motifs for a much more complex function.

Diamonds are not overrepresented in the TRNs of bacteria[2] or yeast[62], but are overrepresented in signaling networks (in which post-translational modification plays a larger role)[63], and in neuronal networks[1]. In our model, we treated the external signal as though it were a transcription factor, simply as a matter of modeling convenience. In reality, signals external to a TRN are by definition not TFs (although they might be modifiers of TFs). This means that our indirect regulation case, in which the signal is not allowed to directly turn on the effector, is the most appropriate one to analyze if our interest is in TRN motifs that mediate contact between the two. Note that if under indirect regulation we were to score the signal as not itself a TF, we would observe adaptive C1-FFLs but not diamonds, in agreement with the TRN data. However, this TRN data might miss functional diamond motifs that spanned levels of regulatory organization, i.e. that included both transcriptional and other forms of regulation. The greatest chance of finding diamonds within TRNs alone come from complex and multi-layered developmental cascades, rather than bacterial or yeast[64]. Multiple interwoven diamonds are hypothesized to be embedded with multi-layer perceptrons that are adaptations for complex computation in signaling networks[65].

Previous work has also identified alternatives to AND-gated C1-FFLs. Specifically, in mixed networks of transcriptional regulation and protein-protein interactions, FFLs did not evolve under selection for delayed turn-on (as well as rapid turn-off)[57]. Indeed, even when a FFL topology was enforced, with only the parameters allowed to evolve, two alternative motifs remained superior[57]. However, one alternative motif, which the authors called "positive feedback" is essentially still an AND-gated C1-FFL, specifically one in which the intermediate TF expression is also AND-gated, requiring both itself and the signal for upregulation. The other is a cascade in which the signal inhibits the expression of an intermediate TF protein that represses the expression of the effector. The cost of constitutive expression of the intermediate TF in the absence of the signal was not modeled[57], giving this cascade an unrealistic advantage.

The importance of dynamics and intrinsic noise

Most previous research on C1-FFLs has used an idealized implementation (e.g. a square wave) of what a short spurious signal entails[4, 48, 66]. In real networks, noise arises intrinsically in a greater diversity of forms, which our model does more to capture. Even when a "clean" form of noise enters a TRN, it subsequently gets distorted with the addition of intrinsic noise[67]. Intrinsic noise is ubiquitous and dealing with it is an omnipresent challenge for selection. Indeed, we see adaptive diamonds evolve to suppress intrinsic noise, even when we select in the absence of extrinsic spurious signals.

The function of a motif relies ultimately on its dynamic behavior, with topology merely a means to that end. To create two pathways that regulate the effector in different speeds, the C1-FFL motif uses a pair of short and long pathways, but these also correspond to fast-degrading and

slow-degrading TFs. This same function was achieved entirely non-topologically in our adaptively evolved diamond motifs. This agrees with other studies showing that topology alone is not enough to infer activities such as spurious signal filtering from network motifs [68-70].

Acknowledgements

Work was supported by the University of Arizona and by a Pew Scholarship to JM, John Templeton Foundation grant 39667 to JM, and by National Institutes of Health grants R35GM118170 to MLS and R01GM076041 to JM. We thank Hinrich Boeger for helpful discussions and careful reading of the manuscript, Jasmin Uribe for early work on this project, and the high-performance computing center at the University of Arizona for generous allocations.

Author Contributions

K.X. and J.M. designed the simulations, analyzed the results, and wrote the manuscript. K.X. performed the simulations and statistical analyses. K.X., A.L., and J.M. wrote the simulation code. M.L.S. and J.M. conceptualized the initial design of the simulations.

Competing Interests: The authors declare no conflicts of interest.

References

1. Milo R, Shen-Orr S, Itzkovitz S, Kashtan N, Chklovskii D, Alon U. Network motifs: Simple building blocks of complex networks. *Science* **298**, 824-827 (2002).

2. Shen-Orr SS, Milo R, Mangan S, Alon U. Network motifs in the transcriptional regulation network of *Escherichia coli*. *Nature Genet* **31**, 64-68 (2002).

3. Alon U. Network motifs: theory and experimental approaches. *Nat Rev Genet* **8**, 450-461 (2007).

4. Mangan S, Alon U. Structure and function of the feed-forward loop network motif. *Proc Natl Acad Sci USA* **100**, 11980-11985 (2003).

5. Jaeger KE, Pullen N, Lamzin S, Morris RJ, Wigge PA. Interlocking feedback loops govern the dynamic behavior of the floral transition in Arabidopsis. *The Plant Cell* **25**, 820-833 (2013).

6. Peter IS, Davidson EH. Assessing regulatory information in developmental gene regulatory networks. *Proc Natl Acad Sci USA* **114**, 5862-5869 (2017).

7. Mangan S, Zaslaver A, Alon U. The coherent feedforward loop serves as a sign-sensitive delay element in transcription networks. *J Mol Biol* **334**, 197-204 (2003).

8. Gould SJ, Lewontin RC. The Spandrels of San Marco and the Panglossian Paradigm: A Critique of the Adaptationist Programme. *Proc R Soc Lond, B, Biol Sci* **205**, 581-598 (1979).

9. Graur D, Zheng Y, Price N, Azevedo RBR, Zufall RA, Elhaik E. On the Immortality of Television Sets: “Function” in the Human Genome According to the Evolution-Free Gospel of ENCODE. *Genome Biol Evol* **5**, 578-590 (2013).

10. Masel J, Promislow DEL. Answering evolutionary questions: A guide for mechanistic biologists. *BioEssays* **38**, 704-711 (2016).

11. Widder S, Solé R, Macía J. Evolvability of feed-forward loop architecture biases its abundance in transcription networks. *BMC Syst Biol* **6**, 7 (2012).

12. Cordero OX, Hogeweg P. Feed-forward loop circuits as a side effect of genome evolution. *Mol Biol Evol* **23**, 1931-1936 (2006).

13. Artzy-Randrup Y, Fleishman SJ, Ben-Tal N, Stone L. Comment on "Network Motifs: Simple Building Blocks of Complex Networks" and "Superfamilies of Evolved and Designed Networks". *Science* **305**, 1107 (2004).

14. Jenkins D, Stekel D. De Novo Evolution of Complex, Global and Hierarchical Gene Regulatory Mechanisms. *J Mol Evol* **71**, 128-140 (2010).

15. Lynch M. The evolution of genetic networks by non-adaptive processes. *Nat Rev Genet* **8**, 803-813 (2007).

16. Mazurie A, Bottani S, Vergassola M. An evolutionary and functional assessment of regulatory network motifs. *Genome Biol* **6**, R35 (2005).

17. Solé RV, Valverde S. Are network motifs the spandrels of cellular complexity? *Trends Ecol Evol* **21**, 419-422 (2006).

18. Tsuda ME, Kawata M. Evolution of Gene Regulatory Networks by Fluctuating Selection and Intrinsic Constraints. *PLoS Comput Biol* **6**, e1000873 (2010).

19. Wagner A. Does Selection Mold Molecular Networks? *Sci STKE* **2003**, pe41 (2003).

20. Kuo PD, Banzhaf W, Leier A. Network topology and the evolution of dynamics in an artificial genetic regulatory network model created by whole genome duplication and divergence. *BioSystems* **85**, 177-200 (2006).

21. Payne JL, Wagner A. Function does not follow form in gene regulatory circuits. *Scientific Reports* **5**, 13015 (2015).

22. Ruths T, Nakhleh L. Neutral forces acting on intragenomic variability shape the *Escherichia coli* regulatory network topology. *Proc Natl Acad Sci USA* **110**, 7754-7759 (2013).

23. Knabe JF, Nehaniv CL, Schilstra MJ. Do motifs reflect evolved function?—No convergent evolution of genetic regulatory network subgraph topologies. *Biosystems* **94**, 68-74 (2008).

24. Raser JM, O'Shea EK. Noise in Gene Expression: Origins, Consequences, and Control. *Science* **309**, 2010-2013 (2005).

25. Kærn M, Elston TC, Blake WJ, Collins JJ. Stochasticity in gene expression: from theories to phenotypes. *Nat Rev Genet* **6**, 451-464 (2005).

26. Eldar A, Elowitz MB. Functional roles for noise in genetic circuits. *Nature* **467**, 167–173 (2010).

27. Draghi J, Whitlock M. Robustness to noise in gene expression evolves despite epistatic constraints in a model of gene networks. *Evolution* **69**, 2345-2358 (2015).

28. Jenkins DJ, Stekel DJ. A New Model for Investigating the Evolution of Transcription Control Networks. *Artificial Life* **15**, 259-291 (2009).

29. Henry A, Hemery M, François P. ϕ-evo: A program to evolve phenotypic models of biological networks. *PLoS Comput Biol* **14**, e1006244 (2018).

30. Brown CR, Mao C, Falkovskaia E, Jurica MS, Boeger H. Linking Stochastic Fluctuations in Chromatin Structure and Gene Expression. *PLoS Biol* **11**, e1001621 (2013).

31. Mao C*, et al.* Quantitative analysis of the transcription control mechanism. *Mol Syst Biol* **6**, 431 (2010).

32. Shahbazian MD, Grunstein M. Functions of Site-Specific Histone Acetylation and Deacetylation. *Annu Rev Biochem* **76**, 75-100 (2007).

33. Voss TC, Hager GL. Dynamic regulation of transcriptional states by chromatin and transcription factors. *Nat Rev Genet* **15**, 69-81 (2013).

34. Katan-Khaykovich Y, Struhl K. Dynamics of global histone acetylation and deacetylation in vivo: rapid restoration of normal histone acetylation status upon removal of activators and repressors. *Genes Dev* **16**, 743-752 (2002).

35. Courey AJ, Jia S. Transcriptional repression: the long and the short of it. *Genes Dev* **15**, 2786-2796 (2001).

36. Poss ZC, Ebmeier CC, Taatjes DJ. The Mediator complex and transcription regulation. *Crit Rev Biochem Mol Biol* **48**, 575-608 (2013).

37. Decker KB, Hinton DM. Transcription Regulation at the Core: Similarities Among Bacterial, Archaeal, and Eukaryotic RNA Polymerases. *Annu Rev Microbiol* **67**, 113-139 (2013).

38. Roy AL, Singer DS. Core promoters in transcription: old problem, new insights. *Trends Biochem Sci* **40**, 165-171 (2015).

39. van Drogen F, Stucke VM, Jorritsma G, Peter M. MAP kinase dynamics in response to pheromones in budding yeast. *Nat Cell Biol* **3**, 1051 (2001).

40. Gillespie DT. Exact stochastic simulation of coupled chemical reactions. *J Phys Chem* **81**, 2340-2361 (1977).

41. Ghaemmaghami S*, et al.* Global analysis of protein expression in yeast. *Nature* **425**, 737-741 (2003).

42. Kafri M, Metzl-Raz E, Jona G, Barkai N. The Cost of Protein Production. *Cell Reports* **14**, 22-31 (2016).

43. Gerrish PJ, Lenski RE. The fate of competing beneficial mutations in an asexual population. *Genetica* **102**, 127 (1998).

44. van Nimwegen E, Crutchfield JP, Huynen M. Neutral evolution of mutational robustness. *Proc Natl Acad Sci USA* **96**, 9716-9720 (1999).

45. Kimura M. On the probability of fixation of mutant genes in a population. *Genetics* **47**, 713-719 (1962).

46. Balázsi G, Barabási AL, Oltvai ZN. Topological units of environmental signal processing in the transcriptional regulatory network of *Escherichia coli*. *Proc Natl Acad Sci U S A* **102**, 7841-7846 (2005).

47. Hooshangi S, Thiberge S, Weiss R. Ultrasensitivity and noise propagation in a synthetic transcriptional cascade. *Proc Natl Acad Sci USA* **102**, 3581-3586 (2005).

48. Dekel E, Mangan S, Alon U. Environmental selection of the feed-forward loop circuit in gene-regulation networks. *Physical Biology* **2**, 81 (2005).

49. Boyle AP*, et al.* Comparative analysis of regulatory information and circuits across distant species. *Nature* **512**, 453-456 (2014).

50. Kemmeren P*, et al.* Large-Scale Genetic Perturbations Reveal Regulatory Networks and an Abundance of Gene-Specific Repressors. *Cell* **157**, 740-752 (2014).

51. Stergachis AB*, et al.* Conservation of trans-acting circuitry during mammalian regulatory evolution. *Nature* **515**, 365-370 (2014).

52. Madan Babu M, Teichmann SA, Aravind L. Evolutionary dynamics of prokaryotic transcriptional regulatory networks. *J Mol Biol* **358**, 614-633 (2006).

53. Kashtan N, Itzkovitz S, Milo R, Alon U. Efficient sampling algorithm for estimating subgraph concentrations and detecting network motifs. *Bioinformatics* **20**, 1746-1758 (2004).

54. Burda Z, Krzywicki A, Martin OC, Zagorski M. Motifs emerge from function in model gene regulatory networks. *Proc Natl Acad Sci USA* **108**, 17263-17268 (2011).

55. François P, Hakim V. Design of genetic networks with specified functions by evolution in silico. *Proc Natl Acad Sci USA* **101**, 580-585 (2004).

56. François P, Siggia ED. Predicting embryonic patterning using mutual entropy fitness and in silico evolution. *Development* **137**, 2385-2395 (2010).

57. Warmflash A, François P, Siggia ED. Pareto evolution of gene networks: An algorithm to optimize multiple fitness objectives. *Physical Biology* **9**, 56001-56007 (2012).

58. Inukai S, Kock KH, Bulyk ML. Transcription factor–DNA binding: beyond binding site motifs. *Curr Opin Genet Dev* **43**, 110-119 (2017).

59. Wang D*, et al.* Loregic: A Method to Characterize the Cooperative Logic of Regulatory Factors. *PLoS Comput Biol* **11**, e1004132 (2015).

60. Crocker J*, et al.* Low Affinity Binding Site Clusters Confer Hox Specificity and Regulatory Robustness. *Cell* **160**, 191-203 (2015).

61. Ramos AI, Barolo S. Low-affinity transcription factor binding sites shape morphogen responses and enhancer evolution. *Philos Trans R Soc Lond, B, Biol Sci* **368**, 20130018 (2013).

62. Lee TI*, et al.* Transcriptional regulatory networks in *Saccharomyces cerevisiae*. *Science* **298**, 799-804 (2002).

63. Ma'ayan A*, et al.* Formation of regulatory patterns during signal propagation in a mammalian cellular network. *Science* **309**, 1078-1083 (2005).

64. Rosenfeld N, Alon U. Response Delays and the Structure of Transcription Networks. *J Mol Biol* **329**, 645-654 (2003).

65. Alon U. *An Introduction to Systems Biology: Design Principles of Biological Circuits*. Chapman and Hall/CRC (2007).

66. Hayot F, Jayaprakash C. A feedforward loop motif in transcriptional regulation: induction and repression. *J Theor Biol* **234**, 133-143 (2005).

67. Pedraza JM, van Oudenaarden A. Noise Propagation in Gene Networks. *Science* **307**, 1965-1969 (2005).

68. Ingram PJ, Stumpf MP, Stark J. Network motifs: structure does not determine function. *BMC genomics* **7**, 108-108 (2006).

69. Wall ME. Structure–function relations are subtle in genetic regulatory networks. *Mathematical Biosciences* **231**, 61-68 (2011).

70. Wall ME, Dunlop MJ, Hlavacek WS. Multiple Functions of a Feed-Forward-Loop Gene Circuit. *J Mol Biol* **349**, 501-514 (2005).

Supporting information for "Feed-forward regulation adaptively evolves via dynamics rather than topology when there is intrinsic noise" by Xiong et al.

Table of contents

Table S1. Major model parameters

Parameter	Values[1]	Bounds[2]	References
Length of cis-regulatory sequence	150 bp		(Yuan et al. 2005)
Length of TF recognition sequence	8 bp		(Wunderlich & Mirny 2009)
Length occupied by a TF on each side of recognition sequence	3 bp		(Zhu & Zhang 1999)
Dissociation constant between TF and perfect TFBS, $K_d(0)$	**$10^{U(-9,-6)}$ mole/liter**[3]	$(0, 10^{-5})$	(Park et al. 2004; Nalefski et al. 2006)
Dissociation constant between TF and non-specific DNA, $K_d(3)$	10^{-5} M		(Maerkl & Quake 2007)
Base rate of transition from Repressed to Intermediate	0.15 min^{-1}		(Katan-Khaykovich & Struhl 2002)
Maximum transition rate from Repressed to Intermediate	0.92 min^{-1}		(Katan-Khaykovich & Struhl 2002; Brown et al. 2013)
Base rate of transition from Intermediate to Repressed	0.67 min^{-1}		(Katan-Khaykovich & Struhl 2002)
Maximum transition rate from Intermediate to Repressed	4.11 min^{-1}		Chosen to give same dynamic range and Repressed to Intermediate
Base rate of transition from Intermediate to Active	0.025 min^{-1}		(Brown et al. 2013)
Maximum transition rate from Intermediate to Active	3.3 min^{-1}		(Brown et al. 2013)
Transition rate from Active to Intermediate, $r_{Act\_to\_Int}$	**$10^{N(1.27, 0.226)}$ min^{-1}**[4]	[0.59, 64.7]	(Guillemette et al. 2005; Pelechano et al. 2010; Brown et al. 2013)
Length of gene, L	**$10^{N(2.568, 0.34)}$ codons**	[50, 5000]	(SGD Project)
Rate of transcription initiation, $r_{max\_transc\_init}$	6.75 min^{-1}		(Brown et al. 2013)
Speed of transcription elongation	600 codon/min		(Dujon 1996; Larson et al. 2011; Hocine et al. 2013)
Time for transcribing UTRs and for terminating transcription	1 min		(Dujon 1996; Larson et al. 2011; Hocine et al. 2013)
Rate of mRNA degradation, r_{mRNA_deg}	**$10^{N(-1.49, 0.267)}$ min^{-1}**	$[7.5\times10^{-4}, 0.54]$	(Wang et al. 2002)
Speed of translation elongation	330 codon/min		(Siwiak et al. 2010)
Translation initiation time	0.5 min		(Siwiak et al. 2010)
Protein synthesis rate, $r_{protein\_syn}$	**$10^{N(0.322, 0.416)}$ molecule $mRNA^{-1}$ min^{-1}**	$[4.5\times10^{-3}, 61.4]$	(Siwiak et al. 2010)
Rate of protein degradation, $r_{protein\_deg}$	**$10^{N(-1.88, 0.561)}$ min^{-1}**	$[3.0\times10^{-6}, 0.69]$	(Belle et al. 2006)
Saturation concentration of effector protein, N_{e_sat}	10,000 molecules/cell		(Ghaemmaghami et al. 2003)
Fitness cost of protein expression for a gene with $L = 10^{2.568}$, c_{transl}	2×10^{-6} $(molecules/min)^{-1}$		(Ghaemmaghami et al. 2003; Kafri et al. 2016)
Maximum number of effector gene copies	5		
Maximum number of TF gene copies, excluding the signal	19		

[1] Parameters in bold can be altered by mutation, and the table shows the distributions from which their initial values are sampled. Estimation of N_{e_sat} is described in the Methods; estimation of the other parameters is described in the Supplementary Text (Sections 1, 2 – 7, and 8).

[2] Same units as the parameter values. Parentheses mean the parameter cannot take the boundary values; square brackets mean it can. We also use these bounds to constrain mutation (see Section 9).

[3] The uniform distribution is denoted U(min, max).

[4] The normal distribution is denoted N(mean, SD).

Table S2. Mutation rates and effect sizes

Mutation	Relative rate	Effect of mutation[1]
Single nucleotide substitution	5.25×10^{-8} per gene	
Gene deletion	1.5×10^{-7} per gene[2]	
Gene duplication	1.5×10^{-7} per gene[2]	
Mutation to consensus sequence of a TF	3.5×10^{-9} per gene	
Mutation to TF identity (activator vs. repressor)	3.5×10^{-9} per gene	
Mutation to $K_d(0)$	3.5×10^{-9} per gene	k = 0.5, μ = -5[2], σ = 0.776
Mutation to L	1.2×10^{-11} per codon	
Mutation to $r_{protein\_syn}$	9.5×10^{-12} per codon	k = 0.5, μ = 0.021[2], σ = 0.760
Mutation to $r_{protein\_deg}$	9.5×10^{-12} per codon	k = 0.5, μ = -1.88, σ = 0.739
Mutation to $r_{Act\_to\_Int}$	9.5×10^{-12} per codon	k = 0.5, μ = 1.57[2], σ = 0.773
Mutation to r_{mRNA_deg}	9.5×10^{-12} per codon	k = 0.5, μ = -1.19, σ = 0.396

[1] Mutation to these quantitative rates takes the form $\log_{10}x' = \log_{10}x + \mathrm{Normal}(k(\mu - \log_{10}x), \sigma)$, where x is the original value of the rate and x' is the value after mutation. See Section 9 for details.

[2] The value of this parameter is different during burn-in. See Section 9 for details.

	Probability that mutation of this type is accepted, given it occurs		Probability that an accepted mutation is of this type, given that it is accepted	
	First 1000 evol. steps	**Last 1000 evol. steps**	**First 1000 evol. steps**	**Last 1000 evol. steps**
Substitution	0.34 ± 0.01	0.35 ± 0.00	0.180 ± 0.005	0.213 ± 0.008
Deletion	0.27 ± 0.01	0.21 ± 0.01	0.360 ± 0.003	0.345 ± 0.005
Duplication	0.34 ± 0.01	0.32 ± 0.01	0.368 ± 0.003	0.343 ± 0.005
TF recognition seq.	0.30 ± 0.02	0.19 ± 0.02	0.009 ± 0.001	0.005 ± 0.000
$r_{Act\_to\_Int}$	0.33 ± 0.02	0.25 ± 0.01	0.012 ± 0.001	0.010 ± 0.001
r_{mRNA_deg}	0.34 ± 0.02	0.27 ± 0.01	0.014 ± 0.001	0.016 ± 0.002
$r_{protein\_syn}$	0.32 ± 0.02	0.23 ± 0.01	0.013 ± 0.001	0.013 ± 0.001
$r_{protein\_deg}$	0.35 ± 0.01	0.26 ± 0.01	0.014 ± 0.001	0.015 ± 0.002
$K_d(\mathbf{0})$	0.28 ± 0.02	0.21 ± 0.02	0.006 ± 0.000	0.005 ± 0.001
TF identity	0.29 ± 0.01	0.29 ± 0.02	0.008 ± 0.000	0.008 ± 0.001
Locus length	0.33 ± 0.01	0.36 ± 0.01	0.017 ± 0.001	0.026 ± 0.002

Table S3. Summary of mutations that replaced the resident genotype. Data is shown as mean $\pm$ SE over the 45 evolutionary replicates under selection for filtering out a spurious signal, with the signal allowed to regulate the effector directly. Without selection, each mutation would have probability 50% of replacing the resident; selection reduces this to around one in three at the beginning of the simulation, down to around one in four at the end. This high rate of accepting mutations after fitness has plateaued suggests significant nearly neutral evolution, i.e. that slightly deleterious mutations fix and are then compensated for. The estimated selection coefficient need only be 10^{-8} for a mutant to replace the resident, which can be easily occur for a slightly deleterious mutation through the error in fitness estimation (see Evolution Simulation in the main text). Single nucleotide substitutions are particularly prone to nearly neutral evolution, whereas changes to the consensus sequence recognized by a TF are under stronger stabilizing selection. Deletion and duplication mutations are the most common forms of substitution not because they are more likely to be accepted, but because they occur at higher mutation rates.

	Signal		TFs		Effector	
	V_n / V_s	M_s / M_n	V_n / V_s	M_s / M_n	V_n / V_s	M_s / M_n
$r_{Act\_to\_Int}$	NA	NA	0.89	0.18	8.26	0.13
r_{mRNA_deg}	NA	NA	2.09	0.98	13.4	2.55
$r_{protein\_syn}$	NA	NA	1.51	8.03	43.1	62.4
$r_{protein\_deg}$	NA	NA	1.28	0.56	7.23	12.5
$K_d(\mathbf{0})$	0.68	0.002	0.67	0.009	NA	NA
Locus length	NA	NA	1.01	0.72	2.07	0.79

Table S4. Evolutionary constraint on parameters in AND-gated C1-FFLs. Adaptive AND-gated C1-FFLs are taken from the 25 high-fitness replicates evolved for filtering out a spurious signal, where the signal directly regulates the effector. For each replicate, we sample one of the last 10,000 evolutionary time steps, and then sample one AND-gated C1-FFL in that genotype, should there be more than one (or resample a time step for that replicate, if there are none). We then take the variance V_s of each C1-FFL parameter value across the 25 replicates. We repeat this sampling process 100 times (using the same 25 replicates) and take the mean in order to obtain a better estimator of the variance in each parameter value. We compare this by a comparable variance V_n given no selection. We obtain these from 30 evolutionary replicates under no selection (from **Fig. 6**), sampling parameter values from the signal, from one TF gene copy, and from one effector gene, without the requirement for C1-FFL presence. Variances are calculated for log-transformed parameter values, except for locus length. For locus length, we use the coefficient of variation rather than variance, i.e. we divide both variances by the square of the average locus length. The table also shows the how the parameter values M_s in adaptive AND-gated C1-FFLs differ from the expected value M_n given no selection. M_s and M_n are calculated as arithmetic means for locus length and as geometric means for all other parameters. The variance ratio is greater than 1 (indicating constraint), for all parameters except $K_d(0)$, where the ratio of mean parameter values indicates that $K_d(0)$ is nevertheless subject to strong directional selection. Effectors are more constrained than TFs, likely because the former are less redundant, having evolved fewer gene copies (4.7 on average for effectors vs. 8.6 for TFs). High degradation rates of effector mRNA and protein suggest selection to shorten the impact of transient expression in response to a short spurious signal (**Fig. S2**). High degradation rates of effector mRNA and protein are also seen in **Tables S5** and **S6**.

	Signal		Fast TFs		Slow TFs		Effector	
	V_n / V_s	M_s / M_n	V_n / V_s	M_s / M_n	V_n / V_s	M_s / M_n	V_n / V_s	M_s / M_n
$r_{Act\_to\_Int}$	NA	NA	1.49	0.44	1.15	0.18	6.64	0.1
r_{mRNA_deg}	NA	NA	5.27	8.21	1.07	0.81	7.99	2.34
$r_{protein\_syn}$	NA	NA	2.10	16.2	1.09	4.96	139	57.8
$r_{protein\_deg}$	NA	NA	12.5	45.3	1.53	0.99	25.7	11.3
$K_d(\mathbf{0})$	0.65	0.005	0.30	0.004	0.18	0.007	NA	NA
Locus length	NA	NA	3.43	0.47	3.40	0.47	5.97	0.74

Table S5. Evolutionary constraint on parameters in isolated AND-gated diamonds. V_n, V_s, M_n, and M_s are defined in the same way as in **Table S4**, and are calculated from 18 high-fitness evolutionary replicates (**Fig. 7B**) in which isolated AND-gated diamonds occur in at least 100 of the last 10,000 evolutionary steps. Because they occur at low rates, we sample 50 times per evolutionary replicate, instead of 100 times as in **Tables S4** and **S6**. There is more constraint on fast TFs than on slow TFs. The fast TFs usually have more gene copies than the slow TFs, therefore redundancy is not the reason for this difference in constraint. As seen for the C1-FFLs in **Table S4**, effectors are more constrained than either TF, $K_d(0)$ shows strong selection for high affinity combined with high variance, and effectors evolve rapid degradation. Fast TFs exhibit not just fast protein degradation (which was used for their identification), but also fast mRNA degradation.

	Signal		Signal-regulated TFs		TF-regulated TFs		Effector	
	V_n / V_s	M_s / M_n	V_n / V_s	M_s / M_n	V_n / V_s	M_s / M_n	V_n / V_s	M_s / M_n
$r_{Act\_to\_Int}$	NA	NA	2.16	0.33	1.03	0.26	6.81	0.13
r_{mRNA_deg}	NA	NA	10.8	8.5	1.40	0.74	12.4	2.36
$r_{protein\_syn}$	NA	NA	4.34	24.9	2.35	9.83	119	58.6
$r_{protein\_deg}$	NA	NA	73.6	49.4	1.50	0.34	34.1	9.92
$K_d(\mathbf{0})$	0.51	0.005	0.29	0.009	0.24	0.002	NA	NA
Locus length	NA	NA	2.52	0.71	2.45	0.71	3.35	0.73

Table S6. Evolutionary constraint on parameters in isolated AND-gated C1-FFLs. V_n, V_s, M_n, and M_s are defined in the same way as in **Table S4**, and are calculated from 12 high-fitness evolutionary replicates (**Fig. 7B**) evolved when the signal cannot directly regulate the effector, and in which isolated AND-gated C1-FFLs occur in at least 1,000 out of the last 10,000 evolutionary steps. Note that the signal-regulated TFs, which are identified via network topology, also have high protein degradation rates, as is used to identify their fast TF counterparts in diamonds – they can thus be seen as a kind of fast TF. Consistent with results on C1-FFLs when direct regulation is allowed (**Table S4**) and results on isolated AND-gated diamonds (**Table S5**), effectors are more constrained than signal-regulated (fast) TFs, which are more constrained than TF-regulated (slow) TFs, despite an opposite trend in gene copy number. Note that selection promotes fast mRNA and protein degradation in fast TFs, but promotes slow degradation of slow TFs; this result is also found more weakly in **Table S5**.

Supplementary Figures

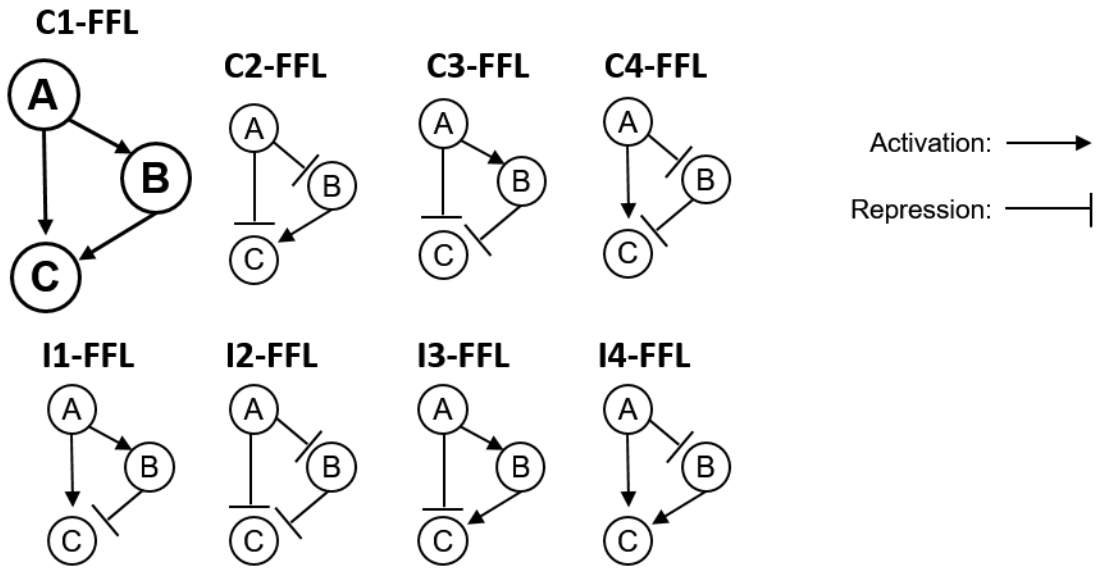

Fig. S1. Feed-forward loops come in eight subtypes. TF A and TF B can activate (indicated by arrows) or repress (indicated by bars) expression of the effector C as well as other TFs. Auto-regulation is allowed, but not shown. Following Milo et al. (2002), we exclude the case in which A and B regulate one another, rather than treating this case as two overlapping FFLs. C stands for coherent and I for incoherent.

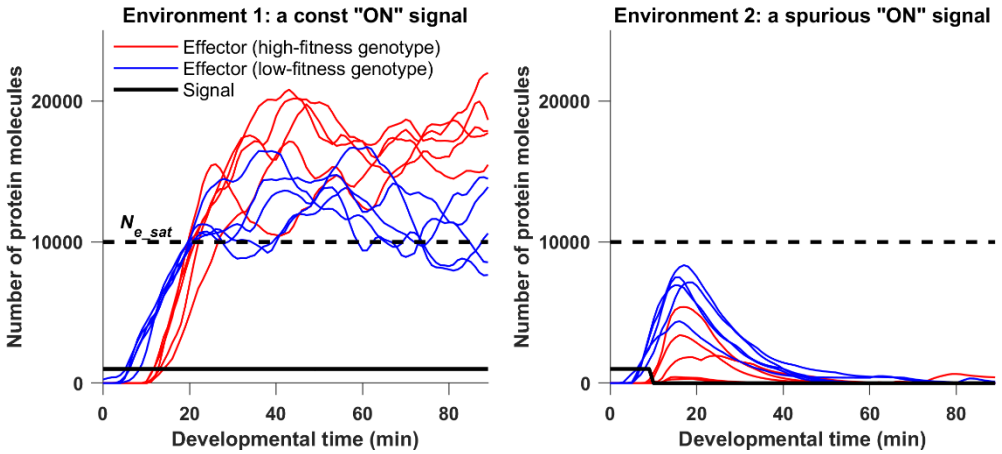

Fig. S2 Examples of evolved phenotypes under selection for filtering out a short spurious signal. The figure shows trajectories of the effector protein in one randomly chosen high-fitness replicate (red) and one randomly chosen low-fitness replicate (blue), as defined in **Fig. 4A**. The genotype of the final evolutionary step is used, and other genotypes were confirmed to behave similarly. Each genotype is illustrated by 5 replicate developmental simulations in each of the two environments. The high-fitness genotype has a longer delay followed by more rapid response given a consistent signal, with this longer delay reducing but not eliminating effector expression given a short spurious signal. The signal is allowed to directly regulate the effector in these simulations. The burn-in period is not shown, with developmental time zero corresponding to the moment the signal is turned on. Among developmental replicates of the same genotype, the concentration at a given time usually has an approximately log-normal distribution, but in environment 2 the distribution has two modes after the spurious signal turns off. One mode corresponds to expression at the basal rate, the other to a burst of expression that has yet to turn off. Because of this bimodality, we plot sample trajectories rather than mean concentration over many replicates.

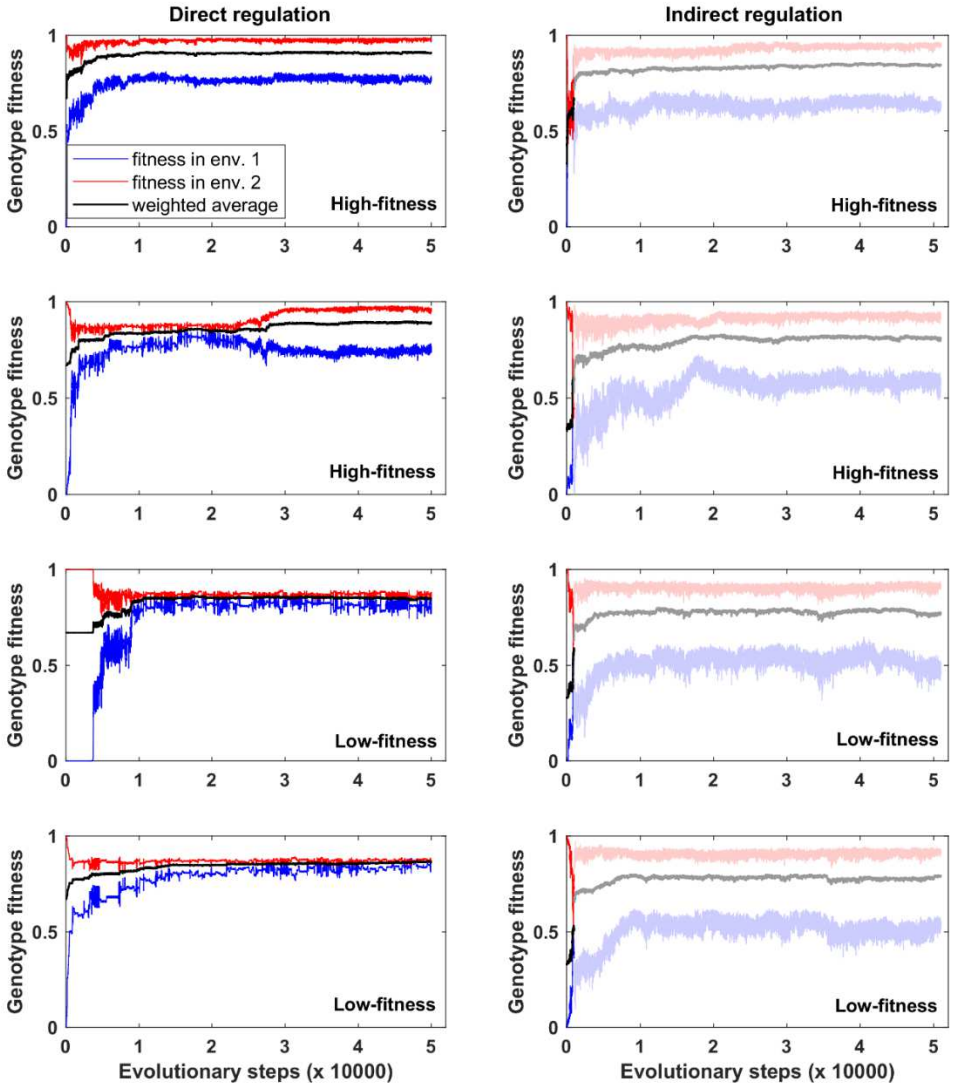

Fig. S3 Representative fitness trajectories under selection to filter out short spurious signals. Left panels: The signal is allowed to directly regulate the effector genes. Panels 1 and 3 correspond to the two genotypes shown in **Fig. S2**. Right panels: the signal cannot directly regulate the effector genes. Average fitness (black) is a weighted average of the blue and red trajectories, with environment 2 (where the signal is spurious) being considered twice as common as environment 1 (where the signal is sustained and real). When the signal cannot directly regulate the effector genes, evolutionary simulations begins with a burn-in phase that lasts 1000 evolutionary steps (see Evolutionary Simulation in the Main Text). We show the burn-in phase in undiluted color, and dilute color after burn-in. Most replicates quickly reach a stable fitness plateau (first and third rows). Certain replicates can be temporarily trapped at a low fitness plateau (second and third rows on the left).

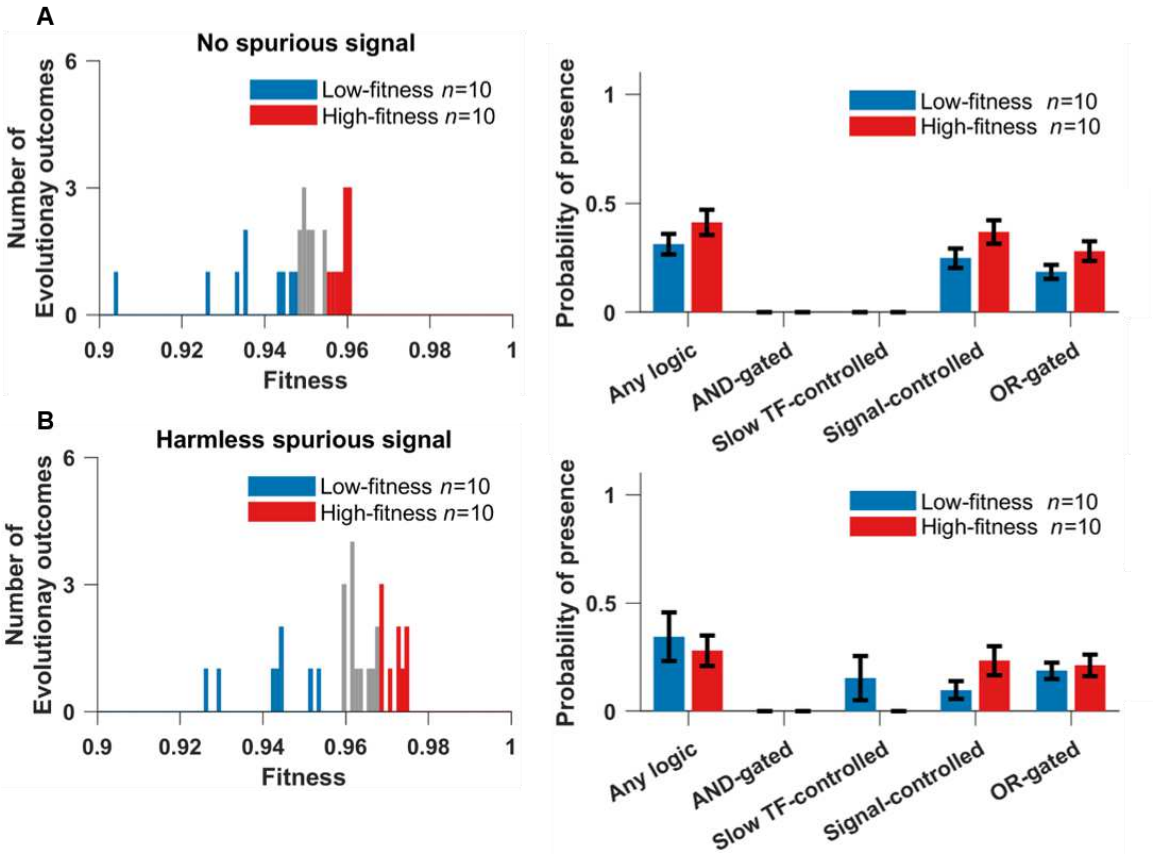

Fig. S4 Genotypes evolved under control selective conditions: (A) "no spurious signal", and (B) "harmless spurious signal". There is no clear evidence of a multimodal distribution of fitness outcomes among replicates (left), and C1-FFLs occur equally in the 10 genotypes of the highest fitness vs. the 10 genotypes of the lowest fitness (right), and so the entire distribution (left) was used to produce **Fig. 6**. Data are shown as mean±SE over evolutionary replicates.

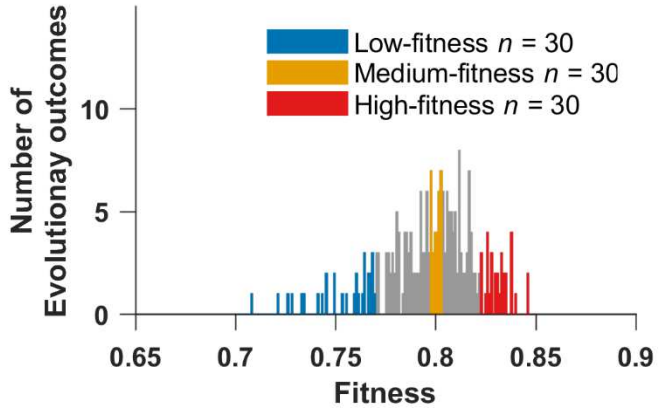

Fig. S5 Fitness distribution of 258 evolutionary replicates under selection for filtering out short spurious signals, when the signal cannot directly regulate the effector. The fitness of a replicate is the average genotype fitness over the last 10,000 evolutionary steps. Colors indicate replicates analyzed elsewhere.

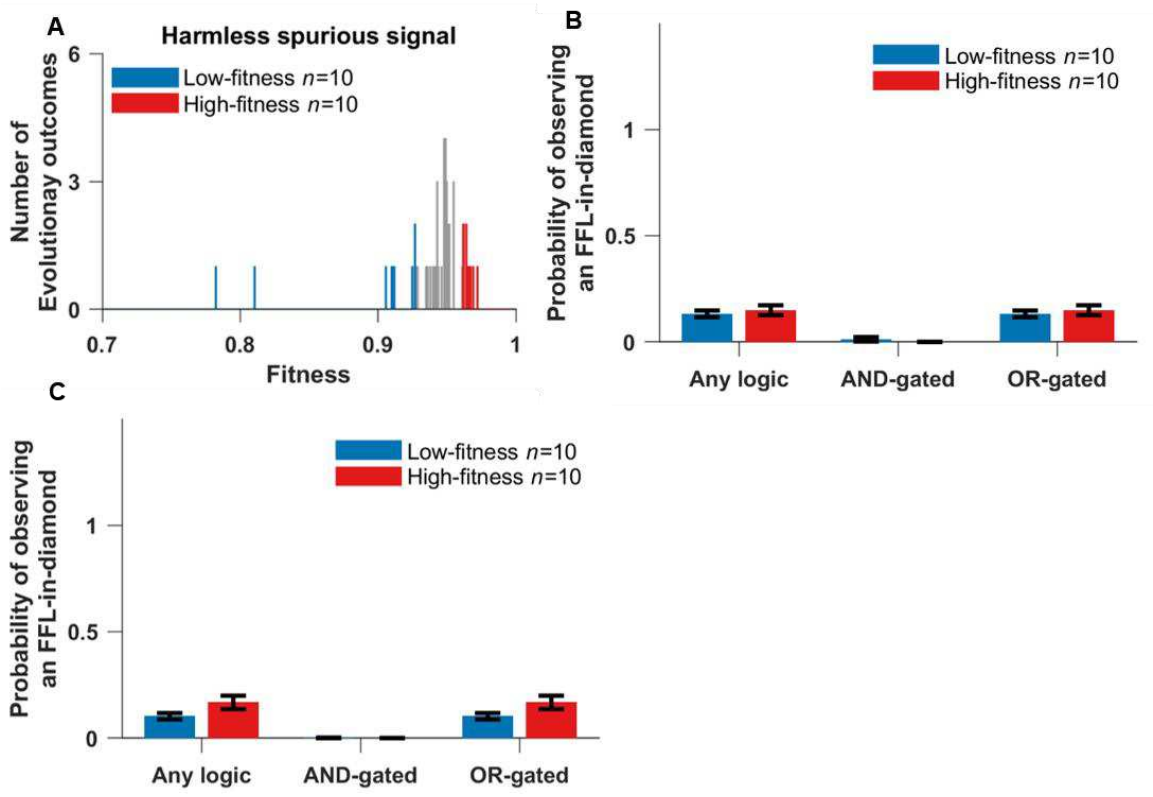

Fig. S6 Evolution when responding to a spurious signal is harmless, when the signal is not allowed to directly regulate the effector. (A) Fitness distribution of 50 replicate simulations. The occurrence of both **(B)** FFL-in-diamonds and **(C)** isolated diamonds were similar in the 10 genotypes with the highest fitness vs. in 10 genotypes with the lowest fitness. Weak (two-mismatch) TFBSs are included when scoring motifs. Data are shown as mean±SE over replicates. Isolated C1-FFLs rarely evolve under this condition, therefore their occurrence is not plotted.

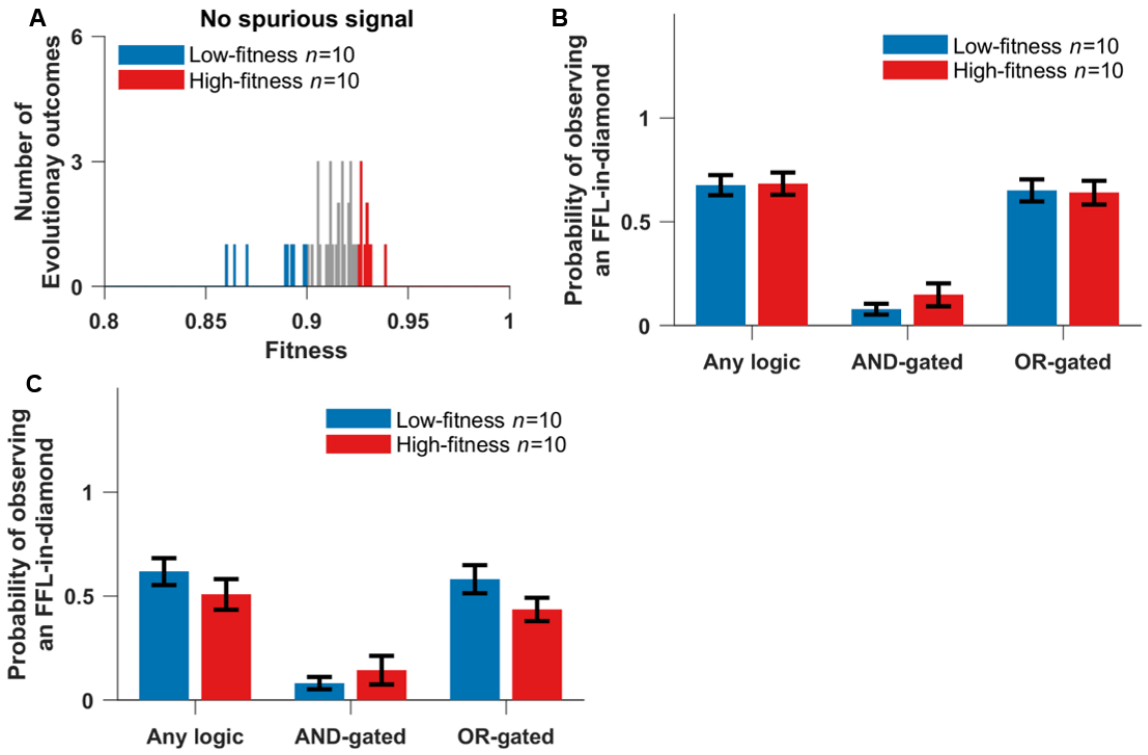

Fig. S7 Evolution when there is no spurious signal, when the signal is not allowed to directly regulate the effector. (A) Fitness distribution of 46 replicate simulations. The occurrence of both **(B)** FFL-in-diamonds and **(C)** isolated diamonds were similar in the 10 genotypes with the highest fitness vs. in the 10 genotypes with the lowest fitness. Weak (two-mismatch) TFBSs are included when scoring motifs. Data are shown as mean±SE over replicates. Isolated C1-FFLs rarely evolve under this condition, therefore their occurrence is not plotted.

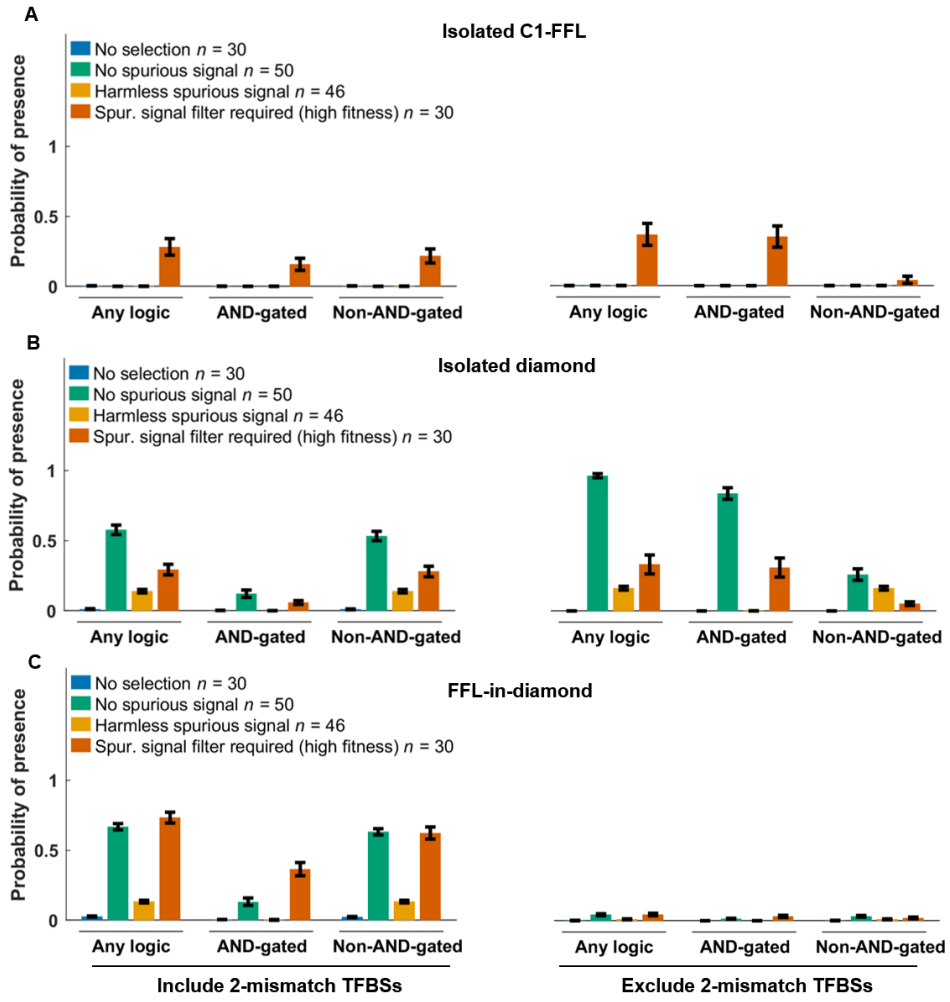

Fig. S8 Selection for filtering out a short spurious signal is the primary way to evolve AND-gated C1-FFLs (A), but AND-gated isolated diamonds also evolve in the absence of spurious signals (B). The signal is not allowed to directly regulate the effector, and the right panels of **(A)** and **(B)** are identical to **Fig. 10**. When scoring motifs, we either include (left) or exclude (right) all two-mismatch TFBSs in the cis-regulatory sequences of intermediate TF genes and effector genes. We excluded "no regulation" (**Fig. 2**) diamonds from the "Any logic" and "Non-AND-gated" tallies in **(B)**; this was necessary because of their high occurrence due to duplication and divergence of intermediate TFs. See Section 11 for the calculation of y-axis. Data are shown as mean±SE over evolutionary replicates.

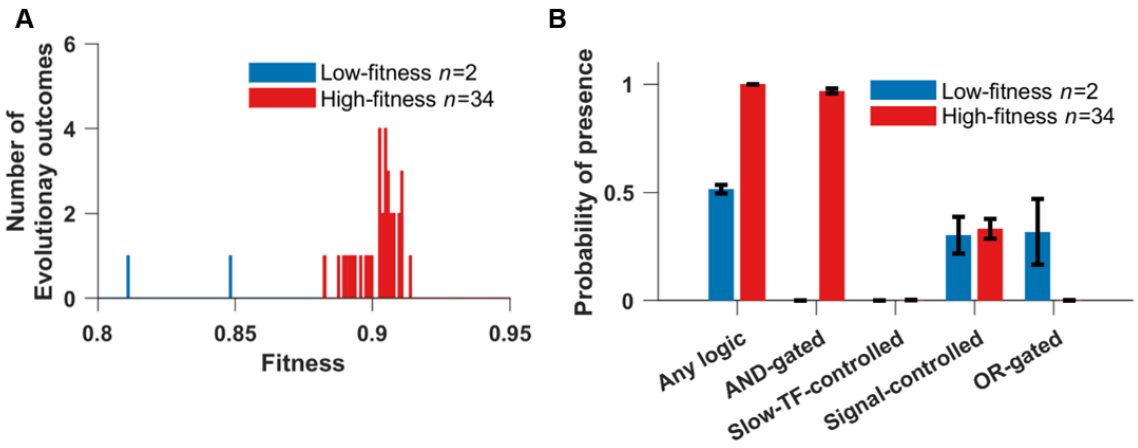

Fig. S9 After removing cost of gene expression, AND-gated C1-FFLs are still associated with a successful response to selection for filtering out a short spurious signal. The signal can directly regulate the effector genes. **(A)** We arbitrarily divide the 36 replicate simulations into high-fitness (red) and low-fitness (blue) groups. **(B)** The high-fitness replicates still evolve AND-gated C1-FFLs. Bars are mean±SE of the occurrence over replicate evolutionary simulations.

Supporting Text

1. TF binding

Transcription of each gene is controlled by TFBSs present within a 150-bp cis-regulatory region, corresponding to a typical yeast nucleosome-free region within a promoter (Yuan et al. 2005). The perfect TFBS for a typical yeast TF has information content equivalent to 13.8 bits (Wunderlich & Mirny 2009); this means that in a simplified model of binding where only one of the four nucleotides is a good match at each site, ~7 bp are recognized as an optimal consensus binding site. Maerkl & Quake (2007) reported that the TFBSs of two yeast TFs, Pho4p and Cbf1p, can have up to 2 mismatched sites within their 6 bp consensus binding sequence, while still binding the TF above background levels (Maerkl & Quake 2007). Our model therefore tracks TFBSs with up to 2 mismatches. This low information content implies a higher density of TFBSs within our cis-regulatory regions than our algorithm was able to handle, so we instead assigned each TF an 8-bp consensus sequence. Two TFs cannot simultaneously occupy overlapping stretches (Fig. S10), which we assume extend beyond the recognition sequence to occupy a total of 14 bp (Zhu & Zhang 1999); this captures competitive binding. The consequences of hindrance between TFBSs for the regulation of effector gene expression are shown in **Fig. 2**.

Fig. S10 TFs (white boxes) recognize 8 bp (red) sites while occupying and thus excluding other TFs from a 14 bp long space. TFs are assumed to bind in either orientations (Sharon et al. 2012). The sequence on the left allows simultaneous binding but that on the right does not.

We denote the dissociation constant of a TFBS with m mismatches as $K_d(m)$. Sites with m>3 mismatches are assumed to still bind at a background rate equal to m=3 mismatches, with dissociation constant $K_d(3) = 10^{-5}$ mole/liter (Maerkl & Quake 2007) for all TFs. We assume that each of the last three base pairs makes an equal and independent additive contribution $\Delta G_{bp} < 0$ to the binding energy (Benos et al. 2002): although not always true, this approximates average behavior well (Maerkl & Quake 2007). We ignore cooperativity in binding. Dissociation constants of eukaryotic TFs for perfect TFBSs can range from 10^{-5} mole/liter (Park et al. 2004) to 10^{-11} mole/liter (Nalefski et al. 2006). We initialize each TF with its own value of $\log_{10}(K_d(0))$ sampled from a uniform distribution between -6 and -9, with mutation capable of further expanding this range, subject to $K_d(0) < 10^{-5}$ mole/liter. Substituting m=0 and m=3 into

$$\Delta G_m = -RTlnK_d(m) = \Delta G_0 - \min(m, 3)\Delta G_{bp},$$

we can solve for ΔG_{bp} and ΔG_0, and thus obtain $K_d(1)$ and $K_d(2)$ (the dissociation constants for TFBS with one and two mismatches, respectively).

Because TFs bind non-specifically to DNA at a high background rate, each nucleosome-free stretch of 14 bp can be considered to be a non-specific binding site (NSBS). A haploid *S. cerevisiae* genome is 12 Mb, 80% of which is wrapped in nucleosomes (Lee et al. 2007), yielding approximately 10^6 potential non-specific binding sites (NSBSs). In a yeast nucleus of volume 3×10^{-15} liters, the NSBS concentration is of order 10^{-4} mole/liter. To find the concentration of free TF [TF] in the nucleus given a total nucleic TF concentration of C_{TF}, we consider

$$K_d = \frac{[\text{binding\_site}][\text{TF}]}{[\text{binding\_site} \cdot \text{TF}]},$$

in the context of NSBSs, substitute [TF·NSBS] with C_{TF} - [TF], and solve for

$$[\text{TF}] = \frac{K_d(3)}{K_d(3)+[\text{NSBS}]} C_{TF} = \frac{10^{-5}}{10^{-5}+10^{-4}} C_{TF} \approx 0.1 C_{TF}.$$

Thus, about 90% of total TFs are bound non-specifically, leaving about 10% free. The relatively small number of specific TFBSs is not enough to significantly perturb the proportion of free TFs, and so for the specific TFBSs with m<3 that are of interest in our model, we simply use $\widehat{K_d}(m)$ = $10K_d(m)$ to account for the reduction in the amount of available TF due to non-specific binding. We also convert $\widehat{K_d}$ from the units of mole/liter in which K_d is estimated empirically to the more convenient molecules/nucleus. The rescaling factor r for which $\widehat{K_d}$(in molecule/nucleus) = $r\widehat{K_d}$ (in mole/liter) is 3×10^{-15} liter/nucleus × 6.02×10^{23} molecule/mole = 1.8×10^{9} molecule cell^{-1} liter mole^{-1}. Taken together, $\widehat{K_d}$(molecule/nucleus) = $10rK_d$ (mole/liter), where the factor 10 accounts for non-specific TF binding.

2. TF occupancy

Here we calculate the probability that there are A activators and R repressors bound to a given cis-regulatory region at a given moment in developmental time. First we note that if we consider TF i binding to TFBS j in isolation from all other TFs and TFBSs, Eq. S1 gives us probability of being bound:

$$P_b(j) = 1 - P_u(j) = \frac{c_i}{\widehat{K_d}+c_i}. \quad \text{(S1)}$$

Let $P_{A,R}^{(n)}$ be a term proportional (for a given value of n) to the combined probability of all binding configurations in which exactly *A* activators and *R* repressors are bound to the first *n* binding sites along the cis-regulatory sequence. We calculate $P_{A,R}^{(n)}$ recursively, considering one additional TFBS at each step. Note that if two different TFs bind to exactly the same location on a cis-regulatory region, we treat this as two TFBSs, not as one, and treat first one and then the other in our recursive algorithm.

Consider the case where the (*n*+1)th binding site belongs to an activator. The case where this activator is not bound contributes $P_{A,R}^{(n)} P_u(n+1)$ to $P_{A,R}^{(n+1)}$. If it is bound, then we must also take into account that the (*n*+1)th binding site overlaps (partially or completely) with the last $H \geq 0$ sites, and so contributes $P_{A-1,R}^{(n-H)} P_b(n+1) \prod_{j=n-H+1}^{n} P_u(j)$. Taken together,

$$P_{A,R}^{(n+1)} = P_{A,R}^{(n)} P_u(n+1) + P_{A-1,R}^{(n-H)} P_b(n+1) \prod_{j=n-H+1}^{n} P_u(j).$$

Similarly, if the (*n*+1)th site belongs to a repressor, we have

$$P_{A,R}^{(n+1)} = P_{A,R}^{(n)} P_u(n+1) + P_{A,R-1}^{(n-H)} P_b(n+1) \prod_{j=n-H+1}^{n} P_u(j).$$

By definition, $P_{A,R}^{(n)} = 0$ for binding configurations that are impossible, e.g. those with negative *A* or negative *R*. We initialize the recursion at *n* = 0, where the only valid binding configuration is for *A* = *R* = 0, i.e. $P_{0,0}^{(0)} = 1$. At *n* = 1, $P_{0,0}^{(1)} \propto P_u(1)$, and if the binding site belongs to an activator, $P_{1,0}^{(1)} \propto P_b(1)$; otherwise, $P_{0,1}^{(1)} \propto P_b(1)$. For *N* = 1, the two probabilities sum to 1 and

normalization is unnecessary. For higher values of $N = N_A + N_R$ TFBSs, we normalize $P_{A,R}^{(N)}$ at the end of the recursion by dividing by $\sum_{A=0}^{N_A} \sum_{R=0}^{N_R} P_{A,R}^{(N)}$ to get the probability of binding configurations that include exactly *A* activators and *R* repressors.

3. $r_{Act\_to\_Int}$

Transcription initiation over an interval of time r_{transc_init} is proportional to the proportion of time spent in the Active state. Assuming a steady state between Repressed, Intermediate, and Active states, as a function of current TF concentrations, we have:

$$\frac{r_{transc\_init}}{r_{max\_transc\_init}} = \frac{r_{Int\_to\_Act}}{r_{Int\_to\_Act} + r_{Act\_to\_Int}} P_{Int\_or\_Act}, \quad \text{(S2)}$$

where $P_{Int\_or\_Act}$ is the probability a gene is at Intermediate or Active. We set $r_{max\_transc\_init}$ (the rate of transcription given 100% Active state) to 6.75 min^{-1}, based on the corresponding rate when a model of the *PHO5* promoter is fit to data (Brown et al. 2013). In this model fit, the constitutively expressed *PHO5* promoter is free of nucleosomes 80% of the time, i.e. $P_{Int\_or\_Act} = 0.8$. We take these two values as universal for constitutively expressed genes, and assume that variation in $r_{Act\_to\_Int}$ is responsible for variation in r_{transc_init}. To identify a set of constitutively expressed genes, we identified 225 genes that have mRNA production rate of at least 0.5 molecule min^{-1} from genome-wide measurements (Pelechano et al. 2010); this threshold corresponds to low H2A.Z occupancy (Guillemette et al. 2005). We set r_{transc_init} to the production rate of mRNA of these 225 genes, and solve for gene-specific $r_{Act\_to\_Int}$ from Eq. S2. We fit the solutions to a log-normal distribution and arrive at $10^{N(1.27,\ 0.226)}$ min^{-1}.

To initialize values of $r_{Act\_to\_Int}$ for each gene, we sample from this distribution. We also set lower and upper bounds for allowable values; if either the initial sample or subsequent mutation put $r_{Act\_to\_Int}$ beyond these bounds, we set the value of $r_{Act\_to\_Int}$ to equal to boundary value. We set the lower bound for $r_{Act\_to\_Int}$ at 0.59 min^{-1}, half the minimum of the values inferred from the set of 225 genes. To set an upper bound, we use the low H2A.Z occupancy bound of $r_{transc\_init} = 0.5$, which gives a solution of 32.34 min^{-1}; we double this to set the upper bound as 64.7 min^{-1}.

4. Transcription delay times

Yeast protein lengths fit a log-normal distribution of $10^{N(2.568,\ 0.34)}$ amino acids (from the Saccharomyces Genome Database (SGD Project), excluding mitochondrial proteins). We sample ORF length *L* from this distribution. To constrain the values of *L*, we set a lower bound of 50 amino acids and an upper bound of 5000 amino acids; the longest protein in SGD is 4910 amino acids. If either initialization or mutation put *L* beyond these bounds, we set the value of *L* to the boundary value.

With an mRNA elongation rate of 600 codon/min (Larson et al. 2011; Hocine et al. 2013), it takes *L* / 600 minutes to transcribe the ORF of an mRNA. Also including time for transcribing UTRs and for transcription termination, and ignoring introns for simplicity, it takes 290 seconds to complete transcription of the yeast *GLT1* gene (Larson et al. 2011), whose ORF is 6.4kb. Putting the two together, we infer that transcribing the UTRs and terminating transcription takes around 1 minute for *GLT1*. Generalizing to assume that transcribing UTRs and terminating transcription takes exactly 1 minute for all genes, producing an mRNA from a gene of length *L* takes 1 + *L* / 600 minutes.

5. Translation delay times and $r_{protein\_syn}$

We model a second delay between the completion of a transcript and the production of the first protein from it. The delay comes from a combination of translation initiation and elongation; it ends when the mRNA is fully loaded with ribosomes all the way through to the stop codon and the first protein is produced. We ignore the time required for mRNA splicing; introns are rare in yeast (Dujon 1996). mRNA transportation from nucleus to cytosol, which is likely diffusion-limited (Niño et al. 2013; Smith et al. 2015), is fast even in mammalian cells (Mor et al. 2010) let alone much smaller yeast cells, and the time it takes is also ignored. The median time in yeast for initiating translation is 0.5 minute (Table 1 in Siwiak et al. 2010), and the genomic average peptide elongation rate is 330 codon/min (Siwiak et al. 2010). After an mRNA is produced, we therefore wait for 0.5 + L / 330 minutes, and then model protein production as continuous at a gene-specific rate $r_{protein\_syn}$.

To calculate $r_{protein\_syn}$, we combine the gene-specific ribosome densities D along the mRNAs and the gene-specific peptide elongation rates E, both measured in yeast (Siwiak et al. 2010). The values of DE across yeast genes fit the log-normal distribution $10^{N(0.322,\ 0.416)}$ molecule mRNA^{-1} min^{-1}; we initialize $r_{protein\_syn}$ for each gene by sampling from this distribution. We set the lower bound for $r_{protein\_syn}$ at half the minimum observed value of DE (4.5×10^{-3} molecule mRNA^{-1} min^{-1}). The upper bound corresponds to an mRNA fully occupied by rapidly moving ribosomes. Each ribosome occupies about 10 codons (Siwiak et al. 2010), and the peptide elongation rate can be as high as 614 codon/min (Waldron et al. 1977). If ribosomes are packed closely together at 10 codons apart, a protein comes off the end of production in the time taken to elongate 10 codons, i.e. proteins are produced at 61.4 molecules per minute. If either initialization or mutation put $r_{protein\_syn}$ beyond these bounds, we set the value of $r_{protein\_syn}$ to the boundary value.

6. mRNA and protein decay rates

We fit the log-normal distribution $10^{N(-1.49,\ 0.267)}$ min^{-1} to yeast mRNA degradation rates (Wang et al. 2002), and initialize the mRNA degradation rate r_{mRNA_deg} for each gene by sampling from this distribution. We set lower and upper bounds for r_{mRNA_deg} at half the minimum and twice the maximum observed values (7.5×10^{-4} min^{-1} and 0.54 min^{-1}), respectively. If either initialization or mutation put r_{mRNA_deg} beyond these bounds, we set the value of r_{mRNA_deg} to the boundary value.

Expressing the estimated half-lives of yeast proteins (Belle et al. 2006) in terms of protein degradation rates, they fit the log-normal distribution $10^{N(-1.88,\ 0.56)}$ min^{-1}; we initialize gene-specific protein degradation rates $r_{protein\_deg}$ by sampling from this distribution. We ignore the additional reduction in protein concentration due to dilution as the cell grows and thus increases in volume. We set lower and upper bounds for $r_{protein\_deg}$ at half the minimum and twice the maximum observed degradation rate (3.0×10^{-6} min^{-1} and 0.69 min^{-1}), respectively. If either initialization or mutation put $r_{protein\_deg}$ beyond these bounds, we set the value of $r_{protein\_deg}$ to the boundary value.

7. Simulation of gene expression

Our algorithm is part-stochastic, part-deterministic. We use a Gillespie algorithm (Gillespie 1977) to simulate stochastic transitions between Repressed, Intermediate, and Active chromatin states, and to simulate transcription initiation and mRNA decay events. We refer to these as "Gillespie events". The completion of transcription to produce a complete mRNA, and subsequent ribosomal loading onto the mRNA, are referred to as "fixed events" (they require fixed times of $1 + L / 600$ minutes and $0.5 + L / 330$ minutes, respectively). Scheduled changes in

the strength of the external signal are also fixed events. Protein production and degradation are described deterministically with ODEs, and updated frequently in order to recalculate TF concentrations and hence chromatic transition rates. Updates occur at the time of Gillespie and fixed events, and also in between.

The total rate of all Gillespie events is

$$r_{total} = \sum_i^{Rep} r_{Rep\_to\_Int\_i} + \sum_i^{Int}(r_{Int\_to\_Rep\_i} + r_{Int\_to\_Act\_i}) + \sum_i^{Act}(r_{Act\_to\_Int\_i} + r_{transc}) + \sum_i^{genes} r_{mRNA\_deg\_i} N_{mRNA\_i},$$

where *Rep*, *Int*, and *Act* are the numbers of gene copies in our haploid model that are in the Repressed, Intermediate, and Active chromatin states, respectively, and N_{mRNA_i} is the number of completely transcribed mRNA molecules from gene *i*. We only simulate degradation of full transcribed mRNA, and not that of mRNA that are still being transcribed, because the latter are already captured implicitly by $r_{max\_transc\_init}$, which is based on mRNAs that complete transcription (Brown et al. 2013). Once an mRNA finishes transcription, it is subjected to degradation regardless of whether ribosome loading is complete.

The waiting time Δt before the next Gillespie event is

$$\Delta t = \frac{x}{r_{total}},$$

where *x* is random number drawn from an exponential distribution with mean 1. Which Gillespie event takes place next is sampled only if a different update does not happen first. If a fixed event is scheduled to happen first at $\Delta t_1 < \Delta t$, we advance time by Δt_1, update the state of the cell, and calculate a new r_{total}'. Since the cellular activity has been going on with the old rate r_{total} for Δt_1, the remaining "labor" required to trigger the Gillespie event planned earlier is reduced. The new waiting time, $\Delta t'$, to trigger the planned Gillespie event is

$$\Delta t' = \frac{x - r_{total}\Delta t_1}{r_{total}'}.$$

Gene duplication creates $n \geq 1$ genes producing the same protein, where each copy *i* might have diverged in their production rate $r_{protein\_syn\_i}$ and degradation rate $r_{protein\_deg\_i}$. Complete proteins are produced continuously once an mRNA molecule is fully loaded with ribosomes, which occurs 0.5 + *L* / 330 minutes after transcription is complete – the concentration of such molecules is denoted $N_{mRNA\_aft\_delay\_i}(t)$. Total protein concentration obeys:

$$N'_{protein}(t) = \sum_i^n \left(r_{protein\_syn\_i} N_{mRNA\_aft\_delay\_i}(t) - r_{protein\_deg\_i} N_{protein\_i}(t) \right). \quad \text{(S3)}$$

Protein concentrations are updated using a closed-form integral of Eq. S3

$$N_{protein}(t_1) = \sum_i^n \left(\frac{r_{protein\_syn\_i} N_{mRNA\_aft\_delay\_i}}{r_{protein\_deg\_i}} + \left(N_{protein\_i}(t_0) - \frac{r_{protein\_syn\_i} N_{mRNA\_aft\_delay\_i}}{r_{protein\_deg\_i}} \right) e^{-r_{protein\_deg\_i}(t_1 - t_0)} \right) \quad \text{(S4)}$$

with this expression updated every time a Gillespie or fixed event at time t_1 changes the value of $N_{mRNA\_aft\_delay\_i}$.

In between updates, values of P_A, P_R, $P_{A\_no\_R}$, and $P_{notA\_no\_R}$, and hence chromatin transition rates, are calculated under the approximation of constant $N_{protein}$. Additional updates, above and beyond fixed and Gillespie events, are performed in order to ensure that chromatin transition rates do not change too dramatically from one update to the next. We use a target of D = 0.01 for the amount of change tolerated in the values of P_A, P_R, $P_{A\_no\_R}$, and $P_{notA\_no\_R}$, in order to schedule updates after time Δt^*, which are triggered when neither a Gillespie event nor a fixed event occurs before this time has elapsed, i.e. when $\Delta t^* < \Delta t_1$ and $\Delta t^* < \Delta t$.

There is the greatest potential for large changes after an update that changes the value of $N_{mRNA\_aft\_delay\_i}$. In this case, we use Eq. S1 to solve for the time interval for which the probability that TF i would be bound to a single perfect and non-overlapping TFBS would change by D, by choosing $\Delta t^* > 0$ that satisfies

$$\left| \frac{N_i(t)}{N_i(t)+K^*_{d,i}(0)} - \frac{N_i(t+\Delta t^*)}{N_i(t+\Delta t^*)+K^*_{d,i}(0)} \right| = D. \quad \text{(S5)}$$

A solution for Δt may not exist, e.g. if the concentration of TF i is decreasing but $P_b(t_2) < D$. In such cases, we set Δt^* to infinity.

When the previous update does not change any $N_{mRNA\_aft\_delay\_i}$ values, then we modify Δt^* adaptively. Let d be the maximum of ΔP_A, ΔP_R, $\Delta P_{A\_no\_R}$, and $\Delta P_{notA\_no\_R}$ during the last update. We then schedule an update at

$$\Delta t^{*\prime} = \frac{D}{d}\Delta t^{*}. \quad \text{(S6)}$$

After an update that changes the value of $N_{mRNA\_aft\_delay\_i}$, we use the smaller value from Eqs. S5 and S6. These additional update times are discarded and recalculated when a Gillespie or fixed event occurs first.

In **Fig. S11**, we see that simulations rarely exceed our target of *D*=0.01, and do so only modestly.

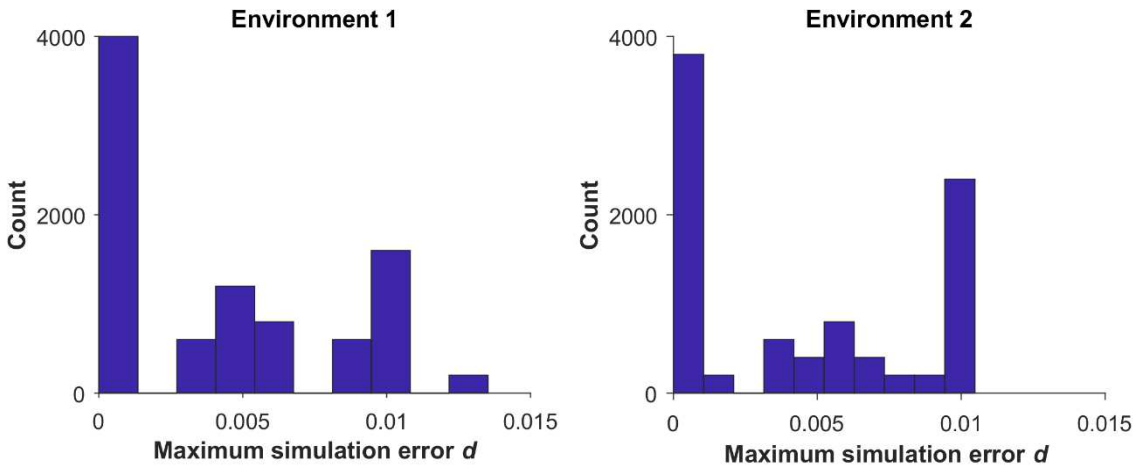

Fig. S11 Our updating algorithm is able to limit simulation errors. The distribution across 9,000 simulations of the maximum value of *d* over the course of development. For each of the 45 evolutionary replicates in **Fig. 4**, we run 200 simulations of development of the final evolved genotype. These genotypes were the outcome of evolution under selection for filtering out short spurious signals, in which direct regulation of the effector by the signal is not allowed. In environment 1 a genotype responds to a constant "ON" signal and in environment 2 it responds to a short spurious signal (**Fig. 3**).

8. Cost of gene expression

The cost of gene expression comes from some combination of the act of expression and from the presence of the resulting gene product. Yeast cells with plasmids carrying fast-degrading GFP had as much growth impairment as those carrying wild-type GFP (Fig. 3 of Kafri et al. 2016), suggesting that the former cost dominates. Universal costs stemming from the act of gene expression include the consumption of energy (Wagner 2005; Wagner 2007) and the opportunity cost of not using ribosomes to make other gene products (Scott et al. 2014). While some costs arise from transcription (Kafri et al. 2016), we simplify our model by attributing all of the cost of expression to the act of translation.

Kafri et al. (2016) reported that, in rich media, the growth rate of haploid yeast is reduced by about 1% when mCherry is expressed to about 2% of proteome. With b_{max} = 1 giving the growth rate of the yeast when mCherry is not expressed, we have the cost of gene expression equal to 0.01. Next, we estimate the production rate of mCherry in Kafri et al. (2016) by assuming that mCherry is in steady state between production and dilution due to cell division; fluorescent proteins tend to be stable such that degradation can be ignored (Snapp 2009). Ghaemmaghami et al. (2003) estimated that a haploid yeast cell contains about 5×10^7 protein molecules, 2% of which are now mCherry. Over a 90 minute cell cycle in Kafri et al. (2016), about 5×10^5 mCherry molecule per cell need to be expressed in order to double in numbers. This yields a production rate of about 5×10^3 mCherry molecules per minute per cell. Because the total cost of gene expression is 0.01, the cost at a protein production rate of one mCherry molecule per minute per cell, c_{transl}, is 2×10^{-6}. Long genes should be more expensive to express than short ones; for a gene of length L, we assume its cost of expression is $c_{transl}L$ / 370, where 370 is the geometric mean length of a yeast protein as described above in Section 4. Results using the length of

mCherry instead, i.e. a slightly higher cost of expression of $c_{transl}L$ / 236, are unlikely to be significantly different.

The overall cost of gene expression at time *t*, *C*(*t*) is:

$$C(t) = c_{transl}(\sum_1^n \frac{L_i}{10^{2.568}} r_{transl\_init\_i} N_{mRNA\_aft\_delay\_i}(t) + \sum_1^n \frac{L_i}{10^{2.568}} \frac{r_{transl\_init\_i}}{2} N_{mRNA\_during\_delay\_i}(t)).$$

The second term represents transcripts that are on average half-loaded with ribosomes, and hence experiencing on average half the cost of translation. We integrate *C*(*t*) within segments of constant *C*(*t*) to obtain the overall cost of gene expression during a simulation.

9. Mutation

Because we use an origin-fixation approach, only the relative and not the absolute values of our mutation rates matter. In *S. cerevisiae,* the rates of small indels and of single nucleotide substitutions have been estimated as 0.2×10^{-10} per base pair and 3.3×10^{-10} per base pair, respectively (Lynch et al. 2008). Thus, cis-regulatory sequences are primarily shaped by single nucleotide substitutions. We do not model small indels in the cis-regulatory sequence, but increase the single nucleotide substitution up to 3.5×10^{-10} per base pair to compensate. This corresponds to a rate of 5.25×10^{-8} per 150 bp cis-regulatory sequence.

Lynch et al. (2008) also report a rate of gene duplication of 1.5×10^{-6} per gene and of deletion of 1.3×10^{-6} per gene (not including non-deletion-based loss of function mutations). These values turned out to swamp the evolution of TFBSs and hence significantly slow down our simulations,

so we chose values 10-fold lower, making both gene duplication and gene deletion occur at rate 1.5×10^{-7} per gene. This preserves their numerical excess but reduces its magnitude.

Our model contains 8 gene-specific parameters, namely L, $r_{Act\_to\_Int}$, $r_{protein\_deg}$, $r_{protein\_syn}$, r_{mRNA_deg}, the $K_d(0)$ of a TF, whether a TF is an activator vs. repressor, and the consensus binding sequence of a TF. We assume mutations to L are caused by relatively neutral small indels, which we assume to be 20% of all small indels; mutation to L therefore occurs at rate 1.2×10^{-11} per codon, i.e. $1.2\times10^{-11}L$ for a gene of length L. For $r_{Act\_to\_Int}$, we assume that it is altered by 10% of all the point mutations (single nucleotide substitution and small indels) to the core promoter of a gene. The length of a core promoter is about 100 bp and is relatively constant among genes (Roy & Singer 2015), yielding a mutation rate of $r_{Act\_to\_Int}$ of 3.5×10^{-9} per gene.

The remaining 6 gene-specific parameter mutation rates are parameterized with lower accuracy due to lack to data; the principal decision is which to make dependent vs. independent of gene length. TF binding to DNA depends on particular peptide motifs whose length is likely independent of TF length, therefore we make mutation rates independent of gene length for mutations to $K_d(0)$, to the consensus binding sequence of a TF, and to the activating vs repressing identity of a TF. We set the rate of each of the three mutation types to 3.5×10^{-9} per gene. In contrast, because the stability of an mRNA mainly depends on its codon usage (Cheng et al. 2017) and thus more codons means more opportunities for change, we assume the rate of mutation to r_{mRNA_deg} does depend on gene length, as do mutations to protein stability $r_{protein\_deg}$. $r_{protein\_syn}$ is determined by the density of ribosomes on mRNA and the elongation rate of ribosomes, and therefore is affected both by ribosome loading speed and by slow spots forming queues in the mRNA. Ribosome loading often relies on the 5'UTR of mRNA (Hinnebusch 2011),

and 5'UTR length is positively correlated with ORF length (Tuller et al. 2009). Slow-spots in mRNA can be due to secondary structure or to suboptimal codons, therefore are also more likely to appear by mutation to long mRNAs, so we assume the rate of mutation to $r_{protein\_syn}$ depends on gene length. We set the mutation rates of $r_{protein\_deg}$, $r_{protein\_syn}$, and r_{mRNA_deg} each to 9.5×10^{-12} per codon; in other words, each mutation rate is 3.5×10^{-9} for a yeast gene of average length (on a log-scale) $10^{2.568}$ = 370 codons.

$r_{Act\_to\_Int}$, $r_{protein\_syn}$, $K_d(0)$, $r_{protein\_deg}$, and r_{mRNA_deg} evolve as quantitative traits. They are assumed to have, in the absence of selection, a log-normal stationary distribution with mean μ and standard deviation σ, with values estimated below and listed in **Table S2**. Denote the values of a parameter as *x* before mutation and *x'* after mutation; mutation takes the form:

$$\log_{10}x' = \log_{10}x + \mathrm{Normal}(k(\mu - \log_{10}x), \sigma), \quad \text{(S7)}$$

where *k* controls the speed of regressing back to the stationary distribution; we set *k* = 0.5 for all 5 parameters. To set values of μ, central tendency estimates of these five values (from **Table S1)** are adjusted according to our expectations about mutation bias. We assume a mutation bias toward faster mRNA degradation r_{mRNA_deg}, faster $r_{Act\_to\_Int}$ (Decker & Hinton 2013; Roy & Singer 2015), slower translation initiation $r_{protein\_syn}$ (Hinnebusch 2011), and larger $K_d(0)$. We assume that the observed log-normal means of r_{mRNA_deg}, $r_{protein\_syn}$, and $r_{Act\_to\_Int}$ differ by 2-fold from the mean expected from mutational bias; for example, the mean of $\log_{10}(r_{mRNA\_deg})$ is -1.49, so the value of μ for r_{mRNA_deg} is -1.49 + $\log_{10}(2)$ = -1.19. We assume a larger bias for $K_d(0)$, namely that mutation is likely to reduce the affinity of a TF for a TFBS down to non-specific levels. Thus, we set $\mu = \log_{10}(K_d(3))$ = -5 for $K_d(0)$; note that in this case μ is equal to one of the boundary values,

which will be hit far more often than during the evolution of other parameters. We assume that the observed central tendency estimate of protein stability does not depart from mutational equilibrium, therefore the value of μ for $r_{protein\_deg}$ is the mean of $\log_{10}(r_{protein\_deg})$ =-1.88.

The value of σ controls mutational effect size. We set the value of σ such that 1% of mutational changes from x=10^{μ} go beyond the boundary values, for simplicity approximating by considering only the closer of the two boundary values on a log scale, i.e. we solve Eq. S8 for σ:

$$\begin{cases} P(\mu + \text{Normal}(0,\sigma) \geq \log_{10} U) = 0.01, & \text{if the upper bound U is closer} \\ P(\mu + \text{Normal}(0,\sigma) \leq \log_{10} L) = 0.01, & \text{if the lower bound L is closer} \end{cases} \quad \text{(S8)}$$

For example, the upper and the lower bounds of r_{mRNA_deg} are 0.54 min^{-1} and 7.5×10^{-4} min^{-1}; on a log-scale, the upper bound is closer to $10^{\mu} = 10^{-1.19}$ min^{-1}. Plugging these values in Eq. S8 and solving for σ, we have σ = 0.396. We set the values of σ for $r_{protein\_syn}$, and $r_{protein\_deg}$ in the same way. However for $r_{Act\_to\_Int}$, σ is set according to the lower bound, even though it is the more distant from 10^{μ}, because otherwise a stable preinitiation complex will evolve too rarely. Under this high mutational variance, evolutionary outcomes at the two bounds are still only observed 5% of the time. For $K_d(0)$, because its upper bound is equal to 10^{μ}, we set σ to 0.776, such that 1% of mutations can change the values of $K_d(0)$ by 100-fold or more.

Mutant values of L, $r_{Act\_to\_Int}$, $r_{protein\_syn}$, $r_{protein\_deg}$, and r_{mRNA_deg} are constrained by the same bounds that constrain the initial values of these parameters (Sections 3-6). If a mutation increases the value of any of these 5 parameters to beyond the corresponding upper bound, we set the mutant value to the upper bound; similarly for a mutant value that is smaller than the lower bound of the corresponding parameter. For mutation to $K_d(0)$, we resample if $x' \geq K_d(3)$,

because otherwise the mutation effectively "deletes" the TF by reducing its affinity to non-specific levels.

10. Burn-in evolutionary simulation conditions

When the signal is not allowed to regulate the effector genes directly, most simulations under selection either to filter out short spurious signals or for simple signal recognition in the absence of spurious signals rapidly found a local optimal solution in which effector genes are never expressed. This local optimum exists in part because we assume that the environment in which the effector is deleterious is twice as common as the environment in which it is beneficial (**Fig. 3**). When the signal is not allowed to directly turn on the effector, then to escape this local optimum, at least one activator must be induced by the signal and then induce the effector. Such activators are rare when genotypes are randomly initialized. Making matters worse, mutation tends to reduce expression after initialization (see Section 9).

To reduce the frequency of this problem, we added a burn-in stage to simulations in which the signal is not allowed to regulate the effector directly. During burn-in, we switch the frequencies of the two environments, so that selection to express the effector is stronger. We also change the mutational bias in $r_{Act\_to\_Int}$, $r_{protein\_syn}$, and $K_d(0)$ to favor higher expression and stronger binding. For $r_{Act\_to\_Int}$ and $r_{protein\_syn}$, we use 0.1 instead of 0.01 as the tolerated fraction of extreme mutations in Eq. S8. For $K_d(0)$, we decrease μ from -5 to -7.5, biasing mutation toward the mean value at which we initialize (**Table S1**). Evolving an activator that can reliably turn on the effector when the signal is "ON" primarily relies on forming strong binding sites and appropriate kinetic constants in expression, assisted by the change in mutational bias above. To better focus the simulations on sampling appropriate mutations during the burn-in phase, we

reduce the rate of gene duplication and the rate of deletion to 5.25×10^{-9} per gene, and limit the maximum number of TF genes to 9 and that of effector genes to 2. Each simulation is run under burn-in conditions for 1000 steps, after which normal model settings and selection conditions are restored. The same burn-in mutational settings are used for the control selection conditions (no selection, no spurious signal, and harmless spurious signal).

11. Quantifying occurrence of network motifs

Scoring the presence of a C1-FFL motif (e.g. **Fig. 4B**) or diamond motif (e.g. **Fig. 7**) is based on scoring whether TF *x* regulates gene *y*. Gene duplication and divergence complicate this scoring, because different gene copies might encode functionally identical proteins, but one copy of gene *y* might have a TFBS for TF *x* and the other might not. For the purpose of scoring motifs, our algorithm begins by simply treating each gene copy as though it were a unique gene.

Following Milo et al. (2002), a C1-FFL is scored if activating TF A can bind to the cis-regulatory sequence of activating TF B and to the effector, if B can also bind to that of the effector, and if B does not bind to that of A. Auto-regulation is allowed. We exclude C1-FFLs in which A and B encode the same TF or variants of the same TF. In the case of direct regulation, A can be the signal rather than a TF. C1-FFLs can then be subdivided into categories based on overlap between the TFBSs in the cis-regulatory region of the effector (**Fig. 2**).

A diamond is scored if two signal-regulated activating TFs, A and B, do not bind to each other's cis-regulatory region, but both bind to that of the effector. We allow auto-regulation and require A and B to not encode the same TF or variants of the same TF.

A FFL-in-diamond is scored if one signal-regulated activating TF A binds to the cis-regulatory region of another signal-regulated activating TF B, but B does not bind to that of A, and both A and B bind to that of the effector. Again, auto-regulation is allowed, and A and B must not encode the same TF or variants of the same TF.

Occurrence within one evolutionary replicate is calculated as the fraction of the last 10,000 evolutionary steps in which at least one motif of the type of interest is present. The mean and standard error of this occurrence metric is then calculated across replicates.

12. Perturbing network motifs

In **Fig. 5** and **Fig. 9**, we add a TFBS to the cis-regulatory sequence of the effector gene, in order to destroy the AND-gate logic of an isolated C1-FFL or diamond. The new TFBS is chosen such that it does not overlap with any existing TFBSs, and has the same affinity as the strongest TFBS that is already present in the cis-regulatory sequence of the effector gene for the signal/fast TF (to convert from an AND-gate to signal-controlled/fast TF-controlled), or for the slow TF (to convert from an AND-gate to slow TF-controlled).

When a TRN has multiple AND-gated motifs of interest, we convert all of them. A perturbation can also affect the logic of other, potentially non-AND-gated motifs in the same TRN (e.g. **Fig. S12**), making it hard to attribute the fitness effect to the AND-gate logic of the targeted motif. For this reason, we perform the perturbation analysis not on a single potentially problematic genotype, but on the last 10,000 evolutionary steps of an evolutionary simulation. Within those 10,000 related genotypes, we exclude those that also contain other motifs that might influence our results. For simulations where the signal is allowed to directly regulate the effector, this

means excluding those with non-AND-gated C1-FFLs. For simulations where the signal is not allowed to directly regulate the effector, we exclude genotypes with either AND-gated or non-AND-gated motifs other those of interest (e.g. if we intend to perturb AND-gated isolated C1-FFLs, we exclude genotypes that also contain either an AND-gated isolated diamond or a non-AND-gated C1-FFL). Both pre-perturbation fitness and post-perturbation fitness are averaged over the remaining genotypes. If no evolutionary step meets our requirement, we exclude the entire evolutionary simulation; this occurs only when the signal cannot directly regulate the effector genes.

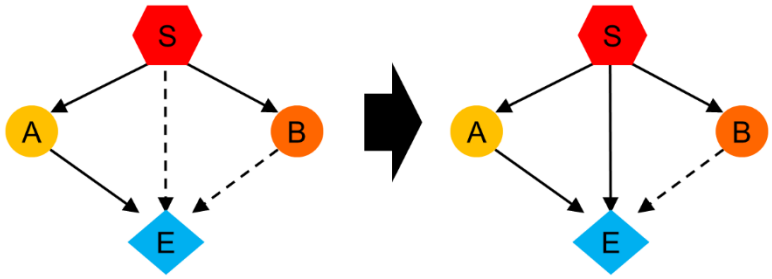

Fig. S12 Examples of confounding motifs in perturbation analysis. The TRN on the left contains a slow TF-controlled C1-FFL (S-A-E) and an AND-gated C1-FFL (S-B-E). To convert S-B-E into a signal-controlled C1-FFL, we need to add one TFBS for the signal to the cis-regulatory sequence of E. However, this change also makes S-A-E OR-gated, making it difficult to conclude whether it is the AND gate logic of S-B-E that matters for fitness.

References

Belle, A, Tanay, A, Bitincka, L, Shamir, R, and O'Shea, EK. 2006. Quantification of protein half-lives in the budding yeast proteome. *PNAS* 103:13004-13009.

Benos, PV, Bulyk, ML, and Stormo, GD. 2002. Additivity in protein-DNA interactions: how good an approximation is it? *Nucleic Acids Res* 30:4442-4451.

Brown, CR, Mao, C, Falkovskaia, E, Jurica, MS, and Boeger, H. 2013. Linking Stochastic Fluctuations in Chromatin Structure and Gene Expression. *PLoS Biol* 11:e1001621.

Cheng, J, Maier, KC, Avsec, Ž, Rus, P, and Gagneur, J. 2017. Cis-regulatory elements explain most of the mRNA stability variation across genes in yeast. *RNA* 23:1648-1659.

Decker, KB, and Hinton, DM. 2013. Transcription Regulation at the Core: Similarities Among Bacterial, Archaeal, and Eukaryotic RNA Polymerases. *Annu Rev Microbiol* 67:113-139.

Dujon, B. 1996. The yeast genome project: what did we learn? *Trends Genet* 12:263-270.

Ghaemmaghami, S, Huh, W-K, Bower, K, Howson, RW, Belle, A, Dephoure, N, O'Shea, EK, and Weissman, JS. 2003. Global analysis of protein expression in yeast. *Nature* 425:737-741.

Gillespie, DT. 1977. Exact stochastic simulation of coupled chemical reactions. *J Phys Chem* 81:2340-2361.

Guillemette, B, Bataille, AR, Gevry, N, Adam, M, Blanchette, M, Robert, F, and Gaudreau, L. 2005. Variant histone H2A.Z is globally localized to the promoters of inactive yeast genes and regulates nucleosome positioning. *PLoS Biol* 3:e384.

Hinnebusch, AG. 2011. Molecular Mechanism of Scanning and Start Codon Selection in Eukaryotes. *Microbiology and Molecular Biology Reviews* 75:434-467.

Hocine, S, Raymond, P, Zenklusen, D, Chao, JA, and Singer, RH. 2013. Single-molecule analysis of gene expression using two-color RNA labeling in live yeast. *Nature Methods* 10:119-121.

Kafri, M, Metzl-Raz, E, Jona, G, and Barkai, N. 2016. The Cost of Protein Production. *Cell Reports* 14:22-31.

Katan-Khaykovich, Y, and Struhl, K. 2002. Dynamics of global histone acetylation and deacetylation in vivo: rapid restoration of normal histone acetylation status upon removal of activators and repressors. *Genes Dev* 16:743-52.

Larson, DR, Zenklusen, D, Wu, B, Chao, JA, and Singer, RH. 2011. Real-time observation of transcription initiation and elongation on an endogenous yeast gene. *Science* 332:475-478.

Lee, W, Tillo, D, Bray, N, Morse, RH, Davis, RW, Hughes, TR, and Nislow, C. 2007. A high-resolution atlas of nucleosome occupancy in yeast. *Nature Genet* 39:1235-44.

Lynch, M, Sung, W, Morris, K, Coffey, N, Landry, CR, Dopman, EB, Dickinson, WJ, Okamoto, K, Kulkarni, S, Hartl, DL, and Thomas, WK. 2008. A genome-wide view of the spectrum of spontaneous mutations in yeast. *Proc Natl Acad Sci USA* 105:9272-9277.

Maerkl, SJ, and Quake, SR. 2007. A Systems Approach to Measuring the Binding Energy Landscapes of Transcription Factors. *Science* 315:233-237.

Milo, R, Shen-Orr, S, Itzkovitz, S, Kashtan, N, Chklovskii, D, and Alon, U. 2002. Network motifs: Simple building blocks of complex networks. *Science* 298:824-827.

Mor, A, Suliman, S, Ben-Yishay, R, Yunger, S, Brody, Y, and Shav-Tal, Y. 2010. Dynamics of single mRNP nucleocytoplasmic transport and export through the nuclear pore in living cells. *Nature Cell Biol* 12:543-552.

Nalefski, EA, Nebelitsky, E, Lloyd, JA, and Gullans, SR. 2006. Single-molecule detection of transcription factor binding to DNA in real time: Specificity, equilibrium, and kinetic parameters. *Biochemistry* 45:13794-13806.

Niño, CA, Hérissant, L, Babour, A, and Dargemont, C. 2013. mRNA nuclear export in yeast. *Chemical Reviews* 113:8523-8545.

Park, S, Chung, S, Kim, KM, Jung, KC, Park, C, Hahm, ER, and Yang, CH. 2004. Determination of binding constant of transcription factor myc-max/max-max and E-box DNA: The effect of inhibitors on the binding. *Biochim Biophys Acta, Gen Subj* 1670:217-228.

Pelechano, V, Chávez, S, and Pérez-Ortín, JE. 2010. A Complete Set of Nascent Transcription Rates for Yeast Genes. *PLoS ONE* 5:e115560.

Roy, AL, and Singer, DS. 2015. Core promoters in transcription: old problem, new insights. *Trends Biochem Sci* 40:165-171.

Scott, M, Klumpp, S, Mateescu, EM, and Hwa, T. 2014. Emergence of robust growth laws from optimal regulation of ribosome synthesis. *Mol Syst Biol* 10:747.

SGD Project. https://yeastmine.yeastgenome.org accessed April 2, 2018.

Sharon, E, Kalma, Y, Sharp, A, Raveh-sadka, T, Levo, M, Zeevi, D, Keren, L, Yakhini, Z, Weinberger, A, and Segal, E. 2012. Articles Inferring gene regulatory logic from high-throughput measurements of thousands of systematically designed promoters. *Nature Biotechnol* 30:521-530.

Siwiak, M, Zielenkiewicz, P, Jacobson, A, Grebogi, C, and Kito, K. 2010. A Comprehensive, Quantitative, and Genome-Wide Model of Translation. *PLoS Comput Biol* 6:e1000865.

Smith, C, Lari, A, Derrer, CP, Ouwehand, A, Rossouw, A, Huisman, M, Dange, T, Hopman, M, Joseph, A, Zenklusen, D, Weis, K, Grunwald, D, and Montpetit, B. 2015. In vivo single-particle imaging of nuclear mRNA export in budding yeast demonstrates an essential role for Mex67p. *J Cell Biol* 211:1121-1130.

Snapp, EL. 2009. Fluorescent proteins: a cell biologist's user guide. *Trends in Cell Biology* 19:649-655.

Tuller, T, Ruppin, E, and Kupiec, M. 2009. Properties of untranslated regions of the *S. cerevisiae* genome. *BMC Genomics* 10:391.

Wagner, A. 2005. Energy constraints on the evolution of gene expression. *Mol Biol Evol* 22:1365-1374.

Wagner, A. 2007. Energy costs constrain the evolution of gene expression. *J Exp Zool Part B* 308B:322-324.

Waldron, C, Jund, R, and Lacroute, F. 1977. Evidence for a high proportion of inactive ribosomes in slow-growing yeast cells. *Biochemical Journal* 168:409-415.

Wang, Y, Liu, CL, Storey, JD, Tibshirani, RJ, Herschlag, D, and Brown, PO. 2002. Precision and functional specificity in mRNA decay. *Proc Natl Acad Sci USA* 99:5860-5865.

Wunderlich, Z, and Mirny, LA. 2009. Different gene regulation strategies revealed by analysis of binding motifs. *Trends Genet* 25:434-440.

Yuan, GC, Liu, YJ, Dion, MF, Slack, MD, Wu, LF, Altschuler, SJ, and Rando, OJ. 2005. Genome-scale identification of nucleosome positions in *S. cerevisiae*. *Science* 309:626-630.

Zhu, J, and Zhang, MQ. 1999. SCPD: a promoter database of the yeast *Saccharomyces cerevisiae*. *Bioinformatics* 15:607-611.